ISTANBUL MEDENIYET UNIVERSITY
INSTITUTE OF GRADUATE STUDIES
DEPARTMENTS OF MOLECULAR BIOLOGY AND GENETICS

The Investigation of the Role of Epibrassinolide-Induced Autophagy During Tamoxifen Resistance in Breast Cancer

Master's Thesis

Esranur Kopal

June 2024

ISTANBUL MEDENIYET UNIVERSITY
INSTITUTE OF GRADUATE STUDIES
DEPARTMENTS OF MOLECULAR BIOLOGY AND GENETICS

The Investigation of the Role of Epibrassinolide-Induced Autophagy During Tamoxifen Resistance in Breast Cancer

Master's Thesis

Esranur Kopal

Supervisor

Prof. Dr. Pınar Obakan Yerlikaya

June 2024

THESIS JURY APPROVAL

This master thesis titled "The Investigation of the Role of Epibrassinolide-Induced Autophagy During Tamoxifen Resistance in Breast Cancer" written by Kopal, Esranur at the Department of Molecular Biology and Genetics was accepted by our jury.

JURY MEMBERS **SIGNATURE**

Supervisor:

Prof. Dr. Pınar OBAKAN YERLİKAYA

İstanbul Medeniyet University

Other Jury Members:

Assoc. Prof. Ayşe KARATUĞ KAÇAR

İstanbul University

Assist. Prof. Ömer Faruk SARIOĞLU

İstanbul Medeniyet University

Date of Defense:12/06/ 2024

STATEMENTS

Style and Reference Manual Statement

Having reviewed this thesis written under my supervision, I confirm that it has been written by APA Manual of Style and consistently used its in text reference format throughout the entire text.

Signature

Prof. Dr. Pınar OBAKAN YERLİKAYA

Declaration of Originality

I hereby declare that all information in this dissertation has been obtained and presented in accordance with academic rules and ethical conduct. I also declare that, as required by these rules and conducts, I have fully cited and referenced all material and results that are not original to this work.

Signature

Esranur KOPAL

ACKNOWLEDGEMENTS

First, I would like to express my deepest gratitude to my precious advisor and mentor Prof. Dr. Pınar OBAKAN YERLİKAYA, who allowed me to work in her laboratory and supported me financially and morally throughout the thesis. Then, I would like to thank my peerless colleagues Zeynep DEMİREL and Nilay DİNÇKURT, who provided me with all kinds of late-night feedback sessions, entertainment, and moral support during my master journey and made this difficult process bearable. I'm also grateful to Zainab AL-LAMI for encouragement and moral support during my master's degree. I had the pleasure of working with Özlem RECİMOĞLU, Ünal ARABACI, and Recep GÜNDOĞDU who motivated me and made my master's journey easier with their versatile support. I'd also like to extend my gratitude to Dr. Gülşen GÜNEL for her ingenious suggestions and helpful contribution. Lastly, I would be remiss in not mentioning my parents and my brother for their belief in me and financial and emotional support. I would like to thank my mother who sends me to school every day with her prayers, my father who comes to my aid whenever I am in trouble, my brother who provides support in technical matters, and my family members for adapting to my changing moods.

Special thanks to Prof. Dr. Elif Damla ARISAN who generously allowed me to access her laboratory at Gebze Technical University.

I would like to thank TUBITAK for financially supporting me during this thesis study within the scope of the BIDEB 2210-A scholarship program. Istanbul Medeniyet University, Scientific Research Projects Unit, Project no: F-GAP-2022-1795

CONTENTS

LIST OF SYMBOLS

α : Alpha

β : Beta

κ: Kappa

°C: Degree Celsius

μ: Micro

LIST OF ABBREVIATIONS

BC: Breast Cancer

LCIS: Lobular carcinoma in situ

DCIS: Ductal adenocarcinoma in situ

IDC: Infiltrating ductal carcinoma

BRCA1: BC susceptibility gene 1

BRCA2: BC susceptibility gene 2

HER2: human epidermal growth factor 2

PR: progesterone receptor

TNBC: Triple-negative BC

GPER: G-protein coupled estrogen receptor-1

ERE: Estrogen response element

PI3K: Phosphatidylinositol 4,5-biphosphate 3-kinase

SERM: Selective estrogen receptor modulator

TAM: Tamoxifen

EGFR: Epidermal growth factor receptor

RTK: Receptor tyrosine kinase

SERD: Selective estrogen receptor degrader

AI: Aromatase inhibitor

CDK: Cyclin-dependent kinase

BR: Brassinosteroid

EBR: Epibrassinolide

SILAC: Stable isotope labeling by amino acids in cell culture technique

UPR: Unfolded protein response

CALR: Calreticulin

ER: Endoplasmic reticulum

BiP: Molecular chaperone-binding immunoglobulin

CANX: Calnexin

PDI: Protein disulfide isomerase

ERAD: ER-associated protein degradation

IRE1α: Inositol requiring protein-1α

PERK: Protein kinase RNA-like ER kinase

eIF2α: Eukaryotic initiation factor 2 α

ATF6: Activating transcription factor 6

ATF4: Activating transcription factor 4

CHOP: C/EBP homologous protein

ROS: Reactive oxygen species

Atg: Autophagy-related gene

mTOR: mammalian targets of rapamycin

AMPK: AMP-activated protein kinase

LC3: microtubule-associated light chain

3-MA: 3-Methyladenine

MDR: Multidrug resistance

ABC: ATP-binding cassette transporters

LIST OF FIGURES

LIST OF TABLES

ABSTRACT

The Investigation of The Role of Epibrassinolide-Induced Autophagy During Tamoxifen Resistance in Breast Cancer Cells

Kopal, Esranur

Master Thesis, Department of Molecular Biology and Genetics

Supervisor: Prof. Dr. Pınar Obakan Yerlikaya

JUNE 2024, 129 Pages.

Breast cancer is one of the leading causes of cancer-associated death among women worldwide. Tamoxifen (TAM) is a widely used hormone therapy approach for the treatment of breast cancer. However, elevated estrogen receptor expression and signaling in breast cancer cells may result in the development of drug resistance. Endoplasmic reticulum stress (ER stress) is one of the combating mechanisms of drug resistance. The activation of apoptosis or autophagy in response to ER stress depends on the extent and duration of the stress. Epibrassinolide, a natural plant steroid hormone, has been shown in previous studies to have anti-cancer properties inducing by apoptosis and autophagy. Autophagy is a crucial recycling process to maintain cellular homeostasis within the cells eliminating mis /unfolded proteins and damaged organelles and aiding stress adaptation. Autophagy has a multifaced role in drug resistance. It can either facilitate or impede resistance based on variables such as the nature of the drug, cellular environment and signaling pathways involved.

In our study, we aimed to investigate the autophagic effect of EBR and/or TAM induced by ER stress to overcome drug resistance in MCF-7 / MCF-7/TAMR and MDA-MB-231 cell lines. For this purpose, relative cell viability analysis (MTT) and cell survival analysis were performed to analyze changes synergistic effect of EBR and TAM on cell viability. Moreover, the colony formation potential of EBR and/or TAM drugs was investigated in 2D and 3D manner Also, the number of death cells, mitochondrial membrane potential loss, and formation of DNA fragmentation were detected by PI, DiOC6, and DAPI respectively. The cell cycle distribution effect of EBR and/or TAM was detected by flow cytometry analysis. Moreover, autophagy induction was evaluated by MDC staining and GFP-LC3 transfection in all cell lines in the presence of 3-MA. Furthermore, expression profile changes of ER stress proteins autophagy proteins (Beclin-1, Atg5, LC3, and p62), resistance marker (MRPI), and apoptosis markers (PARP, caspase 9, caspase 3) were evaluated in the presence of 3-MA either alone or in combination EBR and/or TAM by immunoblotting in all cell lines.

As a result, EBR in combination with TAM decreased the cell viability in 2D and 3D cell cultures. In addition, EBR+TAM combination increased the number of fragmented DNA also decreased mitochondrial membrane potential. Moreover,

following exposure to EBR+TAM, cell cycle arrest was observed at G1 stages in MCF-7/TAMR cells. Furthermore, autophagic vacuole formation also LC3 puncta formation were augmented following EBR+TAM administration and reversed in the presence of 3-MA in breast cancer cell lines. Moreover, elevation of ER stress markers was detected in the same treatment conditions in all breast cancer cell lines. Also, EBR in combination with TAM increased the autophagic marker expression. On the one hand, decreasing in apoptotic marker expression was observed. Furthermore, following EBR+TAM administration expression of the drug-resistance gene was downregulated and reversed with the addition of 3-MA.

In conclusion, our results revealed that EBR in combination with TAM may play a crucial role in elevating TAM sensitivity by overcoming drug resistance through ER stress-induced autophagy in breast cancer cell lines.

Key words: Autophagy, Drug resistance, Endoplasmic Reticulum Stress, Epibrassinolide, Tamoxifen

ÖZET

Epibrasinolidin Otofajiyi Tetiklemesindeki Rolünün Tamoksifene Dirençli Meme Kanseri Hücre Hatlarında İncelenmesi

Kopal, Esranur

Yüksek Lisans Tezi, Moleküler Biyoloji ve Genetik Bölümü

Danışman: Prof. Dr. Pınar OBAKAN YERLİKAYA

Haziran 2024, 129 Sayfa.

Meme kanseri, dünya genelinde kadınlar arasında kansere bağlı ölümlerin önde gelen nedenlerinden biridir. Tamoksifen (TAM) meme kanseri tedavisinde yaygın olarak kullanılan bir hormon tedavi yaklaşımıdır. Ancak, meme kanseri hücrelerinde yüksek östrojen ifadesi ve sinyali, ilaç direncinin gelişimine neden olabilir. Endoplazmik retikulum (ER) stresi, ilaç direncine karşı mücadele mekanizmalarından biridir. ER strese yanıt olarak apoptoz veya otofajinin aktivasyonu, stresin şiddeti ve süresine bağlıdır. Epibrasinolid (EBR), önceki çalışmalarda apoptoz ve otofajiyi tetikleyen anti-kanser özelliklere sahip doğal bir bitki steroid hormon olarak gösterilmiştir. Otofaji, hücreler arası homeostazı korumak için önemli bir geri dönüşüm sürecidir, hücrelerdeki yanlış katlanmış/katlanmamış proteinleri ve zarar görmüş organelleri temizleyerek stres adaptasyonuna yardımcı olur. Otofajinin ilaç direncinde çok yönlü bir rolü vardır. İlaç türü, hücresel ortam ve ortama dahil olan sinyal yolakları gibi değişkenlere bağlı olarak ilaç direncini destekleyebilir veya engelleyebilir.

Çalışmamızda EBR ve/veya TAM'ın ER stresi tarafından tetiklenen otofajik etkisinin ilaç direncini kırmaya yönelik etkisini MCF-7, MDA-MB-231 VE MCF-7/TAMR hücre hatlarında inceledik. Bu amaçla göreceli hücre canlılığı analizi (MTT) ve hücre sağkalım analizi, EBR ve TAM'ın hücre canlılığı üzerindeki sinerjik etksinin değişimlerini analiz etmek için yapıldı. İlaveten, EBR ve/veya TAM ilaçlarının koloni oluşturma potansiyeli 2D ve 3D olarak incelendi. Ayrıca, ölü hücre sayısı, mitokondriyal membran potansiyel kaybı, DNA parçalanmasının oluşumu sırasıyla PI, DiOC6 ve DAPI ile tespit edildi. EBR ve/veya TAM'ın hücre döngüsü dağılım dengesi akış sitometrisi analizi ile belirlendi. Ayrıca, otofajinin tetiklenmesi, 3-MA varlığında tüm hücre hatlarında MDC boyama ve GFP-LC3 transfeksiyonu teknikleriyle değerlendirildi. Dahası, ER stresi proteinlerinin, otofaji proteinlerinin (Beclin-1, Atg5, LC3 ve p62), direnç belirleyicisinin (MRPI) ve apoptoz belirteçlerinin (PARP, kaspaz 9, kaspaz 3) anlatım ifadelerinin değişiklikleri, 3-MA'in tek başına veya EBR ve/veya TAM'ın kombinasyonu varlığında immünoblotlama ile değerlendirildi.

Sonuç olarak, EBR'nin TAM ile kombinasyonu, 2D ve 3D hücre canlığını azaltmıştır. İlaveten EBR+TAM kombinasyonu, parçalanmış DNA sayısını ve mitokondriyal membran potansiyelini azaltmıştır. Dahası, EBR+TAM'a maruz kalan MCF-7/TAMR hücrelerinde G1 evresinde hücre tutulumu gerçekleştirilmiştir. Ayrıca, EBR+TAM

uygulamasına takiben otofajik vakul oluşumu ve LC3 punkta oluşumu meme kanseri hücre hatlarında artmış ve 3-MA varlığında geri çevrilmiştir. Ek olarak, aynı tedavi koşullarında ER stresi belirteçlerinde anlatım seviyesinde yükselme meme kanseri hücre hatlarında tespit edilmiştir. Ayrıca, EBR'nin TAM ile kombinasyonu otofajik belirteçlerinin ifade anlatımını arttırmıştır. Öte yandan, apoptotik belirteç ifadelerinde azalma gözlenmiştir. İlaveten, EBR+TAM uygulamasını takiben, ilaç direnci geninin ifadesi düşük seviyede tespit edilmiş ve 3-MA varlığında geri çevrilmişitir.

Sonuç olarak, EBR'nin TAM ile kombinasyonunun, ER stresi tarafından tetiklenen otofaji aracılığıyla ilaç direncini aşarak, TAM duyarlılığını arttırmada meme kanseri hücre hatlarında kritik bir rol oynayabileceği ortaya koyulmuştur.

Anahtar Kelimeler: Endoplazmik Retikulum Stres, Epibrasinolid, İlaç Direnci, Otofaji, Tamoksifen.

1. INTRODUCTION

1.1 BREAST CANCER

Breast cancer (BC) is the most frequently diagnosed malignancy in women worldwide. According to the most current global cancer burden estimates, 2.26 million new cases of BC will be diagnosed in 2020, making it the most prevalent cause of cancer death among women (Wilkinson et al., 2022). BC is the most prevalent cancer among Turkish women, accounting for 25,249 new cases in 2022 and 23.5% of all female malignancies countrywide, according to the Globocan Cancer Observatory (Ferlay et al., 2024).

Breast tissue comprises 15-20 lobs and contains many lobules, also known as glands, that play a role in milk production. It also involves ducts that connect the lobules through the nipple and connective tissue, lymphatic tissue, and fatty tissue. BC occurs when the unregulated growth of the cells is found in any components of the mammary gland. The histological categorization of BC is based on the diversity of pathological growth patterns. At least 18 different histological types of breast cancer are distinguished by the World Health Organization (Łukasiewicz et al., 2021). Most BCs are carcinomas, tumors that start in the epithelial cells that line the body's organs and tissues. Up to 25% of all invasive BCs are histologically special forms of BC (Weigelt et al., 2010). Adenocarcinoma is a more specific type of carcinoma. It typically starts in the cells in the ducts (milk ducts) or lobules (milk-producing glands), which is the name given to carcinomas that develop in the breast. However, it generally occurs inside the lobules or ducts. Therefore, they refer to lobular carcinoma in situ (LCIS) or ductal adenocarcinoma in situ (DCIS). DCIS is the most common type of non-invasive BC (90%) rather than LCIS (Wehweck et al., 2021). Although the non-invasive type of BC is detected, most BCs are the invasive type which means cancer cells spread around connective or fatty tissues of the breast. The most widely

diagnosed (80%) invasive type of cancer is infiltrating ductal carcinoma (IDC). The other frequent type is invasive lobular carcinoma. Also, medullary carcinoma is a different type of invasive BC, and only 5% of patients suffer from this type. The other invasive BC type is mutinous carcinoma, a rare type obtained from mucus-producing cancer cells. Moreover, tubular carcinoma, a special IDC type, accounts for around 2% of BC. In elderly women tubular carcinoma is more seen (Makki et al., 2015). Inflammatory BC is a rare type of invasive BC, but it is more aggressive and fast-growing (Weigelt et al., 2010). All in all, numerous classifications have been proposed based on molecular and histological characteristics. All these features have critical implications for therapy (Makki et al., 2015).

1.1.1. Risk Factors of Breast Cancer

BC risk factors are categorized *as non-modifiable and modifiable factors*. The non-modifiable risk factors include gender, age, race/ethnicity, genetic predisposition or family history, mutations, and hormonal imbalance (Łukasiewicz et al., 2021). One of the most significant non-modifiable risk factors for the contribution of BC in the female sex due to enhancing hormonal stimulation. Although men have insignificant estrogen levels, women present vulnerable levels of estrogen and progesterone in a particular manner. Any distributions of these sex hormones within the physiological levels have been linked to an increased risk of BC for premenopausal and postmenopausal women (Mayrovitz (Ed.)., 2022). Even though BC cases are rare for men and occurrence is less than 1%, the diagnosis is more advanced than in women(Łukasiewicz et al., 2021) The occurrence of BC increases proportionally with age like other carcinogenesis. Nowadays, 80% of BC patients are detected >50, and at the age of 60, the peak of the disease is observed throughout the world. Accumulation of cellular alterations increases with age on account of carcinogenesis and increases with time (Łukasiewicz et al., 2021). The diagnosis of age is highly correlated with outcome prognosis. Women diagnosed with BC in young patients (ages lower than 50) have a lower survival rate compared to those diagnosed at ages 50-70. The most likely reason for triple negative BC (TNBC) occurrence in patients 40 years old or younger (Mayrovitz (Ed.)., 2022). However, the mechanism is not identified, the disparities of race and ethnicity are the other affecting factors for BC carcinogenesis. The mortality

rate of BC in black women is higher than in whites because of socioeconomic disparities. Also, the genetically more aggressive type of BC is detected in black women compared with other ethnicities. The genetic predisposition is another risk factor for BC development. Approximately 13-19% of BCs are inherited and correlated with family history (Łukasiewicz et al., 2021). In general, a woman who has a first-degree relative with BC increases her risk of acquiring the disease 1.5 to 3 times. Moreover, a person's increased relative risk (RR) of early-onset BC (before the age of 35) is associated with having a first-degree relative who had the disease (Harbeck et al., 2019). The number of affected first-degree relatives also increases the risk of developing BC in patients. The BC susceptibility gene 1 (*BRCA1*) or BC susceptibility gene 2 (*BRCA2*) as the primary gene related to hereditary BC has been found in most women who have familial BC. The mutations of these genes are inherited mainly in an autosomal dominant manner. According to a large study, the cumulative cancer risk has been reported as 72% in *BRCA1* mutation carriers and 69% in *BRCA2* mutation carriers (Mayrovitz (Ed.)., 2022). Besides the above-mentioned high penetrance genes, several genes and their mutations are linked with the induction of BC. Tumor protein 53 (*TP53),* cadherin 1 *(CDH1),* phosphatase and tensin homolog deleted on chromosome ten (*PTEN),* and serine-threonine kinase 11 (*STK11)* are the other highly penetrant genes for BC occurrence. Also, there are lower penetrance genes including various DNA repair genes such as ataxia-tel-angiectasia mutated (*ATM),* checkpoint kinase 2 *(CHEK2),* partner and localizer of *BRCA2 (PALB2 and BRAC1* interacting helicase 1 *(BRIP1)* associated with BC development (Łukasiewicz et al., 2021; Sarhangi et al., 2022). Further research has revealed a strong correlation between exposure to endogenous hormones such as progesterone and estrogen, and the risk of BC in females. Consequently, the potential for certain events harboring pregnancy, breastfeeding, menopause, and menarche, along with their duration and the associated hormonal imbalance, is significant (Łukasiewicz et al., 2021) For instance, studies indicate that starting the early menstruation cycles below the age of 12 increases the exposure time of the endogenous hormones in this manner increases the rate of BC risk.

Besides the non-modifiable factors, modifiable risk factors harboring dietary factors, chemical alcohol consumption, and physical activity are affected by the occurrence of

BC (Harbeck et al., 2019). According to data from epidemiological studies obesity is linked with an increased probability of BC risk. This association primarily affects obese post-menopausal women who are at increased risk of developing estrogen receptor-positive BC. Nonetheless, obese women get poor clinical outcomes independent of menopause. Following study results by Wang et al., women aged 50 or older who have a higher Body Mass Index (BMI) than those who have a lower BMI are more likely to get BC. Furthermore, the researchers observed that higher BMI correlated to more aggressive biological characteristics of the tumor, such as a larger size and a higher percentage of lymph node metastasis. In addition, women who are exposed to chemical compounds on a long-term basis have a much higher chance of progression of BC. This risk slightly increases with the length of exposure. So far, several chemicals have been studied in BC development, the most studied ones are polychlorinated biphenyls (PCB) and dichlorodiphenyltrichloroethane (DDT). These studies put forward that early exposure to these compounds negatively affects the development of the mammary glands. Other drugs harbors antibiotics, antihypertensive compounds, antidepressants, etc. also may include potential risk factors for the progression of BC (Łukasiewicz et al., 2021). Alcohol consumption is another risk factor for the development of BC. The elevated estrogen levels are carried on by the consumption of alcohol and the resulting hormonal imbalance that affects the risk of carcinogenesis within the female organs. Furthermore, research has shown that consuming alcohol increases the incidence of estrogen-positive BC in certain. Moreover, studies have noted that drinking alcohol raises the risk of breast tumors that are estrogen-positive in particular (Łukasiewicz et al., 2021). Various studies indicate the association between increased physical activity and lower BC risk. In this manner, the protective effect of physical activity was put forward in all women who had family-diagnosed diseases (Mayrovitz (Ed.)., 2022). Several theories explain the preventive impact of physical exercise against BC incidence. These include the possibility that physical activity lowers cancer risk by modifying immune system responses, lowering estrogen levels and insulin-like growth factor-1 levels, or limiting exposure to endogenous sex hormones. To sum up, ages, genetics, reproductive history, environmental factors, and multiple factors that are still undiscovered have

complicated roles in the development of BC. In this context, these many factors need to be considered in treatment approaches.

1.1.2. Molecular Classification of Breast Cancer

BC is a genetically heterogeneous neoplasm with multiple subtypes. Basis of histological and molecular characteristics, BC is classified into four categories: luminal A and luminal B (estrogen receptor-positive group), basal-like- and human epidermal growth factor 2 (HER2) according to a study by Perou and Sorlie (Jones et al., 2012)(Figure 1).

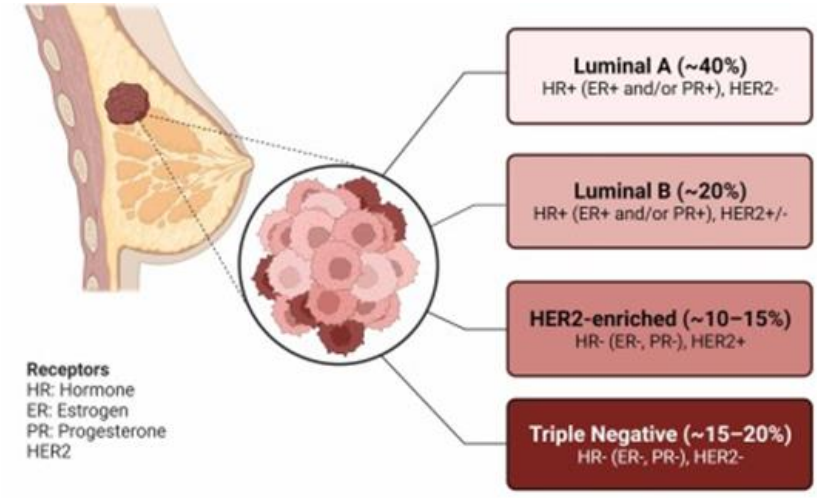

Figure 1. Molecular classification of breast cancer (Lazaratos, A. (2020) BioRender).

1.1.2.1. Estrogen receptor positive group (Luminal A and B)

The most general type of BC is Luminal A, and it is almost 40-50% of all BC cases (Sarhangi et al., 2022). Luminal A subtypes are the presence of the estrogen receptor, progesterone receptor (PR), and a lack of HER2 receptor. The cell proliferation marker which is Ki-67 is low almost less than 20% in the luminal A subtypes. The most well-known mutations in Luminal A incorporate *PIK3CA (45%), TP53, CDH1, GATA3, MAP3K1,* and *MAP2K4* (Sarhangi et al., 2022). Clinically, they are low-grade, slowly developing, and have the best chance of survival with a lower recurrence rate. Chemotherapy has a more restricted efficacy on these carcinomas. However, hormone therapy (tamoxifen or aromatase inhibitors) has a high response rate (Mayrovitz (Ed.)., 2022).

Luminal B types are the members of hormone estrogen receptor-positive tumor groups. The incidence of Luminal B (20-30%) is less than Luminal A. Luminal B types are categorized into two subgroups. The first group is HER2- and has a higher degree of estrogen receptor and PR expression besides the high expression of Ki-67. In the second group, it can be PR negative (-) in some cases in the presence of the expression of estrogen receptors and HER2. In addition, the second one the expression of K-i67 is either high or low depending on the condition (Sarhangi et al., 2022). Generally, Luminal B types display an expression of Ki-67 of more than 20%. The detection of the most common type mutations in luminal B types is *TP53* and *PI3KCA* mutations. They are of a high histological grade. The luminal B subtypes exhibit more aggressive behavior than luminal A. It is related to the worst prognosis group of luminal tumors. These tumors may benefit from hormonal therapy together with chemotherapy (Mayrovitz (Ed.)., 2022).

1.1.2.2. HER2 positive

The high expression of HER2 besides the absence of estrogen receptors and PR receptors is detected in HER2-positive tumor subtypes. Approximately 15-25% of BCs consist of overexpression of HER2. It has a poor prognosis. Two subcategories are harboring HER2-enriched (HER2+, estrogen receptor-, PR-, Ki-67 30%) also luminal HER2 (HER2+, estrogen receptor +, PR+, and Ki-67: 15-30%) (Mayrovitz (Ed.)., 2022). The frequency of *TP53* and *PI3K* mutations in HER2-positive tumors is higher than in luminal subtypes (in order of 72% and 39%) (Sarhangi et al., 2022). This subtype demonstrates a more aggressive course of disease and growth faster than luminal ones. Also, it has a high risk of recurrence especially five years after the treatment. Chemotherapy is highly responsive to HER2 patients. In addition, chemotherapy-specific drug candidates directed to the HER2 receptor are used for therapeutic response (Mayrovitz (Ed.)., 2022).

1.1.2.3. Basal-like /Triple-negative

TNBC is a heterogeneous type of BC. Its name suggests that it is a triple negative for all three receptor expressions: estrogen receptor, PR, and HER2. 15–20% of all BC cases are constituted of TNBC tumor and TNBC frequency varies depending on

ethnicity. It seems to be by young women at age 40, especially younger black women (Mayrovitz (Ed.)., 2022). The well-recognized characteristics of TNBC are aggressiveness compared to other types, poor prognosis, and distinct metastatic properties. Even though *BRCA1/BRCA2* mutations are associated with all BCs, the TNBC subtype has the greatest prevalence of *BRCA1/BRCA2*. Approximately 20% of TNBC patients are thought to have a germline mutation of *BRCA1/BRCA2*. (Sarhangi et al., 2022). In conclusion, BC has several biological subgroups that differ in incidence, progression risk, metastasis potential, and treatment response.

1.1.3. Molecular Mechanisms in Breast Cancer Development and Progression

Hanahan and Weinberg defined in 2011 that cancer cells exhibit a set of properties or hallmarks harboring incessant growth, evading growth suppressors, evasion of cell death, activating invasion & and metastasis, genomic instability, inducing vascularization, escaping immune destruction, creating self-sufficiency metabolism (Hanahan and Weinberg., 2011). Hanahan exhibited four more cancer hallmarks in 2022, including non-mutational epigenetic reprogramming, polymorphic microbiomes unlocking phenotypic plasticity, and senescent cells. Modifications of signal transduction pathways are fundamental for forming many of these hallmarks. These signaling pathway changes result from proto-oncogene mutations or inactivation of tumor suppressor genes, and mutated proteins with uncontrolled activity (Hanahan, 2022). Diverse signaling pathways with multiple genes have been affected in the pathophysiology of BC. Estrogen receptor signaling and HER2 receptor signaling pathways are the most studied pathways directly related to BC progression. Moreover, the PI3K/Akt/mTOR, Notch, and Ras pathways also correlate with the progression of breast carcinogenesis (Feng et al., 2018)

One of the most affected signaling paths for the tumorigenesis of BC is the estrogen signaling pathway. A class of female hormones known as "estrogens" includes estrone, estradiol, estriol, and estretrol. Regarding chemistry, estrogens are members of the chemical molecule family known as steroids (Fuentes et al., 2019). To date, three distinct estrogen receptors have been put forward in breast tumors; two of them are nuclear receptors, estrogen receptor alpha (α) and estrogen receptor beta (β), and the

other one is G-protein coupled estrogen receptor-1 (GPER) that triggers non-genomic effects of estrogen in the cytosol (Girgert et al., 2019). The human gene ESR1, located at location 6q25.1 on chromosome 6, encodes the estrogen receptor α. Apart from the 66kDa full-length estrogen receptor α isoform, multiple other shorter isoforms (36kDa and 46kDa) have been detected due to different start codons or alternative splicing outcomes. Conversely, the ESR2 gene, located on chromosome 14 (14q23–24), encodes estrogen receptor β, of which five recognized isoforms exist. The GPER1 gene, which codes for the membrane receptor, is located at locus 7p22.3 on chromosome 7 (Fuentes et al., 2019). The structures of the estrogen receptors, estrogen receptor α, and estrogen receptor β, share several structural regions and are composed of multiple functional domains, as they belong to the nuclear hormone receptors superfamily of transcription regulators. There are no structural similarities between GPER1 and estrogen receptor α or estrogen receptor β. The binding affinity of this receptor is lower than that of other estrogen receptors. This could be significant, though, since GPER1 is responsible for the activation of second messenger-mediated intracellular signaling cascades and quick response to estrogen. Thanks to their steroid structures, estrogen gets into the plasma membrane and triggers an intercellular signaling cascade by association with GPER, estrogen receptor α, and estrogen receptor β. Estrogen-mediated signaling pathways can be categorized into two groups: genomic and non-genomic in terms of binding estrogen receptor complexes to DNA directly or indirectly. In direct genomic signaling, which is a known classical signaling mechanism, the estrogen receptor complex translocates the nucleus and interacts with specific DNA sequences named estrogen response elements (EREs). In the indirect genomic signaling pathway, estrogen receptor complexes have been related to the activation of other signal transduction mechanisms and protein kinase cascade consequences with the phosphorylation of transcription factors. In this way, it regulates transcription with the interaction of DNA sequences. Some transcription factors impacted by these signaling pathways include CCAAT-enhancer-binding protein beta (C/EBP), Elk-1, CREB, the NF-κB complex, and the signal transducer and activator of the transcription (STAT) family. Moreover, protein cascades comprising the four major classes are the Ras/Raf/MAPK pathway, cAMP/ protein kinase A (PKA) signaling pathway, the phospholipase C (PLC)/ protein kinase C

cascade (PKCs), and the phosphatidylinositol 3 kinase (PI3K)/Akt kinase signaling pathway also take the role in the indirect signaling pathway. Convergence of the two conventional estrogen receptor regulatory mechanisms might thus lead to increased transcriptional activity in certain tissues and physiological processes (Fuentes et al., 2019). The specific action that the activated estrogen receptor produces is dependent on the chemical structure of the ligand that the receptor is coupled to in addition to the cellular environment. As a result, considerable effort has been expended on studying the structure-activity links underlying the estrogen receptor. Selective estrogen receptor modulators (SERMs), phytoestrogens, endoestrogens, xenoestrogens, and metalloestrogens are five major groups of ligands that bind to estrogen receptors. Investigations into structure-activity and estrogen receptor relationships have yielded successful anti-estrogen therapeutics harboring tamoxifen (TAM), anastrozole, raloxifene, and others. In BC pathogenesis, approximately 75% positive estrogen receptor α expression is detected. In this context, new information continues to unveil new insights into pharmacological intervention for cancer particularly through studies on estrogen receptors in BC (Clusan et al., 2023; Fuentes et al., 2019; Schuur et al., 2015).

Another pathway that is associated with the progression of BC is the HER2 signaling path. A member of epidermal growth factor receptors (EGFR) is HER2. It constitutes four tyrosine kinases EGFR (HER1), HER2 (ErB2/c-neu), HER3 (ErB3), and HER4 (ErB4). These kinases have many domains including the extracellular ligand binding domain, intracellular domain, and transmembrane domain for controlling several biological processes (Feng et al., 2018). The activation of HER2 receptors leads to turning on other signaling mechanisms that intersect with cell proliferation, cell cycle progression, cell differentiation, survival, migration, and adhesion such as phosphatidylinositol 4,5-biphosphate 3-kinase (PI3K), mitogen-activated kinase (MAPK), and glycogen synthase kinase-3 (GSK-3) (Crusio et al., 2021.; Ortega et al., 2020). The HER2 overexpression seems to be the mark of various BC cell lines. Abnormal amplification of HER2 protein is associated with the tumorigenesis of BC via affecting downstream signaling pathways. Targeted therapy is a strategy to directly engage specific molecules in these signaling pathways to prevent the progression of tumors. The first direct therapy against the extracellular subdomain of HER2 emerged

as a humanized monoclonal antibody called trastuzumab (Herceptin). Despite the poor effectiveness of monoclonal antibodies as therapies at the time, studies including the addition of trastuzumab to routine adjuvant chemotherapy were started. The outcomes of these studies showed that, in comparison to adjuvant chemotherapy alone, targeting HER2 with trastuzumab improved disease-free survival in women with HER2-positive patients. Patients will respond well to therapy, as is all too often in cancer cases, only for that same drug to lose its effectiveness a few weeks, months, or years later, and the disease relapses. This phenomenon is likewise seen in the HER2 system (Schuur and DeAndrade, 2015). Understanding the mechanism behind trastuzumab resistance has proven challenging, primarily because of the difficulty in obtaining tumor samples that are resistant to trastuzumab. Additional investigation into the biology of HER2 signaling in invasive BC (IBC) has provided an understanding of the resistance mechanisms. Resistance to anti-HER2 agents can occur through a mechanism where HER2 forms dimers with EGFR (HER1) or HER3 family members, enabling signaling even in the presence of HER2 inhibitors. Pertuzumab, another monoclonal antibody targeting HER2, prevents this dimerization process and proves to be an effective therapy for HER2-positive BC. Importantly, it can complement the action of trastuzumab, leading to an enhanced therapeutic outcome. These results support the principle that blocking "rescue" signaling overcomes therapy resistance. Developing new treatment methods by targeting downstream pathways of HER2 is a crucial factor in increasing the effectiveness of the therapeutic response. For instance, overactivity in the PI3K/AKT pathway downstream of HER2 has been commonly detected in biopsy samples of BC that are resistant to trastuzumab (Crusio et al., 2021). In preclinical studies, Buparlisib (BKM120), a broad inhibitor of PI3K, has been shown to demonstrate synergistic effects in inhibiting growth when combined with agents that target the HER2 receptor (Ortega et al., 2020).

Besides the estrogen and HER2 signaling the PI3K/Akt/mTOR is one of the critical pathways for BC tumorigenesis. The PI3K/Akt/mTOR signaling pathway regulates cell growth, proliferation, survival, motility, metabolism, and immune response. The dysregulation of this pathway has been linked with a broad spectrum of cancer symptoms such as uncontrolled cell proliferation, metabolic reprogramming in tumor cells, and genomic instability. Furthermore, activation of the PI3K/Akt/mTOR

pathway is one of the primary reasons for cancer cell resistance to anticancer treatments. In nearly all human cancers including BC, this pathway has been altered where up to 60% of tumors contain various variants that hyperactivate this system (Feng et al., 2018; Ortega et al., 2020). Activation of PI3K is a crucial stage in oncogenesis and contributes to treatment resistance in estrogen receptor +/HER2+ breast tumors. *PI3KCA* mutations are more prevalent in luminal A subtype tumors, occurring in 45% of cases, with HER2+ mutations following in 39% of cases, luminal B in 30% of cases, and TNBC mutations in 9% of instances. Currently, the PI3K inhibitors have been improved for preventing cancer tumorigenesis. The FDA just approved alpelisib as the first PI3K inhibitor for the treatment of BC, therefore actual research on this kind of inhibitor is becoming increasingly interesting. Taselisib's effectiveness in treating BC in cellular models with *PIK3CA* mutations has also been documented in other preclinical investigations (Feng et al., 2018; Ortega et al., 2020).

Another critical pathway for the progression of BC is the Notch pathway. The Notch pathway is known as an evolutionarily conserved pathway that mediates cell fate, stem cell differentiation, and organ development. The Notch signaling comprises four receptors including Notch 1, 2, 3, 4, and five ligands harboring Delta-like (DLL) 1, 3, 4 and Jagged (Jag) 1, 2. The Notch ligand-receptor complex is subsequently proteolytically cleaved many times, resulting in the formation of the Notch extracellular domain and the Notch intracellular domain (NICD). NICD functions as a transcription factor, regulating downstream target genes (Feng et al., 2018). Any perturbation of this pathway including activation of mutations in the Notch receptor, amplification of ligands and/or receptors, and/or overexpression of its target genes results in cellular transformation, heightened proliferation, and drug resistance in breast, prostate, multiple myeloma, T-cell acute lymphoblastic leukemia, and other cancers (BeLow and Osipo, 2020). Since overexpression of Notch 1, 3, and 4 was observed in the transition from normal breast cells into cancerous cells, it has been revealed that Notch exhibits oncogenic properties in breast tumor formation. Moreover, high levels of expression of Jag1 and/or Notch1 in tumors were indicated to be correlated with poor prognosis and to be an independent prognostic factor in primary human BCs. Additionally, Notch signaling interacts with the HER2 signaling

system, which is linked to more aggressive disease and is activated in about 20% of breast tumors (BeLow and Osipo, 2020; Feng et al., 2018).

One more pathway taking a role in tumorigenesis of breast tissue is the Ras pathway. The Ras pathway mediates the activation of extracellular signaling and cytoplasmic signaling networks by receptor tyrosine kinases (RTKs) (Crusio et al., 2021). The epidermal growth factor receptor (EGFR), belonging to the RTK family, is a well-documented activator of Ras signaling. This activation occurs through the recruitment of the molecular scaffolding protein growth factor receptor-bound protein 2 (GRB2). The Ras-guanine exchange factor (Ras-GEF) SOS1, which is attracted to GRB2, causes the exchange GDP for GTP, resulting in activating the Ras protein (Gimple and Wang, 2019). The Ras protein family consists of four members which are H-Ras, N-Ras, K-Ras A, and K-Ras B. There are several downstream effector pathways found for Ras. The best-characterized pathways are the MAPK/ERK pathway and PI3K-Akt pathway. Ras pathways play a role in the proliferation of cells, growth, and survival of the cell, motility, and metabolism. The first identified mutated oncogene in humans is Ras. The oncogenic activity of Ras is detected in many cancers frequently amongst the other mutations. Also, oncogenic activation of Ras is shown in the progression of BC. Overexpression of HER2 and EGFR receptors and loss of expression of Ras GTPase activating proteins (RasGAPs) are frequently detected in human BC. The H-Ras and N-Ras isoforms are the most detected mutated forms in aggressive types of BC (Galiè, 2019). Therewithal in basal-like cancer, the activation of K-Ras is observed (Crusio et al., 2021). These isoforms demonstrate functional diversity in the progression of BC. These diverse functions harbor metabolic reprogramming, epithelial-mesenchymal transition (EMT), proliferation, cell death mechanism, and so on. Invasive properties of BC cells are demonstrated via activation of H-Ras. Furthermore, *de novo* lipogenesis and activation of autophagy-related genes also the formation of autophagic vacuole are triggered via oncogenic K-Ras (Crusio et al., 2021.; Galiè, 2019). Oncogenic Ras proteins serve a promoter role in cell cycle progression via inhibiting CDKs which are p21 and p27. Moreover, the anti-apoptotic and pro-apoptotic effects of Ras depend on the Ras effector status. The function of oncogenic Ras in cancer is directed towards pro-survival (Crusio et al., 2021). Furthermore, the immune evasion role of the Ras/MAPK pathway was determined in

triple-negative BC cells (Galiè, 2019). Apart from its strong role as a modulator of tumor transformation and progression, Ras may potentially contribute to treatment resistance in BC. The act of Ras in breast tumorigenesis and resistance to treatments justifies considering Ras as a target in BC treatment. In this context, the inhibition of Ras signaling pathways has great potential as a therapeutic candidate for BC. Therefore, multiple signaling pathways contribute to the progression of BC tumorigenesis in a different direction.

1.1.4. Treatment Options

Breast cancer patients are diagnosed via physical examination, mammography, and diagnostic ultrasound. Moreover, magnetic resonance imaging, positron emission tomography/computerized tomography (PET/CT), and scintigraphy are available in clinics for diagnosis (Schuur and DeAndrade, 2015). Biopsy is the gold standard for the assessment of the BC probability from the tissue specimens. Fine needle aspiration (FNA), core needle biopsy, and excisional biopsy are the three types of biopsy techniques. After the biopsy, pathological analysis was performed for examination of biomarkers of tumor samples. The prognosis of BC types is an important factor in determining the correct treatment approach (Schuur and DeAndrade, 2015). Entirely BC is a heterogeneous disease on the molecular level thereby this property gives the directions for new treatment approaches such as biologically directed therapy for any molecular subtype. Current treatment strategies for BC are radiotherapy, surgery, chemotherapy, hormonal therapy, and targeted therapy (Clusan et al., 2023).

1.1.4.1. Surgery, radiotherapy, chemotherapy, hormone therapy, targeted therapy

For invasive BC, the removal of breast tumor tissues is contributed via two major surgical procedures; breast-conserving surgery (BCS) and mastectomy. While the BCS, also known as lumpectomy, provides the partial removal of the cancerous breast tissues via preserving surrounding healthy breast tissue, mastectomy is the removal of a complete breast tumor and is related to the reconstruction of the breast immediately. Axillary lymph node dissection (ALND) and sentinel lymph node biopsy (SLNB) are the affected lymph nodes during BCS so the removal of these is required. Even though,

in stages 1 and III, BCS is preferred primarily as a treatment option, the tendency of mastectomy is detected because of the local recurrence. The local recurrence rates are variable significantly between breast tumor subtypes in patients.

Chemotherapy is the most known systematic therapy strategy for the treatment of high-risk BC patients. The most known chemotherapeutic drug families are anthracycline and taxane. They are applied either before surgery (as neoadjuvant) or after surgery (as adjuvant) according to the breast tumor characteristics. Choosing the appropriate chemotherapy drug is critical since the preoperative chemotherapy response differs in variable breast tumor subtypes. However, chemotherapy seems to be an effective strategy for therapy. Its application causes various side effects such as vomiting, hair loss, fatigue, diarrhea, and so on.

After the surgery and chemotherapy, radiotherapy which is the local therapeutic option is applied to ensure the destruction of all cancerous cells decreasing the recurrence of BC. Depending on the surgery types, several choices are detected for radiotherapy. Breast radiotherapy, chest-wall radiotherapy, and breast boost therapy are the most common techniques. Some of the most prevalent side effects of radiation therapy in BC patients include skin irritation and darkening in the treated area, tiredness, and lymphoedema. Nonetheless, radiation treatment is strongly associated with improved overall survival rates and reduced risk of cancer recurrence (Łukasiewicz et al., 2021).

To provide the most effective treatment in the most suitable scenarios, targeted medicines are designed to associate with signaling pathways molecules that are crucial for the genesis and progression of cancer. Hormonal (endocrinal) therapy and biological therapy are the most studied strategies for therapeutic options for BC development nowadays. The hormonal therapy can be received in patients with all estrogen receptor-and/or PR- and/or PR-positive (Luminal) subtypes of BC in cases of recurrence or metastasis of BC (Łukasiewicz et al., 2021; McDonald et al., 2016). The detection of high expression of hormone receptors in BC patients leads to a development phenomenon which is blockage of hormone expression as a treatment modality. In these ways, the selective estrogen receptor modulators (SERMs) and selective estrogen receptor degraders (SERDs) have been improved. While the SERMs which include TAM, toremifene aim to block estrogen receptors, SERDs that harbor

aromatase inhibitors (AIs) (such as exemestane, letrozole anastrozole) goal to reduce estrogen levels (Łukasiewicz et al., 2021). This therapy can be applied as either neoadjuvant or adjuvant therapy in BC patients. After surgery, adjuvant hormonal therapy has been used as a standard for at least 5 years. Extending this therapy up to 10 years or 15 years seems beneficial for patients prone to relapse (Harbeck et al., 2019). However, during this treatment, almost 50% of patients developed progressive resistance to hormonal therapy (Łukasiewicz et al., 2021). Therefore, further investigation will be required to overcome this situation.

Biological therapy (targeted therapy) can be administered at any stage of BC treatment. Targeted therapy is commonly applied in HER2-positive BC patients; prominent medicines comprise trastuzumab (HER2-specific monoclonal antibody), pertuzumab (a monoclonal antibody), deruxtecan, lapatinib, and neratinib (Łukasiewicz et al., 2021; McDonald et al., 2016). The overall survival is extended via anti-HER2 therapy, most patients develop resistance to this therapy. To minimize resistance combined treatment approaches with chemotherapy provide significant long-term benefits compared to alone (Crusio et al., 2021.). Cyclin-dependent kinase (CDK) inhibitors are another type of targeted therapy approach. Particularly, CDK4 and CDK6 inhibitors including palbociclib, abemaciclib, and ribociclib, block the proliferation of cyclin-dependent kinase in hormone receptor-positive cancer cells. The ER-positive and HER2-negative BC cells are treated with a higher response rate when the CDK inhibitors and endocrine therapy combine. Furthermore, to enhance survival for ER-positive patients who harbor *BRCA1* and *BRCA2* mutation, PARP inhibitors (olaparib and talazoparib) have been applied (Sarhangi et al., 2022). Moreover, these inhibitors are also used for TNBC patients who have *BRCA1* and *BRCA2* mutations (Shaikh et al., 2022). Also, in BC patients who have mutated PI3KCA, alpelisib is developed to target the PI3K protein to prevent abnormal cell proliferation. Furthermore, targeting signaling pathways is another biological therapy strategy for BC therapy. For instance, everolimus which is an mTOR inhibitor helps to stop new vessel formation for the growing tumors in postmenopausal women. Besides these strategies, immunotherapy approaches have been seen as targeted therapy approaches. For example, for metastatic TNBC patients atezolizumab which is a programmed cell death-ligand 1 (PD-L1) antagonist is approved by the FDA. Moreover, some antibody-drug conjugates

(ADCs) such as sacituzumab govitecan (SG), and ladiratuzumab vedotin have been developed to target cell surface proteins for the TNBC. The success of the SG has been demonstrated in the clinic and is the first drug approved by the FDA in the ADC category (Shaikh and Emens., 2022; Zhu et al., 2023). In conclusion, new biologic drugs and treatment strategies that address the unique and complex molecular characteristics of tumors in each BC patient are revolutionizing treatment algorithms for BC patients and are expected to provide increasing benefits to BC patients with an expanding pipeline of promising agents (Kumar et al., 2023; Tarantino et al., 2020).

1.2. TAMOXIFEN AND BREAST CANCER

The hormone-dependent BC types have been detected in almost 70% of patients. Almost two-thirds of the proliferation of BC cells relies on the activation of the estrogen receptor α. Therefore, hormone therapy is recommended for treatment options for patients with estrogen-positive BC. TAM is the first and most widely used chemo-preventive reagent for BC. TAM, which is known as an estrogen receptor α antagonist, is categorized under the selective estrogen receptor modulator (SERM) (Ahmed et al., 2021; Clusan et al., 2023). The major human estrogen, which is 17β-estradiol, binds to estrogen receptor α and closes the hydrophobic pocket via the helix-12 domain. Estrogen receptor α translocates to the nucleus, where it activates the estrogen response element, promoting the transcription of estrogen-dependent genes. TAM is converted into 4-hydroxytamoxifen (4OH-TAM), which binds to estrogen receptor α. Unlike 17β-estradiol, this causes a distinct conformational shift and does not close the hydrophobic pocket with helix-12. Consequently, 4OH-TAM inhibits the activation of estrogen receptor-α through its triphenylethylene backbone structure (Bekele et al., 2016). Besides estrogen receptor-positive patients' TAM may be an additional option for treating estrogen receptor-negative tumors. Initial findings claimed that TAM caused estrogen receptor-negative tumors to undergo apoptosis by elevating the oxidative state of the cells, blocking Protein Kinase C (PKC), and ultimately preventing DNA synthesis and proliferation in malignant gliomas (Radin and Patel, 2016). Various studies have put forward the anti-tumor effects of TAM such

as inhibition of tumor growth and invasion capacities, leading to apoptosis and autophagy (Ahmed et al., 2021; Shagufta, 2018; Wu et al., 2016).

TAM has been the sole therapy approach for advanced BC for over 20 years. For premenopausal and postmenopausal women, 5 years of TAM therapy is applied and seen as the preferred treatment. Although TAM has excellent clinical results, most patients with metastases and around 40% of individuals on adjuvant TAM relapse (Barazetti et al., 2021; Howell and Howell, 2023). Understanding the mechanisms of TAM resistance is critical to creating effective countermeasures against relapse. TAM resistance has been linked to a variety of pathways. One of them is the loss of ER expression. Activation of oncogenic signaling cascades for instance, PI3K/Akt/mTOR resulted in the overexpression of the receptor tyrosine kinases (RTKs) which seems to be one of the other TAM resistance mechanisms. Moreover, some transcription factors, cell cycle regulators, and protective autophagy have critical roles in resistance mechanisms (Ahmed et al., 2021; Barazetti et al., 2021; Yao et al., 2020).

1.3. EPIBRASSINOLIDE

The diversity of the chemical structure of the plants has great biological potential, at this moment approximately 60% of FDA-approved drugs for cancer have a natural origin like taxanes, vincristine, irinotecan, etc. However, up to the present, few studies have been conducted on the potential of natural plant hormones in preventing cancer (Steigerová et al., 2010). In this context, brassinosteroids (BRs) which are polyhydroxysteroid phytohormones have been investigated due to their highest bioactivity and structural similarity to animal steroid hormones. The BRs play a crucial role in various physiological functions of plants and take a role in the developmental processes of plants either at the organ level or at the cellular level. They take a role in the hormonal balance regulation, synthesis of nucleic acid and proteins, regulation of enzyme activity, growth, and development, etc. BRs have a dynamic role in response to stress conditions. Until recently, 70 different kinds of BRs have been analyzed in various plants (Kaur Kohli et al., 2020). Based on the highest bioactivity and commercial availability the 24-epibrassinolide (EBR) and 28-homobrassinolide (28-

HomoBL) are the most investigated BR compounds (Kvasnica et al., 2019). BRs were initially thought to only affect hormones like NHR inhibitors due to their resemblance to steroid-like composition. However, when the nuclear hormone receptor (NHR) and EBR interaction was investigated, it was revealed that it caused cell death both in NHR-expressing and non-NHR-expressing cancer cells (Malíková et al., 2008; Steigerová et al., 2010, 2012). Malikova et al., study was conducted on hormone-sensitive/insensitive breast (MCF-7/MDA-MB-468) and prostate (LNCAP/DU-145) cell lines. It was put forward those cell inhibitory responses of EBR through the cell cycle arrest at the G1 phase for MCF-7, MDA-MB-468, and LNCAP cell lines, whereas G2 arrest in DU-145, and triggering apoptosis (Malíková et al., 2008). Our earlier investigation also indicates that EBR induced apoptosis in prostate cancer cell lines which are LNCAP and DU-145 in a caspase-dependent manner by changing the expression of the BCL-2 family members (Obakan et al., 2014a). Moreover, our previous findings revealed that after EBR treatment in mouse embryonic fibroblast cells (MEF), there was no change in cell viability (Adacan, Obakan-Yerlikaya, et 2020a). This suggests that natural BRs generate distinct responses in cancer and normal cells, indicating a significant therapeutic potential due to their selective cytotoxic effects on cancer cell lines rather than untransformed human fibroblasts (Huskova et al., 2020).

The significant therapeutic potential of the BRs has been revealed in many cancer models in recent studies. Steigerova et al. studied the antiproliferative mechanism of EBR and 28-homocastasterone (28-homoCS) in breast and prostate cancer cell lines however the main mechanism behind their activities is not completely understood (Steigerová et al., 2010). Some investigations demonstrated that EBR triggers the production of reactive oxygen species (ROS). This production of ROS influences polyamine metabolism resulting in mitochondria-mediated apoptosis through the PI3K/MAPK pathway (Coskun et al., 2015). Furthermore, the antiangiogenic properties of BRs also were put forward in studies. Human umbilical vein endothelial cells (HUVEC) and human microvascular endothelial cells (HMEC-1) were utilized to test the antiangiogenic properties of BRs and their derivatives. It was found that EBR and 28-HomoCS significantly reduced cell adhesion, which affected the antiproliferative potential of the cells. They also inhibited the migration of HUVEC

cells and HMEC-1 cell proliferation in a dose-dependent manner (Kaur Kohli et al., 2020). These studies put forward the diverse action mechanisms of BRs such as anticancer, antiproliferative, anti-angiogenesis, antiviral, and so on (Huskova et al., 2020).

Utilizing the stable isotope labeling by amino acids in cell culture techniques (SILAC), diverse cellular functions of EBR and novel targets of EBR were identified firstly in the Obakan et. al 2015 study (Obakan et al., 2015). In this way, the alterations profile of 160 protein expressions in a various cellular function was analyzed between EBR-treated and untreated control samples. For instance, in this investigation, dramatic downregulation of calreticulin (CALR) which is the unfolded protein response (UPR) chaperone was detected after 12 h EBR exposure, also other UPR-related proteins were affected after exposure to EBR. Thus, EBR has been demonstrated to have an endoplasmic reticulum inducer effect in prostate and colon cancer cell lines (Obakan et al., 2015). Moreover, EBR causes the imbalance of the Ca^{+2} homeostasis leading to endoplasmic reticulum stress-mediated apoptosis in colon cancer cells SW480 and DLD-1 (Obakan-Yerlikaya et al., 2017). Furthermore, EBR induced autophagy Atg5 independent manner on the account of ER stress via acting on CALR in MEF cells (Adacan, Obakan-Yerlikaya, et al., 2020a). Also, activation of autophagy in polyamine metabolism via EBR is put forward in colon cancer cells in SW480 and DLD-1 (Adacan and Obakan Yerlikaya, 2020b). Further step the induction of autophagy with EBR was detected in the SCID mouse xenograft model in this way impaired the progression of colon cancer (Obakan Yerlikaya et al., 2023).

EBR will be a promising anti-cancer agent for preventing cancer progression through mediating cell death mechanisms and its effectiveness will be tested in different types of tumors. Especially considering these findings the novel BR drugs and nanocarriers for these drugs have been improved to prevent the progression of cancer. (Banerjee et al., 2019; Zhou et al., 2022).

1.4. ENDOPLASMIC RETICULUM STRESS AND UNFOLDED PROTEIN RESPONSE IN BREAST CANCER

The endoplasmic reticulum (ER), one of the largest organelles, is made up of tubular and reticular structures that extend through the cell and connect to other organelles for maintaining physiological conditions in a normal stage in eukaryotic cells (Huang et al., 2023). This multifunctional organelle takes a role in various functions involving calcium storage and signaling, lipid synthesis, metabolism, synthesis and transport of membrane proteins, cytoplasmic proteins, and secretory proteins. According to functional and physical characteristics, two types of ER are categorized: rough and smooth. The smooth ER (SER) which does not contain ribosomes plays a role in the production of hormones and lipids. While the rough ER (RER) which contains ribosomes is crucial for the synthesis, folding, and modifying post-translational manner, quality checks also transport at least one-third of total proteins in cells (Bonsignore et al., 2023). The primary role of the ER is to effectively regulate quality so that only correctly folded proteins may get to their intended location. The array of enzymes located in ER harboring specific chaperons, foldases, oxidoreductases, and glycosylating enzymes regulate the maturation process of proteins starting from nascent polypeptides form to properly folded and modified state (Oakes, 2020). The specific ER-resident chaperons are categorized into three subgroups. One of them is molecular chaperone-binding immunoglobulin (BiP; also known as 78kDa glucose regulatory protein (GRP78)) and GRP94 which also take the role in assembling also folding unspecified proteins. The other ones are CALR, calnexin (CANX), and lectins facilitate the maturation of the glycoproteins. The last one is the Heat shock protein 47 (Hsp47) plays a role, particularly in collagen. Moreover, other functional classes of enzymes known as protein disulfide isomerases (PDIs) facilitate the synthesis and/or dissociation of disulfide bonds. Furthermore, the Ca^{+2} trafficking in and out of ER is known to control a wide range of cellular processes and signal transduction pathways. The Ca^{+2} binding chaperons, of which calreticulin is one of the prominent examples, control proper protein folding of the newly synthesized proteins and other quality control pathways in the ER. As a result, the fluctuations of the Ca^{+2} levels are also critical to the folding capacity of the ER (Sano and Reed, 2013). Under a normal state,

the elimination of misfolded or damaged proteins is mediated via the ER-associated protein degradation (ERAD) mechanism to protect the cells (Sisinni et al., 2019).

Although the functions of ER are tightly regulated, the disruption of protein folding capacity or calcium homeostasis in ER due to various external events and cell-intrinsic stimuli provokes ER stress (Chen and Cubillos-Ruiz., 2021; Hetz et al., 2020). These stress stimuli harbor decreasing oxygen levels which takes a role in the formation of disulfide bonds to keep the conformation of protein stable, lacking nutrients (specifically glucose deficiency leads to disturbance in protein glycosylation), rapid cell proliferation, perturbation in redox homeostasis, decreased calcium ions levels and accumulation of misfolded or unfolded proteins in the ER lumen (Rozpedek et al., 2016). In response to ER stress, unfolded protein response (UPR) which is an adaptive mechanism of ER stress is triggered to cope with stress conditions (Chen and Cubillos-Ruiz, 2021; Hetz et al., 2020). Activation of UPR contributes to the restoration of homeostasis of proteins (proteostasis) in ER by enhancing protein folding capacity, decreasing protein overload, and raising the degradation of misfolded protein through reprogramming gene expression. In mammals, the basic UPR signaling pathway is initiated via three key ER transmembrane proteins which act as sensors of an ER stress including inositol requiring protein-1α (IRE1α), activating transcription factor 6 (ATF-6) and protein kinase RNA-like ER kinase (PERK). These sensors consist of three domains. One of them is a luminal domain which senses the unfolded protein peptides and misfolded proteins in the ER lumen. The transmembrane and cytoplasmic domains are the other ER stress sensor domains that coordinate translation or transcription by transmitting signals through the nucleus (Chen and Cubillos-Ruiz, 2021; Hetz et al., 2020; W. Huang et al., 2023). During non-stress conditions, BiP binds to these ER stress sensors (IRE1α, PERK, and ATF-6) thereby keeping them in an inactive state by blocking the UPR signal. Under the ER stress conditions, BiP demonstrates a higher tendency for binding of misfolded proteins or unfolded proteins, by this way dissociate from these sensors to be activated via autophosphorylation, homodimerization, and cleavage process, resulting in induction UPR (Huang et al., 2023).

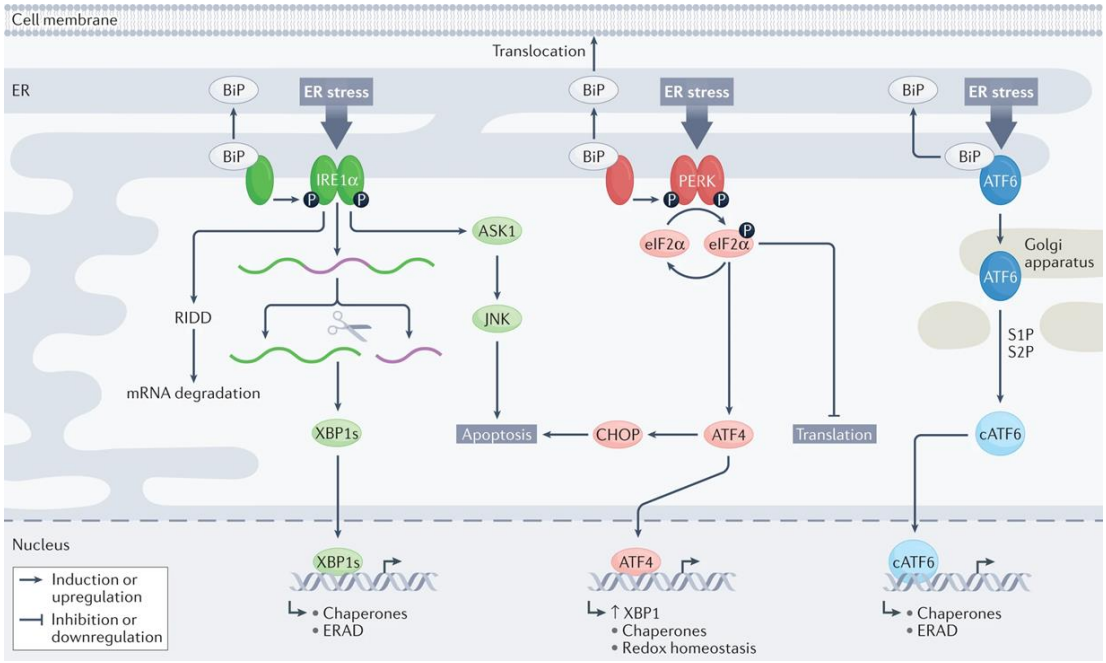

Figure 2. Unfolded protein response mechanisms (de la Calle et al., 2022).

1.4.1. Endoplasmic Reticulum Stress Signaling Pathways

The most evolutionary conserved arm of the UPR, also the first characterized ER stress sensor is IRE1 – X box binding protein 1 (XBP1) (Hetz et al., 2020; W. Huang et al., 2023). There are two isoforms of IRE1- X binding protein which are IRE1α and IRE1β. The *ERN1* gene encodes IRE1α. Two enzymatic activities: serine/threonine kinase and endonuclease are detected in the cytoplasmic domain of IRE1α. When the accumulation of misfolded or unfolded proteins, they either connect directly to the luminal domain of IRE1α or bind to BiP promoting dimerization of IRE1α and activation of its kinase activity by autophosphorylation and endonuclease activity. The active state of IRE1α leads to splice intron from X-box binding protein 1 to obtain functionally active protein XBP1. Afterward, XBP1 translocates to the nucleus where it provides transcription of UPR targeting genes in the nucleus also ER-related protein degradation components (ERAD) via promoting transcription of genes (Chen and Cubillos-Ruiz, 2021; Huang et al., 2023). The activated IRE1 RNAse domain also facilitates the degradation of mRNAs localized in ER through a process termed regulated IRE1-dependent decay (RIDD). As a result of this process, cellular metabolism, inflammation, protein folding load, and inflammasome signaling

pathways are all regulated, which reduces ER stress and encourages cell recovery to homeostasis. Under chronic ER stress, the cytoplasmic domain of IRE1α also functions as a scaffold to attract adaptor proteins, such as members of the tumor necrosis factor receptor-associated (TRAF) family, to trigger inflammatory responses. IRE1α recruits TRAF2 in cases of severe and prolonged endoplasmic stress. This also triggers cell death and subsequent activation of c-Jun N-terminal kinase (JNK). As an alternative, upon activating the RIDD pathway, the cascade of caspase 8 or caspase 2 triggers apoptosis (Qing et al., 2023).

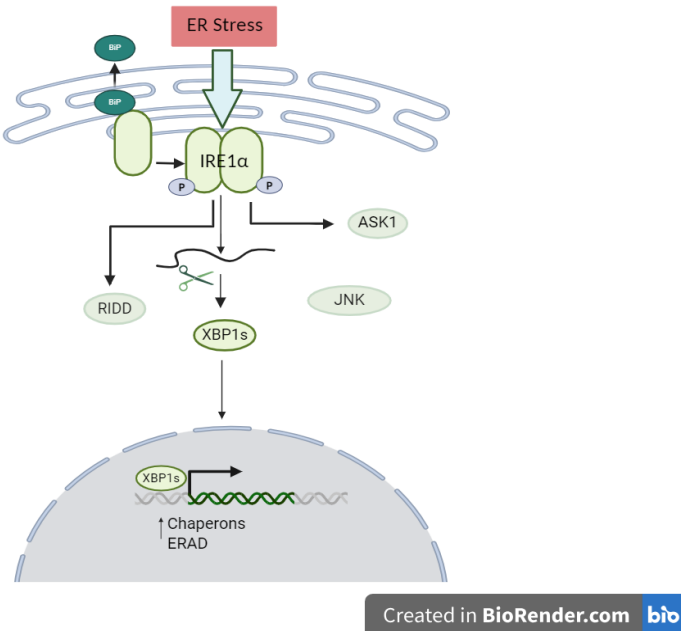

Figure 3. IRE1α pathway.

Like IRE1α, PERK is one type of ER-resident type-1 transmembrane protein. PERK is also known as serine-threonine kinase, the best substrate for eukaryotic translation initiation factor 2α (eIF2α). While the N-terminal region of PERK is in the ER lumen and associated with BiP, the C-terminal region is linked with the cytoplasmic kinase domain. In response to ER stress conditions, BiP is released from sensors and binds to misfolded proteins with higher affinity, thereby activating PERK via homodimerization and autophosphorylation. Activated PERK phosphorylates both itself and eIF2α. The eIF2α diminishes the mRNA translation by interfering with 5'-cap assembly, thus reducing protein synthesis so that ER stress load (Huang et al., 2023). Although the phosphorylation of eıF2α resulted in reduced mRNA translation the selective mRNAs such as triggering the activation of transcription factor 4 (ATF4)

are preferentially translated. ATF4 serves as a crucial transcriptional regulator that targets genes involved in protein folding, amino acid metabolism, autophagy, and apoptosis, triggering the cell fate response. A double-edged sword effect is observed in ATF4 under ER stress. At one point, ATF4 induces proapoptotic factor C/EBP homologous protein (CHOP; also referred to as GADD153) and GADD34 which provide mRNA restoration thanks to the dephosphorylation of eIF2α via targeting protein phosphatase 1 (PP1). This loop ends with the restoration of the synthesis of protein and termination of stress response signaling. On the other hand, if severe ER stress continues, ATF4 activates caspase 8 expression in response to the activation of GADD34 and CHOP, hence inducing apoptosis (Qing et al., 2023). Moreover, it is worth noting that CHOP stimulates the expression of ER oxidoreduction 1α *(ERO1α)* genes. Under physiological conditions, these enzymes are exclusively connected to the ER membrane and take a critical role in disulfide bond formation for recently translated proteins. Furthermore, the *ERO1α* is a needed oxygen molecule for the oxidation of PDI that catalyzes disulfide bond formation. As a result, it can be hypothesized that under conditions of prolonged ER stress, *ERO1* produces H_2O_2 and promotes a hyper oxidizing environment that induces apoptosis (Rozpedek et al., 2016).

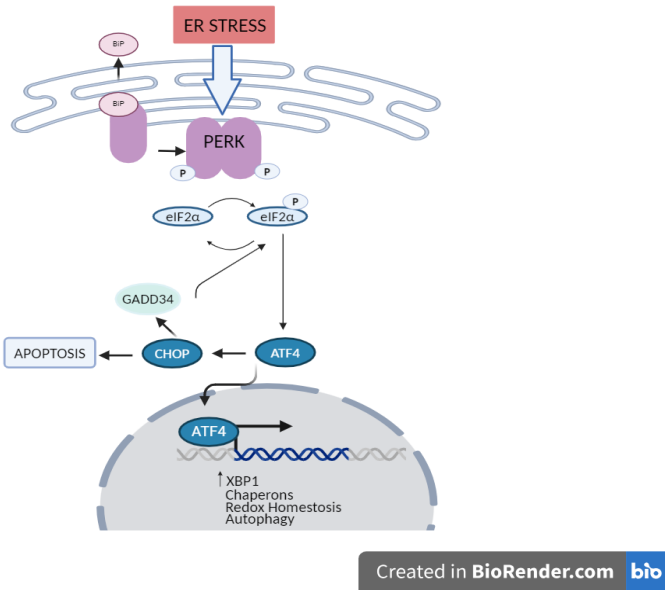

Figure 4. PERK signaling pathway.

Activating transcription factor 6 (ATF-6) is the third pathway in UPR signaling. ATF6 is a member of ER-resident type II transmembrane protein, consisting of cytoplasmic

N-terminal Zip transcription factor domain and a major ER luminal domain. ATF-6 has two types that differ in transcriptional effects ATF-6α and ATF-6β. The ATF-6α transcriptional activation is highly potent compared to the ATF-6β (Huang et al., 2023). Under prolonged ER stress, unlike the IRE1α and PERK, the luminal domain of ATF-6α is translocated through the Golgi apparatus via direct separation of BiP. In the Golgi, ATF-6α is cleaved via two proteases, S1P and S2P (site-1 and site-2 proteases, also known as MBTPS1 and MBTPS2) resulting in releasing basic leucine zipper (bZIP) fragment harboring N- terminal fraction (ATF6p50). Following this type of regulated intramembrane proteolysis (RIP), ATF6p50 transports to the nucleus. It mediates the ER stress response elements that take a role in protein folding processes such as chaperones, foldases, etc, also in the ERAD complex (Chen and Cubillos-Ruiz, 2021; Hillary et al., 2018; Qing et al., 2023). For instance, the induction of primary (unspliced) *XBP1* transcript and BiP via ATF6α contributes to proteostasis and enhancement of the regulatory output of the IRE1α arm. Moreover, additional targets identified in ATF6's regulatory repertoire are protein disulfide isomerase-associated 6 (PDIA6) and ER degradation enhancing α-mannosidase-like protein 1 (EDEM1) which facilitate the degradation of misfolded proteins (Figure 5) (Hillary et al., 2018).

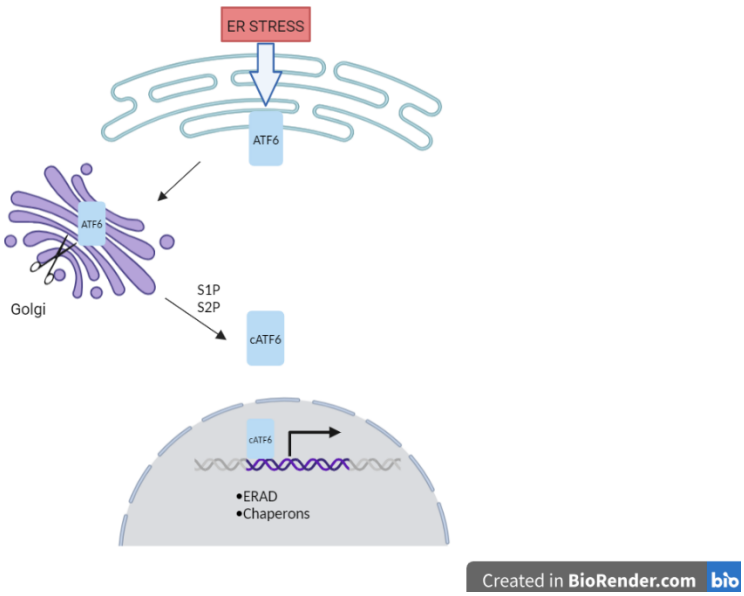

Figure 5. ATF6 signaling pathway.

1.4.2. Endoplasmic Reticulum Stress Response in Breast Cancer Cells

A tumor occurs when abnormal cell accumulation occurs in any body part. This excessive proliferation of tumor cells and insufficient angiogenesis can trigger the perturbation of ER stress homeostasis. The hypoxic conditions also cause the activation of ER stress. In addition, genetic instability, and somatic mutations in secretory pathway proteins in tumor cells can affect their folding and result in ER stress (Y. Lin et al., 2019; Oakes, 2020). Under pathological settings, ER stress is linked to a variety of metabolic illnesses, including cardiovascular disease, diabetes, and cancer. The relevant role of ER stress response and cancer have been investigated in the past 15 years (Chen and Cubillos-Ruiz, 2021). Several studies put forward that activation of ER stress also UPR under stressful conditions is one of the survival strategies in cancer cells (Fu et al., 2021). Initially, the UPR response generated by mild ER stress was assumed to be a self-regulating mechanism for protecting cells from permanent damage (Xu et al., 2022). Both autophagy and UPR signaling pathways are considered cell self-protection strategies; nevertheless, when cellular stress persists or intensifies, these pathways may trigger cell death. The activation of ER stress is a complex molecular process comprising signaling pathways involved in cellular autophagy, apoptosis, oxidative stress, and inflammatory responses (Chen and Cubillos-Ruiz, 2021). Even while there is still much to learn, new research has begun to shed light on the connection between cancer and dysregulated UPR. Various lines of evidence have demonstrated that persistent activation of the UPR is linked to treatment resistance and recurrence of disease. In such a scenario, the molecular mechanisms driving prolonged activation of the UPR are considered new potential targets for restoring drug sensitivity in breast tumors (Sisinni et al., 2019).

ER stress in breast tumors results from hypoxia and nutrient deprivation caused by cytotoxic and endocrine therapeutic interventions. The progression of the ER stress is variable in the three UPR arms in different subtypes of breast tumors. In BC cells, the overexpression of BiP protein has been analyzed both in the estrogen-positive and anti-estrogen-resistant BC cells. Moreover, a study demonstrated that elevated estrogen levels can trigger the expression of BiP and XBP1. Moreover, IRE1α-XBP1 and PERK signaling plays a key role in the progression of the ERα positive breast tumor. Moreover, upregulation of these UPR components might correlate with contributing

resistance to chemotherapeutic drugs and anti-estrogenic drugs such as faslodex and TAM (Bonsignore et al., 2023). Within the scope of this information, the UPR response elements have become targeted mechanisms for therapeutic purposes nowadays. Several small molecule inhibitors that target the UPR pathway have been found to interfere with the development of BC. For instance, MKC8866, one type of IRE1α inhibitor, has been used in IRE1α activity in Phase 1 clinical trials for BCs. Also, GSK260414 has been found to interfere with PERK activity and observed to prevent metastasis in TNBC, therefore it has entered the Phase 1 clinical trial of BC (Patra et al., 2023).

In conclusion, the ER is a dynamic organelle that coordinates signaling pathways to promote cell adaptation, survival, and cellular resistance. Although ER stress has been linked to several disorders, there are still many unsolved concerns about its role in health and disease. Several disorders have been linked to ER stress-mediated cell death either apoptosis or autophagy which makes this mechanism a desirable target for the therapy. Thus, understanding the process behind ER stress responses could help shape future treatment methods for cancer therapy (Sano and Reed, 2013).

1.5. AUTOPHAGY

Autophagy is an evolutionarily highly conserved catabolic process from yeast to mammals. Firstly, the “autophagy” term was used by De Duve to describe self-destruction at the cellular level in the 1960s. Under normal physiological conditions, autophagy takes a role in maintaining cellular homeostasis via recycling of cellular content and elimination of misfolded protein aggregates or dysfunctional organelles. In this manner, this process is essential for maintaining a balance of the intracellular environment and protecting the cells from death. In the case of cells facing intrinsic and extrinsic stress conditions which comprise such as nutrient starvation, energy deprivation, ER stress, hypoxia, ROS, growth factor deficiency, tumor microenvironment, etc. Autophagy is triggered to recover metabolic requirements to increase cell survival (Kocaturk et al., 2019). Besides normal physiological conditions, autophagy is also detected in the pathological conditions of various diseases such as

tumors, infection, neurodegenerative disorders, aging, and diabetes (Chavez-Dominguez et al., 2020).

1.5.1. Types of Autophagy

Autophagy is also known as an intracellular lysosome-dependent pathway. In research done so far, autophagy has been categorized into four major classes based on the delivery strategies of intracellular components (cargo) to lysosomes for degradation; macro-autophagy (referred to as autophagy here), micro-autophagy, and chaperon-mediated autophagy (CMA) and selective autophagy (Wu and Sharma, 2023).

The term "microautophagy" describes a process in which the lysosome membrane is deformed to allow cytoplasmic contents to invaginate. Through membrane protrusion and invagination, lysosomes and late endosomes immediately take up autophagic payloads during microautophagy. Then, the autophagic cargoes are broken down in the endolysosomal lumen (Wang et al., 2023). Microautophagy is observed in cases of nutrient deficiency. Both nitrogen deprivation and rapamycin promote micro autophagy of soluble components, even though, pexophagic vacuole invagination is dependent on autophagy related gene (Atg) proteins. A vacuolar transport chaperone (VTC) complex is required for microautophagy. This complex is in the ER, vacuoles, and the cell periphery. This process does not cause membrane loss caused by classical autophagy (Uttenweiler et al., 2007).

CMA is one of the specific protein degradation processes. The individual cargo protein is directly translocated through the lysosomal membrane for degradation via CMA. The cargo protein which carries the KFERQ motif for the recognition binds to heat shock protein cognate 71 (HSC70) which is a key chaperone for CMA. Once this connection occurs the HSC70/cargo complex is delivered to the lysosome surface and interacts with the lysosome-associated membrane protein type 2A (LAMP2A). The translocation complex is then formed by assembling LAMP2A monomers into multimeric complexes. Once this structure is created appropriately, translocation of proteins across the lysosomal membrane occurs, at the same time lysosomal-HSC70 draws into the lumen to prevent it from out of the membrane. During this process, stability of the LMP2A is provided via HSC90 which takes a role in covering

lysosomal protease binding regions preventing degradation during this transition. Lastly, the protein degrades within the lysosome later, and the translocation complex disassembles (Auzmendi-Iriarte and Matheu, 2021).

Selective autophagy is the name that suggests select targets specifically for degradation at a specific cellular organelle. According to their targets, several pathways were identified in studies harboring mitophagy, ER-phagy, xenophagy, lysophagy, pexophagy, lipophagy, ribophagy, aggrephagy, etc. Many selective autophagy receptors (SARs) have been identified against specific cargo such as NBR1, p62, TOLLIP, NIX, NCOA4, and Cue5 (Alvarez-Meythaler et al., 2020). The recognition of cargo can be achieved via cargo ubiquitylation which differs in non-selective autophagy.

The term autophagy refers to macroautophagy in literature according to general acceptance. Nowadays various studies have been focused on understanding the molecular mechanism of macro-autophagy. The initiation of autophagy occurs with the formation of autophagosomes which engulf cytosolic components either cytoplasmic proteins or aggregates or damaged organelles, later followed by lysosomal fusion where the proteases disrupt the cargo material. The process of autophagy is mediated by sequential five steps: initiation, membrane nucleation, phagophore formation, phagophore elongation (autophagosome maturation), fusion, and degradation of cargo (Figure 6).

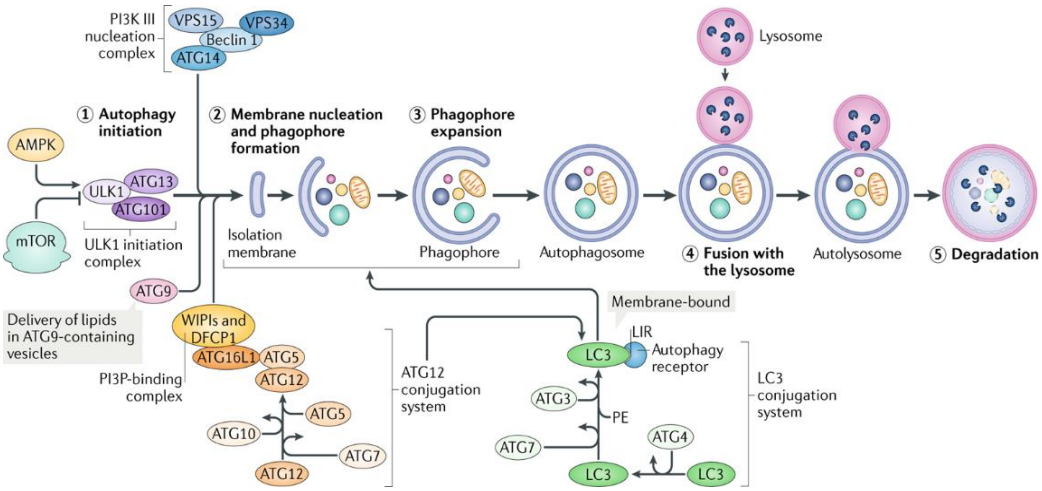

Figure 6. Mechanism of autophagy (Hansen et al., 2018) .

The autophagy mechanism is highly correlated with several protein complexes and the two ubiquitin-conjugation-like systems. The Atgs were characterized as key players in every step of the autophagic pathway because of initial studies of yeast in the 1990s (Kocaturk et al., 2019). Autophagy is activated and progresses because of intrinsic and environmental stressful situations. At the same time, the occurrence of autophagy is controlled via an assortment of signaling pathways. The execution of autophagy relies on master regulators of cellular energy metabolism which are mammalian targets of rapamycin (mTOR) and AMP-activated protein kinase (AMPK). The mTOR consists of two different signaling pathways referred to as mTORCI and mTORC2, however only mTORC1 is directly correlated with the autophagic process (Cocco et al., 2020). Under nutrient-rich conditions, the mTORC1 negatively regulates autophagy by suppressing the formation of the ULK complex that constructs ULK1/2, ATG13, and FIP_{200} (ULK interacting protein). Whereas the AMPK which is a serine protein kinase positively regulates autophagy in response to nutrition starvation via two distinct mechanisms (1) suppression of the mTORC1 complexes, (2) activation of the ULK complex through class III phosphatidylinositol 3- kinase (PI3K) bypassing mTOR (Cocco et al., 2020). Moreover, two major complexes of protein take a role in the initiation step of autophagy. The first complex is the ULK1/2 and FIP_{200}. The PI3K complex is a second major effector protein complex for autophagy consisting of VSP34, VSP15, Beclin-1, Atg14, and UV radiation resistance-associated gene (UVRAG) proteins. This complex is responsible for membrane nucleation and phagophore formation which is a cup-shaped structure. One of the main proteins for the nucleation process is Beclin-1 which binds with VSP34. The VSP34 takes a role in the production of the phosphatidylinositol 3-phosphate (PI3P) which is essential for the phagophore nucleation. Moreover, Beclin1 interacts with various other mediators like UVRAG, Atg14L, Beclin-1 regulated autophagy protein 1 (AMBRA1), and vacuole membrane protein 1 (VMP1) to mediate the membrane formation differently. Accumulation of the PI3P promotes additional binding of Atgs to expand phagophore formation (Kocaturk et al., 2019). In the maturation stage of phagophore two-ubiquitin-like protein (UBL) conjugation systems are detected. The first system comprises of conjugation of Atg12-Atg5 UBL and later conjugates with Atg16L1 to form the Atg12-Atg5-Atg16L1 complex contributing to enlarging of phagophore for

forming a large multimeric complex. This complex also serves as a function of the E3-like kinase to the second conjugation system. This conjugation process, which involves the formation of autophagosomes, occurs in a stepwise manner depending on the E1-like enzyme Atg7. Atg7 stimulates the activation of the Atg8. With the help of the E3-like Atg12-Atg5 conjugate, the conjugation of microtubule-associated light chain B (LC3B) protein which is the mammalian homolog of yeast Atg8 is linked to phosphatidylethanolamine (PE) by an amide bond. Then cleavage of the LC3B precursor protein is mediated with Atg4B protease for modifying LC3B to LC3B-I (Finnegan et al., 2022; T. Huang et al., 2018; J. Zhang et al., 2023). Then the LC3B-I subsequently transported to Atg3 and linked with PE to construct the LC3B-II-PE complex, referred to as a marker of autophagosome formation. When autophagosome formation is completed LC3B-I dissociates from PE via the outer membrane Atg4 and returns to the cytosol. Whereas the LC3B-II on the membrane's inner side remains attached to the membrane and degrades the substrates in the cargo. Gamma-aminobutyric acid receptor-associated protein (GABARAP), an LC3-related protein, has a comparable role in autophagosomal expansion, including autophagosome formation and substrate sequestration into double-membrane vesicles. Atg9, a transmembrane protein, also contributes to the phagophore expansion by supplying lipid bilayers to the nascent phagophore, allowing for additional elongation of the autophagosome before it is completed (Yun et al., 2020). After the autophagosome membrane's completion, intracellular cargo is engulfed by autophagic vesicles to deliver lysosomes for degradation by hydrolyses into lysosomes. The fusion of the autophagosome with the lysosome is referred to as autophagolysosome (AL). Several autophagy receptors/adaptor proteins including sequestosome 1 (SQSTM), nuclear dot protein 52 kDa (NDP52), a neighbor of BRCA1 (NBR1), and autophagy-linked FYVE protein (ALFY) have been responsible for the selective recognition also the recruitment of autophagosomal cargoes for the targeted autophagic response. SQSTM1 which is known as p62 is the best-characterized autophagy receptor up to date (Huang et al., 2018; Yun et al., 2020). In addition, multiple proteins such as soluble N-ethylmaleimide sensitive factor attachment protein receptor (SNARE) proteins including syntaxin 17 (STX17), synaptosomal-associated protein 29 (SNAP29), and vesicle-associated membrane protein 8 (VAMP8), Rab GTPases

proteins especially Rab7, lysosomal integrin protein (LAMP2), and membrane tethering proteins play critical roles in this fusion process. Thereafter fusion process degradation of products which includes amino acids, sugars, nucleotides, and fatty acids, where in content onto autophagolysosome by the lysosomal proteases are returned to cytosol in the reason for the reuse in the metabolic process.

1.5.3. Dual Role of Autophagy for Cancer

The first direct correlation between autophagy and cancer was identified by Beth Levin's groups in 1999. They put forward deletions of the monoallelic *BECN1* (*Atg6* gene in yeast) gene in human cells might promote tumorigenesis both *in vitro* and *in vivo* manner. In this context, initial studies have shown a tumor-suppressive role of autophagy. Indeed, autophagy has a double-edged sword effect in cancer progression in a context-dependent manner. At the early stage of malignant formation, autophagy is responsible for preventing tumorigenesis. Once tumorigenesis has occurred, autophagy has been indicated to take a role in encouraging tumor growth. The onco-suppressive role of autophagy may exert many mechanisms comprising; degradation of oncogenic proteins, maintenance of cell metabolism, preservation of genomic stability, and so on (Rybstein et al., 2018). Contrary to the tumor-suppressive mechanism of autophagy, the tumor-promoting functions of autophagy have been detected in several of the hallmarks of cancer. One of them is that autophagy contributes to cell proliferation by supplying nutrients and energy requirements for cancer cells under stress conditions (Chavez-Dominguez et al., 2020; Rybstein et al., 2018). For instance, environmental stress contributes to the inactivation of PI3K and AKT/mTOR pathways to activate autophagy for sustaining survival mechanisms in breast cells. Moreover, autophagy promotes the contribution of the stemness phenotype to induce the expression of the stem cell markers and signaling pathways. In a murine model, stimulation of stemness of two stem-like BC cell lines has occurred via autophagy activation of the EGFR also TGFβ/Smad paths (Wu and Sharma, 2023). Furthermore, autophagy provides tumor dormancy under unfavorable conditions. This dormancy is highly correlated with the recurrence of the disease, metastasis, and therapy resistance later. The growth and extravasation of the dormant cells are

mediated via autophagy within the tumor microenvironment. Dormant BC models both *in vivo* and in preclinical human models have been put forward that autophagy inhibition in such a model resulted in decreasing cell viability also the burden of metastasis (Wu and Sharma, 2023). In addition, autophagy provides the resistance of cancer cells to therapy. For example, autophagy promotes resistance to treatment for TAM in BC cell lines. According to Samaddar et al. and Qadir et al., TAM/4-OHT coupled with autophagy suppression (3-Methyladenine (3-MA), bafilomycin A1, siRNAs targeting Atg7, Atg5, and Beclin1) restored the sensitivity of TAM/4-OHT in resistant MCF-7 cells (Mele et al., 2020). This autophagy-related drug resistance mechanism has been seen as a barrier to cancer therapy because of that the role of autophagy in the resistance mechanism is not fully defined. Hence, suppressing autophagy can be exerted as an alternative strategy (or novel therapeutic target) to re-sensitize cancer cells to therapy.

1.5.4. Targeting Autophagy in Breast Cancer

The complex relationship between autophagy-related genes and BC has been put forward in various aspects because of the paradoxical role of autophagy. Moreover, due to the variety of the expression profile of BC subtypes, different outcomes in response to autophagy have been identified. In the estrogen receptor-positive breast tumors, an autophagy-mediated drug resistance mechanism was observed against the endocrine therapy. In this case, the inhibition of autophagy provides the reverse of drug resistance through the promotion of apoptosis. For instance, the cytoprotective autophagy ensures the reverting of the Exemestane (aromatase inhibitor) resistance in BC models (Cocco et al., 2020). Moreover, low levels of autophagy have been detected in HER2+ tumors. The association between the deficiency of the Beclin 1 expression and the amplification of HER2 was observed in in vitro studies. For this reason, according to studies, the overexpression of the Beclin 1 gene hinders the progression of HER2+ tumors (Wu and Sharma, 2023). Furthermore, elevated levels of autophagy are the most detected in the TNBC subtype compared to other subtypes of BC cells. The higher levels of autophagy led to invasive properties of the TNBC tumors. Thus, targeting autophagy-related genes in TNBC tumors seems to be a potential target for therapeutic purposes. For instance, a study showed that the knockdown of the LC3 and

Beclin1 genes resulted in the inhibition of the autophagy process and prevent the proliferation of the cells migration of the cells also triggered apoptosis in MDA-MB-231 and BT-549 cells (Cocco et al., 2020). Moreover, the enrichment of Atg7 provides better prognostic outcomes for TNBC patients. Whereas the higher expression of the Atg7 leads to apoptosis in TNBC cells, the negative effect on the growth and progression of the TNBC cells was detected in the presence of the Atg7. In addition, silencing of the Atg7 in MCF-7 cell lines promotes the anticancer effects of docetaxel via increasing apoptotic efficiency based on a study (M. Li et al., 2019; Wu and Sharma, 2023). Consequently, modulation of autophagy as a therapeutic candidate can reduce the progression of the tumor and enhance the effectiveness of conventional therapy.

1.6. CROSSTALK BETWEEN ENDOPLASMIC RETICULUM STRESS, APOPTOSIS, AND AUTOPHAGY

Accumulation of unfolded or misfolded proteins in the ER lumen leads to the dysfunction of the ER resulting in ER stress. The ER stress triggers UPR which is known as an adaptive mechanism for the cells. It activates various complementary signaling mechanisms to cope with any protein folding alterations. The UPR-linked pathways provide the restoring homeostasis of the cell either blocking or enhancing cell death according to its capacity to get rid of stress conditions or not (Sisinni et al., 2019). The UPR coordinates the regulation of reciprocal integration of apoptosis and autophagy maintaining the maintenance of the cell homeostasis. Apoptosis refers to the programmed cell death that happens not only in response to cell injury or external stress but also throughout development and morphogenesis (Jan and Chaudhry, 2019). Autophagy is linked with both cell survival and cell death processes. A natural process of autophagy provides recycling of the damaged or old organelles as misfolded or unfolded proteins in the cells for cell survival. Like UPR, in a physiological condition, autophagy correlated with cell survival. The persistence of ER stress resulting from UPR initiates the autophagic process through multiple pathways resulting in apoptotic or autophagic cell death (Lin et al., 2019). Molecular crosstalk has been identified

between three UPR transducers with autophagy and apoptosis in several studies (Lin et al., 2019; Song et al., 2018).

1.6.1. Apoptosis and Unfolded Protein Response

Apoptosis is one of the cell death mechanisms and is categorized into two pathways: intrinsic apoptotic machinery and extrinsic apoptotic pathway. The pro-apoptotic proteins are exposed via stimulating apoptotic signals which change the mitochondrial inner membrane potential and end up with activation of the intrinsic apoptotic signaling mechanism. In the extrinsic apoptotic pathways referred to as death receptor (DR) mediated apoptosis which promotes the FAS-associated death domain (FADD) to create a death-inducing signaling complex (DISC).

During the intrinsic pathway of apoptosis, the correlation between ER and apoptosis is identified. Ca^{+2} is released through the cytosol from the ER lumen and enhances the caspase 12 activation. When caspase-12 is triggered, it enhances the activation of the downstream caspases harboring caspase-7 and caspase-9 ends up with the activation of caspase-3 ultimately apoptosis starts (Kara and Oztas, 2020). Moreover, the activation of the UPR sensors is highly detected with the triggering apoptotic machinery. The phosphorylation of elF2α via PERK triggers the ATF4 activation which in turn stimulates the expression of CHOP. CHOP enhances the expression of many pro-apoptotic BCL-2 family members while inhibiting the expression of the Bcl-2 gene. Then these genes activate caspase 3 and caspase 9 as a result in triggering apoptosis. Recent investigations have identified that specific BCL-2 members, well-characterized ones BAX and BAK can be in the ER. These precise proteins in the ER take a role in regulating calcium homeostasis and are disrupted under prolonged ER stress (Kara and Oztas, 2020; Scull and Tabas, 2011). Moreover, it is highlighted that PERK and ATF4 are mainly pro-survival pathways, but they can also enhance apoptosis by activating CHOP, the primary mediator of UPR-induced apoptosis.

During ER stress, the extrinsic apoptotic pathway is triggered via promoting activation of the JNK signaling cascade which is primarily linked with IRE1α paths. This signal operated via the TRAF2 and the apoptosis signal-regulating kinase 1 (ASK1) which form a complex IRE1α. The IRE1α-TRAF2-ASK1 pathway induces the downstream

of the stress kinases, JNK, and p38 MAPK. Whereas the activation of JNK triggers the activation of BH3-only protein Bim, p38 MAPK promotes and activates the CHOP which induces genes harboring Ero1α and DR5 associated with favor apoptosis (J.-X. Zhang et al., 2023). Furthermore, under severe ER stress, Bak and Bax are also activated directly via IRE1α induction (Kara and Oztas, 2020). The relationship between ER stress apoptosis has been pointed out in the literature to date.

1.6.2. Autophagy and Unfolded Protein Response

ER stress activates two protein degradation pathways: ERAD-mediated ubiquitin-proteasome degradation and autophagy-mediated lysosome degradation. In ERAD, unfolded protein is retranslated to the cytosol, where the proteasome ubiquitinates and degrades them. As a secondary response mechanism, autophagy is activated since the ER stress capacity exceeds the accumulation of misfolded/unfolded proteins. Even though many studies have demonstrated that ERAD is the primary cellular mechanism to get rid of unfolded proteins in the presence of ER stress, several studies have recognized that autophagy is strongly stimulated in the context of ER stress (Sano and Reed, 2013).

In the process of autophagy, each of the UPR transducers is involved in different stages of autophagy, from autophagy initiation to autophagosome formation. The PERK arm of the UPR is associated with the elongation also autophagosome formation process of autophagy (Song et al., 2018). Activation of PERK suppresses global protein translation by phosphorylating eIF2α, which in turn facilitates the selective translation of transcripts containing an alternative open reading frame, comprising ATF4, a crucial transducer. The ATF4 expression regulates one of the autophagy-related genes ATG12, moreover, CHOP regulates the expression of ATG5. These genes are involved in the elongation of the autophagosome (Lin et al., 2019; Sisinni et al., 2019; Song et al., 2018). Furthermore, the TAM treatment also triggered the autophagy process through the ATF-4-induced LAMP3 manner. Moreover, bortezomib treatment of BC leads to an increase in LC3B expression resulting in autophagy via an ATF4-dependent manner. In addition to chemotherapeutic drugs, radiotherapy induces PERK-dependent autophagy in BC (Bonsignore et al., 2023). The IRE1α branch of UPR

boosts autophagy through the activation of stress kinases J-N terminal kinases (JNK) pathway. The activation of JNK concludes with the phosphorylation of BCL-2 in the complex of BCL-2/Beclin1, ending up releasing Beclin1. The Beclin-1 enhances isolation membrane nucleation which is the first step of autophagy. In addition, the transcription factor of XBP-1 which is mediated via IRE1α also activates Beclin1 expression resulting in autophagy (Song et al., 2018). Moreover, the XBP-1 tends to recruit soluble LC3-1 to structures of membranes giving cause for autophagosome formation (Sisinni et al., 2019). Research on IRE1α, PERK, and ATF6 impairment in ER stress discovered that autophagy was reduced in the IRE1α signaling pathway but not in the PERK or ATF6 pathways. This implies that the IRE1α signaling pathway is highly correlated with ER stress-induced autophagy (Lin et al., 2019). Multiple studies revealed that ATF-6 is needed to induce autophagy with the help of the overexpression of death-associated kinase which plays a role in autophagosome formation via phosphorylation of Beclin1 (Oakes, 2020). Moreover, the ATF6 arm of UPR also regulates autophagy indirectly through the XBP-1 and CHOP (Hillary and FitzGerald, 2018). In conclusion, the crosstalk between ER stress and autophagy has been investigated through the distinct mechanism for discovering novel targets for therapeutic purposes.

1.7. DRUG RESISTANCE MECHANISM IN BREAST CANCER

Cancer is the disease with the highest mortality rate worldwide. To date, many treatment strategies have been developed to overcome cancer. However, tumor cells have been unaffected by various chemotherapeutic agents also other cancer-related drugs because of multidrug resistance (MDR). This MDR is classified as intrinsic and acquired resistance. Intrinsic resistance in other terms natural resistance is a crucial factor in the effectiveness of medications as it develops before the patient is exposed to them. Activating internal cellular defense mechanisms can reduce the therapeutic effect of a given medication. The widely known reasons for innate resistance in tumors are pre-existing genetic mutations, insensitive subpopulations, and internal defense mechanisms against environmental toxins (Mehdizadehtapeh and Obakan Yerlikaya, 2021). On the other hand, acquired resistance has arisen after the administration of

chemotherapeutic agents or other drugs. Acquired resistance may be promoted on account of activation of the proto-oncogene, expression changes of drug targets due to mutations also changes in the tumor microenvironment (TME) following treatment. To prevent tumor recurrence in the later stages of treatment, as acquired drug resistance progresses, the treatment plan must be redesigned according to acquired resistance. The MDR mechanism is a complex process since several pathways are associated with this process. The MDR mechanism is divided into seven parts. They include reducing drug absorption with the help of the solute carriers, elevating drug efflux via membrane transporters especially ATP-binding cassette transporters (ABC), altering the target of the drug, activation a detoxification system, preventing drug-inducing cell death by the blockage of the cell death mechanism signaling, changing in the microenvironment, and finally providing adaptation via some epigenetic regulation, according to Li et al (Li et al., 2017).

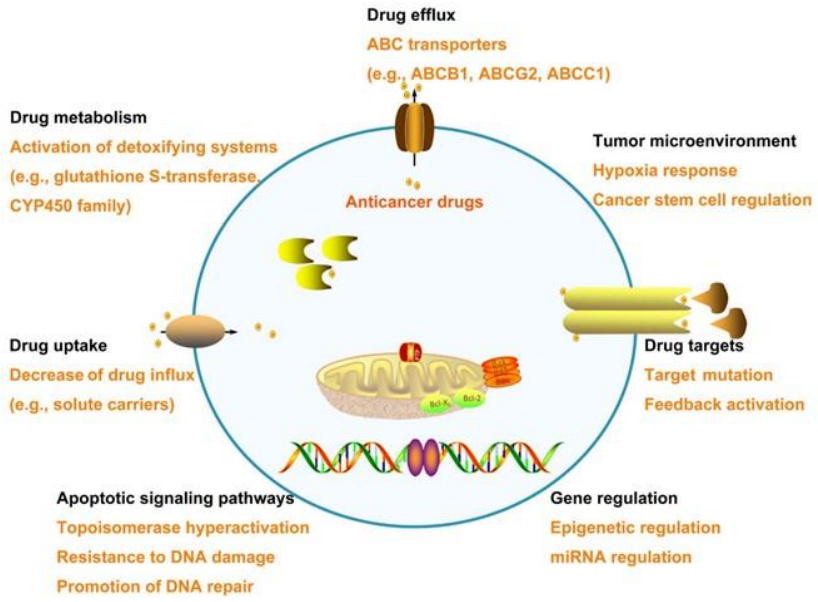

Figure 7. Multidrug resistance mechanisms (Li et al., 2017).

Both in the healthy cells and cancerous cells, the membrane transporters that contribute to the pharmacokinetic effect of the drugs are expressed and comprise nearly 49 genes categorized into 7 subfamilies from A to G (Kumar and Jaitak, 2019). P-glycoprotein (P-gp) also MDR1/ABCB1, multidrug resistance-associated protein 1 (MRP1/ABCC1), and BC resistance protein (BCRP/ABCG2) are only a few of the fifteen ABC transporter proteins that have been identified to far as drug efflux pumps

in MDR (İsaoğlu et al., 2020). In tumor cells, overexpression of these transporters is the main contributor to drug resistance against treatment strategies.

ER is one of the corresponding mechanisms having an impact on MDR. The association between ER stress and chemoresistance mechanism has been analyzed in various tumor types. Drugs that confer acquired resistance to ER stress can activate membrane transporter genes such as P-gp, MRP1, and BCRP. Therefore, it was stated that ER stress sensors may be inducers of MDR. According to investigations, BiP (GRP78), one of the ER stress pathway members, induces tumor MDR mainly in two ways. One of them, GRP78, can reduce ER stress and cell apoptosis resulting in enhancing the resistance of tumor cells to chemotherapy and radiotherapy. Another function of GRP78 is that it conveys signals to promote EMT and stemness of cancer cells when located on the cell surface, consequent with activation of MDR (Qing et al., 2023). For instance, in drug-resistant BC cells, the inhibition of BiP via siRNA enhances the cells undergoing apoptosis and elevates the sensitivity of the chemotherapy and modulates the anti-estrogen sensitivity. Considering studies related to GRP78 and MDR, BiP can be a novel therapeutic candidate for MDR in cancer cells. Moreover, the PERK pathway, which is the key signaling path of UPR, is closely related to drug resistance mechanisms. Studies in various tumor cells found that PERK activation increases P-gp expression, leading to drug resistance. Also, further studies have revealed that PERK and Nrf2 regulate the transcription of the MRP1 genes so that the PERK/Nrf2/MRP1 axis can be targeted to overcome resistance to chemotherapy. The IRE1α which is the other conserved arm of the UPR also linked with the MDR. The XBP1 takes a unique role in encouraging cell survival and MDR. Thereby, this close relationship contributes to the development of therapeutic approaches against MDR. For the treatment of ER-positive BC patients' TAM is used as one strategy, however almost half of these patients demonstrate resistance to chemotherapy. To overcome this situation molecular analysis was performed and the high expression of the XBP1 was detected in ER-positive BC patients. The inhibition of XBP1 via a splicing inhibitor known as STF-083010 reverses the drug sensitivity of the TAM-resistant cells and leads to apoptosis. ATF6 is the most enigmatic of the three UPR pathways, and the relationship between ATF6 and tumor MDR has not been widely investigated. The research potential of ATF6 is quite high based on the crucial

effect of the conversion of drug resistance mechanisms (Qing et al., 2023). In the aggressive types of tumors ER-stress-mediated drug resistance is widely detected (Mehdizadehtapeh and Obakan Yerikaya, 2021).

Autophagy is the other corresponding mechanism of the MDR. Based on the studies the relationship between drug resistance and autophagy is complicated due to the double-edged effect. Autophagy either promotes drug resistance or creates sensitivity against the drugs. Since a cytoprotective mechanism of autophagy is activated, MDR treatment is more complicated.

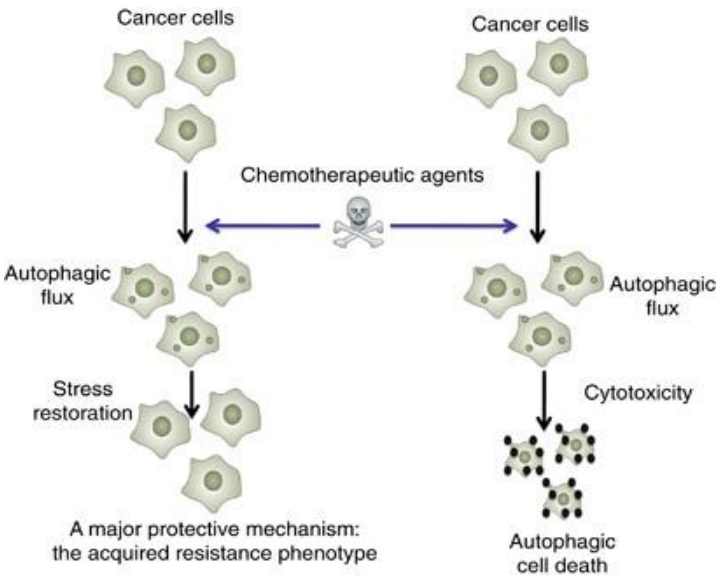

Figure 8. Paradoxical role of autophagy and multi-drug resistance (Sui et al., 2013).

BC cells are dead because of the cytotoxic effects of the drugs. Under these circumstances, autophagy degrades all the cell's debris to provide reusable nutritional support for promoting tumor cell growth. This means cytoprotective autophagy plays a role in such a condition (Wen et al., 2020). In this case, inhibition of autophagy may re-sensitize resistant cancer cells and thus make chemotherapy more effective. In turn, autophagy can also sometimes cause autophagic cell death, which is different from apoptosis. As a result, autophagy may increase the effectiveness of MDR therapy in some cancers (İsaoğlu et al., 2020). In BC cell lines drug resistance mechanism is also highly related to the autophagic process. For instance, increased levels of autophagy have been analyzed in TAM-resistant ER-positive cells, epirubicin-resistant MCF-7 cells also trastuzumab-resistant HER-2-positive BC cells compared to the drug-sensitive cell types (Wen et al., 2020). It means that a high level of autophagy is

associated with resistance mechanisms for the drugs during systemic treatment. In this case, the inhibition of autophagy seems to be one of the treatment options for resistant cancer cell lines. For example, pharmacological inhibition of autophagy via hydroxychloroquine (HCQ) or chloroquine (CQ) has resulted in decreased viability of BC cells (Sameiyan et al., 2019).

2. MATERIALS AND METHODS

2.1. CELL CULTURE

2.1. 1. Cell Lines

The metastatic mammary adenocarcinoma MDA-MB-231 is one type of triple-negative BC cell line. The Michigan Cancer Foundation (MCF-7) is the estrogen, progesterone HER2 positive cell line. MCF-7-TAMR which was obtained from MCF-7 cell line via long-term 1μM TAM exposure, was used. These MDA-MB-231, MCF-7, and MCF-7/TAMR, human BC cell lines were obtained from the American Type Culture Collection (ATCC**)** (https://www.atcc.org/).

2.1.2 Passage, Cell Counting and Seeding

MDA-MB-231, MCF-7, and MCF-7/TAMR cell lines were routinely growing, passaging, seeding, thawing, and freezing in this investigation. MDA-MB-231, MCF-7, and MCF-7/TAMR were grown in Dulbecco Modified Eagle Medium (DMEM) (Gibco, Grand Island, New York) supplemented with 10% FBS (fetal bovine serum) (Gibco, UK), 1% penicillin-streptomycin (Gibco) and maintained in a humidified incubator at 37^0 C with 5% CO_2 (Binder). In addition to these components of the complete DMEM for MCF-7/TAMR, 4 mg/ml insulin (Gibco) and 10 μl/ml Tamoxifen (TAM) (Cayman Chemical) were added. The cells were grown in the T-25 flask (Nest, CA, USA). When the cells grow cell surface confluency into the flask reaches 80%, and the cells are passaged. Firstly, a medium in the flask was discarded with a pipette, afterward the adherent cells onto the surface were washed with the needed amount (1ml) of 1X phosphate buffer saline (PBS) (EcoTech), 1-2 times depending on their debris. Once the PBS was removed, the required amount (1ml) of trypsin-EDTA (ethylenediamine tetraacetic acid) (0.25%) (Gibco, Grand Island, New York) was added to the flask for harvesting cells onto the surface. Later, the flasks were placed into the incubator and incubated for 2-4 minutes based on the confluency of the cells. When the time was out, the cells were controlled under the microscope (ECLIPSE TS100, Nikon) to check the dissociation of the cells through the cell

surface. If this separation was not enough, the mechanical power was applied gently, and the removal of the cells was checked again. Then to inhibit the trypsin activation 1:1 ratio of DMEM was poured into the flask. Cell suspension (including detaching cells) was collected from the flask and transferred into the 15 ml conical tube. The flask was completed with a certain amount of medium which was determined based on the surface area of the flask. After that, the cell suspension was centrifugated at 2500 rpm for 5 minutes (Centrifuge Z 206 A, Hermle), and the supernatant part was discarded. According to the amount of pellet an appropriate amount of DMEM was added to dissolve the pellet. The cell suspension, which was pipetted thoroughly and became homogeneous, was prepared for cell counting. After the cell suspension was ready for counting, the 10µl of cell suspension was taken and placed into a hemocytometer. The four sets of 16 squares part of the hemocytometer were counted under the light microscope (ECLIPSE TS100, Nikon) and an average was taken. Then to obtain viable cell quantity in the 1ml of cell suspension, the average cell numbers were multiplied by 10^4. Lastly, according to cell types, the appropriate number of cells were seeded again into the flask for continuing cells grown as a main stock. The passage number was increased to +1 after each passage procedure. On the other hand, a suitable number of cells were also seeded into plates either 6-well plates or 96-well plates (BIOFIL) Petri dishes (60mm or 100 mm (BIOFIL) based on an ongoing experiment.

2.1.3. Freezing and Thawing

A cell freezing procedure was performed to create cell stock to back up cells with low passage numbers to maintain the stocks. The passage procedure was applied as mentioned above. The cells were passaged, and then the cells were collected from the 15 ml conical tube and centrifuged at 2500 rpm for 5 minutes (Centrifuge Z 206 A, Hermle). The pellet was dissolved with 1 ml freezing medium composed of 10% Dimethyl sulfoxide (DMSO (Riedel-De-Haën) and 90% FBS (Gibco, UK), as a 1:9 ratio mixture. The cells within the DMSO: FBS solution were placed into cryovial tubes (Biosigma, Sentezlab). These cryovial tubes were labeled including cell line name, passage number, and dates of preservation. Lastly, the cryovial tubes were put

into an ultra-low temperature freezer at -80^0 C for freezing (Haier). When we need a cell with a low passage number or when we need to open a new cell because of any contamination, we perform the cell thawing process. At first, the new cell stocks were taken from the cell stock in an ultra-low temperature freezer -80ºC (Haier). The solution in the tube was dissolved by half at that point the 1:1 medium was added into the tubes and mixed gently. After that, this mixture was placed into a 15ml conical tube. Later, the cell suspension was centrifuged at 2500 rpm for 5 min (Centrifuge Z 206 A, Hermle) and cells were collected at the bottom of the falcon. The supernatant was removed after centrifugation; the pellet was dissolved with an approximate amount of medium. The new flask was opened, and the complete medium was seeded onto the T-25 flask (NEST), for the final volume of the medium as 4 ml. The cell suspension was transferred into a newly opened flask and the cells were controlled under the microscope (ECLIPSE TS100, Nikon). Then the cells remained in an incubator for growth.

2.2. CELL VIABILITY ASSAY

The MTT assay was performed to indicate the cell viability of the cells based on measuring the metabolic activity of the cells. MDA-MB-231, MCF-7, and MCF-7/TAMR cells were seeded into a 96-well plate (BIOFIL) at 7.500 cells/well. Then cells were incubated for 24 h in the incubator for attaching and growing. Later, the cells were exposed to drugs; EBR (Apollo Scientific), (E/Z)-4-hydroxy Tamoxifen (4OH-TAM), (Cayman Chemical), and 3-Methyladenine (3-MA) (Cayman Chemical) according to the required concentrations. MCF-7/TAMR was also treated with Tunicamycin (Tun) (Cayman Chemical). After 24 h incubation, 10µl of MTT (3-(4,5-dimethylthiazol-2-yl)-2,5-diphenyltetrazolium bromide)/ (thiazolyl blue tetrazolium bromide) reagent (Bio Basic) (0.1g MTT was dissolved with 10ml autoclaved ddH_2O water) was added onto each well and incubate them 4-6 hours in an incubator at 37ºC (Binder) for obtaining insoluble purple formazan crystals. Ensuring incubation, the medium was discarded for each well of the plate being careful not to pull any crystal. Then, formazan crystals were solubilized with 100µl dimethyl sulfoxide (DMSO) (Riedel-De-Haën) and incubated for 5 minutes in a dark place at RT. Following the

last incubation, the density of cell viability was measured with a microplate reader (Thermo Scientific, Multiskan FC 357) at 570 nm. Lastly, the cell viability percentage was calculated based on absorbance values. Thus, both the effects of different doses of drugs and the combination effects of these drugs were determined.

2.3. TRYPAN BLUE DYE EXCLUSION ASSAY

The trypan blue exclusion assay was performed to put forth the survival rate of the cells in 24, 48, and 72 h intervals. At first, MCF-7 TAMR cells were seeded into a 6-well plate (BIOFIL) at a density of 75 $x10^3$ cells/well in a final volume of 1.5 ml medium and incubated overnight. Treatment was carried out at doses which were determined as 30µM EBR and 10µM TAM by MTT assay. After completion of 24, 48, and 72 h drug treatment periods, all the media in each well was collected into Eppendorf tubes separately. The tubes were centrifuged at 13.200 rpm at 1 min (Centrifuge 5418 R, Eppendorf). Then, supernatant parts were removed. During centrifugation, wells were washed with 1 ml of 1X PBS (EcoTech). After the discarding supernatant, PBS within each well was collected from the Eppendorf tubes one by one and the tubes were centrifuged again at 13.200 rpm at 1 min (Centrifuge 5418-R Eppendorf). The supernatant was taken off the tubes. At that time the harvesting cells, 500µl trypsin-EDTA (Gibco) were given for each well and incubated the 2-3 min in an incubator at 37ºC (Binder). Then, to inhibit trypsin activation 1:1 ratio medium was added into each well. Later, the cells into wells were collected into the Eppendorf tubes respectively and centrifuged again at 13.200 rpm at 1 min (Centrifuge 5424-R Eppendorf). At that point, the supernatant was removed from each well and the pellet was dissolved with a 1:1 ratio of trypan blue dye (0.4% solution w/v) (EcoTech) medium according to the amount of pellet. Afterward, the 10µl suspension was taken onto each tube and put into a hemocytometer for counting viable (white) cells in the four sets of 16 squares under the inverted light microscope (Hermle, Centrifuge Z206A). The cell survival curve created with the data which was repeated at least three times, obtained for 24, 48, and 72 h was drawn with the GraphPad application. The curve indicated the cytostatic and cytotoxic effects of the drugs on the cells.

2.4. COLONY FORMATION ASSAY

For analyzing the colony formation potential of the cells based on selected doses of drugs, a colony formation assay was applied. MCF-7/TAMR cells were seeded onto the 6-well plate (BIOFIL) at a density of 3.0 x10^4 per well within 1.5 ml medium for each well and incubated into an incubator until the cells adhered to the surface. Afterward, the medium was aspirated into each well and the wells were rinsed with 1 ml of 1X PBS (EcoTech) at one time and removed. According to the determined dose of drugs, each well was treated respectively except for control wells. Only fresh medium was given to control well. After 24 h incubation at 37^{o}C, the drugs + medium combination was removed from the wells and then 3 ml fresh medium was given for each 6-well plate. Later, the plates were incubated in an incubator for approximately 14-21 days at 37^{o}C. Each day the cells were checked. At the end of the incubation periods, the medium was discarded and washed with 1X PBS twice. Then the fixation was performed with a 1:3 ratio of acetic acid (BioRad): methanol (Riedel-de-Haën) into a shaker (Sk-O180-S, DLAB) at 45 minutes in RT. Next, the removal of the fixation solution was done and 1 ml of 0.5% crystal violet (Merck) was for each plate and incubated them 2 hours at RT. Later, the dye was washed with distilled water. The image of each well was pictured. Lastly, the colony numbers were encountered via ImageJ software, and the graph was obtained based on the encountered numbers.

2.5. HANGING DROP ANALYSIS

According to the counting result obtained after passaging of MDA-MB-231, MCF-7, and MCF-7 /TAMR cell line, a homogeneous solution was created with 2x10^4 cells included in each 20 µl droplet. Selected drug doses for EBR, TAM, and 3-MA were calculated according to the amount of solution prepared and drug treatment was carried out. Next, 2 ml of 1X PBS (EcoTech) was added to a 60mm Petri dish (BIOFIL). Afterward, on the cover side of the Petri dishes, 20µl of droplets of drug-treated cell suspension were placed in approximately 7-8 droplets. The lid of the Petri dish was

then carefully turned and closed. Later, Petri dishes were placed into the incubator cautiously. The Petri dish was taken off the incubator at specified time intervals (24, 48, and 72 h), and 3D images of the cells were taken under the microscope (H600L, Nikon) at 4X size, taking care not to disrupt the droplets on the cover. The size of the sphere was measured by Image J and graphed via GraphPad.

2.6. FLUORESCENCE STAINING ASSAYS

2.6.1 Propidium Iodide Staining Assay

The PI staining was performed to evaluate the cell viability of the cells because it binds to damaged or dead cells. MCF-7/TAMR cells were seeded in a 96-well plate (BIOFIL) at a density of 10 x 10^2 for each well. One day later cells were grown and ready for drug exposure with determined doses and incubated overnight in an incubator at 37ºC (Binder). Later incubation, the medium was removed from the wells, and a 1:1000 ratio of PI (Sigma-Aldrich, Saint Louis, UK) /medium mixture was given to each well as a final volume of 1.5 ml. The stock concentration of PI was 1mg/ml The plate was incubated for approximately 10 minutes in the incubator (Binder) The fluorescence results were obtained under fluorescence microscopy at ex/em: 535/615 wavelength (Axio Observer 5 Colibri7, Carl Zeiss Microscopy).

2.6.2. DAPI (4′,6-diamidino-2-phenylindole) Staining Assay

The DAPI assay was performed to stain DNA by this way visualizing and fixing the viable cells. MCF-7/TAMR cells were seeded into a 6-well plate at density 10 x 10^4 a final volume of 1.5ml of each well. The cells were incubated in an incubator for adherence and growing of the cells. Then, treatment was done at the determined doses and left for 24 h incubation. After the 24 h incubation, the medium was thrown away from the wells, and the 1:1000 DAPI (Thermo): medium mixture was prepared as 1µl/mL. The stock solution of DAPI was 5mg/mL. Later, 1.5 ml of this mixture was distributed into each well. This plate was incubated in an incubator for almost 20 min. Afterward, the dye and medium mixture were removed from each well, and 1 ml of

1X PBS was added to the wells. The results were taken under fluorescence microscopy at ex/em: 358/461(Zeis, Oberkochen, Germany).

2.6.3. DiOC6 (3) (3,3'-Dihexyloxacarbocyanine Iodide) Staining Assay

DiOC6 (3) (3,3'-Dihexyloxacarbocyanine Iodide) staining was performed to detect the mitochondrial membrane potential of healthy cells. MCF-7/TAMR cells were seeded onto the 6-well plate as 50 x 10^3 / 75 x 10^3 cells/well into 1.5 ml medium for each well. Day after, the selected doses of drugs were administered to cells and incubated them 24 h in the incubator. Then, the medium was thrown away from the cells. The medium with DiOC6 dye (Thermo) (Stock 1 to 5 μM) at a ratio of 1:1000 was given for the cells. Afterward, the stained cells were incubated for 15 min incubator, and fluorescence images were taken by fluorescence microscopy at ex/em 482/504nm (Zeis, Oberkochen, Germany).

2.6.4. Monodansylcadaverine Staining Assay

Autophagic vacuole formation was detected via monodansylcadaverine (MDC), which is a weak base fluorescent stain, and staining assay. After trypsinization, MCF-7 and MDA-MB-231 cells were seeded onto 6- a well plate at a density of 50 x 10^3 as a final volume of 1.5ml/well. MCF-7/TAMR cells were seeded onto the 6-well plate at 75 x10^3 cells/well in a 1.5ml medium. After overnight incubation, cells were treated with determined drug doses and incubated for 24 h. Then, the medium was discarded into the plate and cells were stained with MDC (stock prepared as 10 mg/ml) (Cayman Chemical, USA) with a ratio of 1:1000. After the incubation of almost 10-20 minutes, autophagic vacuole formation was detected under fluorescence microscopy at ex/em 335/525nm. (Zeis, Oberkochen, Germany).

2.7. FLOW CYTOMETRY

MCF-7/TAMR cells were seeded onto the 6-well plate as $25x10^4$ cells/wells. Then the cells were placed in an incubator for adhering and growing. Later on, the cells were treated with a decided dose of drugs, and they were incubated for 24 h. After that the medium was collected into the Eppendorf tubes and centrifuged at 13.200 rpm for 1 min (Centrifuge 5424 R, Eppendorf). At this time cells were rinsed with 1ml of 1X PBS (EcoTech). When the centrifugation finished supernatant was discarded and PBS onto wells was collected onto Eppendorf tubes and centrifuged again at 13.200 rpm at 1 min (Centrifuge 5424 R, Eppendorf). Then the supernatant was removed, and cells that were harvested with trypsinization were collected and put into Eppendorf tubes and centrifuged at 13.200 rpm for 1 min (Centrifuge 5424 R, Eppendorf). The supernatant part was removed, and the pellet was dissolved with 1ml 70% ice-cold ethanol (ISOLAB) dropwise. In this way, the cells were fixed and stored at $+4^0$ (Flavel) C for 4-6 months. Before reading samples, the following steps were applied. Firstly, the suspension was centrifuged at 13.200 rpm for 1 min (Centrifuge 5424 R, Eppendorf) to remove ethanol from the samples. Afterward, 1 ml of 1X PBS (EcoTech) was added to each sample for washing. Later, 300µl 1X PBS +3µl PI+1µl RNase A (EcoTech, EcoZyme) was put into each sample and pipetted then incubated on ice for 15 min. Lastly, cell cycle phases for each sample were detected by flow cytometry using BD Accuri C6 software (BD Bioscience).

2.8. GFP-LC3 PLASMID TRANSFECTION

The EGFP-LC3 (plasmid #11546) was obtained from addgene (https://www.addgene.org/11546). After that, plasmid isolation was performed following the EcoSpin Plasmid Isolation Kit (EcoTech) protocol. Later plasmid isolation, the cells were transfected with GFP/LC3 (addgene no: 11546) plasmid using iN-fect™ in vitro Transfection Reagent. MDA-MB-231 cells were seeded onto the 6-well plate as $10x10^4$ cells/wells. MCF-7 cells and MCF-7/TAMR cells were seeded

into the 96-well plate as 5 x10^3 and 7.5x10^3 respectively. When the cell grew properly, transfection suspension was ready to prepare. First, serum-free DMEM (120µl/well) for each 6-well collectively was taken into 1.5ml Eppendorf tubes. Also, the serum-free DMEM (10µl/well) was collected for each 96-well. The desired plasmid: transfection ratio was calculated as either 1:3 or 1:6. Then appropriate amount of transfection reagent was added into serum-free DMEM and incubated them 5 min at RT. Later, the 1µg plasmid/6-well or 0.2 µg or 0.4 µg plasmid/96-well was added to serum-free DMEM mixed gently, and incubated for 30 min. Meanwhile, complete DMEM into the plate washed with 1X PBS to remove the complete DMEM totally from the plate. Then appropriate amount of serum-free DMEM was added to each 6-well and 96-well plate respectively. At the end of the incubation, the total volume transfection mixture of each well was added dropwise manner for each well already containing serum-free DMEM. After the 4-6 hours of incubation, 20%FBS containing DMEM with the suitable amount was added for each well. The plate was left to determine adequate time whether the 24 or 48 h for the transfection. When the transfection was done after checking, the cells were treated. The transfection reagent was removed in all and drugs harboring complete DMEM were given for each well according to their conditions. For starvation conditions 0.01%FBS containing DMEM was given for selected wells and incubated 24 h. Lastly, the GFP-LC3 puncta formation was observed via fluorescence microscopy at (ex/em 488/510 nm) wavelength (Zeis, Oberkochen, Germany).

2.9. TOTAL PROTEIN ISOLATION

The cells were seeded onto 60mm Petri dishes (BIOFIL) at density 4.0 x10^5 in 3ml medium. After the trypsinization procedure incubated in an incubator at 37^{o}C (Binder) until the cells adhered and grew appropriate confluency. Later, drug treatment was performed according to selected doses of EBR, TAM, and 3-MA based on MTT assay. Afterward, the cells were left for 24 h in the incubator at 37^{o}C (Binder). Then the cells that were controlled and treated were taken off the incubator for isolation. The medium in all conditions (except control) was collected into the 1.5ml Eppendorf tubes and centrifuged at 13.200 rpm for 1 min (Centrifuge 5424 R, Eppendorf). After that, the

supernatants of each tube were discarded. This step was repeated two times. In a while, the medium into control dishes was discarded directly and the Petri was rinsed with 1ml 1X PBS (EcoTech) and removed. After these steps, 1 ml of ice-cold 1X PBS was added to the all-Petri dishes including the control, and then the cells were collected via scraping procedure with the back of the pipette tip. The cells that were collected by scraping were put into the Eppendorf tubes and centrifuged again at 13.200 rpm for 1 min (Centrifuge 5424 R, Eppendorf). Next, the supernatant was removed for all tubes without disrupting pellets. These steps were followed two times. As follows, according to pellet density, an appropriate amount of ice-cold Mammalian Protein Extraction Reagent (M-PER) (+) (Thermo) was added for each, and the pellets were dissolved properly. Later, the tubes were placed onto a shaker (Sk-O180-S, DLAB) for 20 min incubation at room temperature. At the end of incubation, if the pellets were precipitated, pipetting was performed again, and tubes were incubated for 2-3 minutes in a shaker (Sk-O180-S, DLAB). After the incubation, the samples were centrifuged at 13.200 rpm for 15 min at 4^{o}C (Centrifuge 5418 R – Microcentrifuge, Eppendorf). Finally, the supernatant parts where the protein was accumulated were collected in new Eppendorf tubes stored at -20^{o}C (Flavel).

2.10. BRADFORD ASSAY

Protein concentration was determined via Bradford assay after the total protein isolation. The 1X Bovine-serum albumin (BSA) (Sigma-Aldrich) standards were utilized as different concentrations 0, 2,4,6, 8 ug/ml into 100µl of Bradford reagent (Sigma Aldrich) for plotting standard curve graphs. At that time for protein samples, the 1µl protein samples for each were added onto 100µl of Bradford reagent. After adding the reagent, the incubation was performed for 15 min in the dark. Later, sample absorbance was measured with a spectrophotometer at 595 nm (Multiskan FC 357 Microplate Photometer, Thermo Scientific). Based on BSA standards concentration versus absorbance graphs were plotted in Excel. According to the graph, the required volume of protein samples was determined.

2.11. SDS-PAGE ANALYSIS

Protein expression was performed via SDS-Page analysis. The appropriate volume of protein samples was calculated based on the equation of the BSA standard curve to achieve equal loading of each sample. Also, 4X Laemmli buffer (EcoTech) amount for each sample was calculated as a final concentration of Laemmli 1X based on an equation of the BSA standard curve. The desired amount of protein samples (20-25µg) and Laemmli buffer (EcoTech) were combined in (PCR) tubes (ISOLAB) and heated them 95^{o}C in a heat-blocker for 5 min (Thermo Scientific). The 12% Tris-glycine gel was poured and waited until the polymerization according to our protocol given in Supplementary Table 1. The polymerized gel was placed into a tank and filled up with a 1X running buffer (EcoTech)The prepared protein samples mix was loaded into 12% gel and running was started at 50V. When the dye reaches the separating gel part the voltage increases to 70V. Lastly, the dye reaching nearly the bottom of the gel voltage was increased to 90V. At the end of the running procedure, the semi-dry (Biometra Fastblot, Analytik Jena) transfer was performed.

Before the transfer procedure, the gel was removed from the running tank, and the stacking part was cut off. Then the gel was incubated in a 1X transfer buffer (handmade). In addition, the polyvinyl-fluoride (PVDF) (0.45µm) (GVS) was activated as follows; 1 min incubation in methanol (Sigma-Aldrich) then washed with 5 min ddH_2O and waited 10 min 1X transfer buffer. Moreover, filter papers were rinsed with a 1X transfer buffer. After the preparation of all these preliminary steps, the 4 filter papers were placed onto the device, then the membrane was put onto the filter paper. Later, the gel was put onto the membrane and 4 filter papers were added to the gel. In this way, the transfer sandwich was prepared. The transfer was done at 200mA either 15 min for < 100kD or 20 min for >100kDa.

When the transfer was done, a blocking step was performed for membranes via 5% skim milk on a shaker (Sk-0180-S, DLAB) for 1 h at RT. The skim milk was prepared as 2.5gr skim milk powder (Bioshop, Canada) dissolving with 50ml 1X TBS-T. At the same time, the gel was stained with Coomassie brilliant blue G-250 dye (B2025-1EA, MERCK,) on a shaker (Sk-0180-S, DLAB) for 1 h at RT. The gels were taken into de-staining solution after the Coomassie staining was removed after the 1h. Afterward,

the membranes were incubated with primary antibodies ATF6 (1:250) (Invitrogen), PERK (1:1000) (CST), IRE1-alpha (1:1000) (CST), Calreticulin (1:1000) (CST), Calnexin (1:1000) (CST), GRP78 (1:1000) (Invitrogen), PDI (1:1000) (CST), Beclin-1 (1:250) (St John's Laboratory), Atg5 (1:500) (St John's Laboratory), LC3A/LC3B (1:500) (St John's Laboratory), SQSTM1 (1:500) (St John's Laboratory), cleaved Caspase 3 (1:1000) (CST), Caspase 9 (1:250) (CST), cleaved PARP (1:1000) (CST), MRP1 (1:500) (Invitrogen), GAPDH (2:5000) (Boster) which were prepared in 5% skim milk overnight $+4^0$C on roller (MX-T6-S, DLAB). When the primary antibody incubation was completed, the membranes were washed with 1x-TBS-T 3 times for 5 min onto a shaker (Sk-O180-S, DLAB) at RT. Then membranes were taken into secondary antibodies (1:1000 ratio prepared in 5% skim milk) which were appropriate primary antibody hosts and HRP-conjugated and incubated overnight $+4^0$C on roller (MX-T6-S, DLAB). After incubation, the membranes were washed with 3 times 1X TBS-T and one times 1X TBS for 5min onto the shaker at RT.

The enhanced chemiluminescence (ECL) solution which was composed of Solution A and B was prepared for chemiluminescence detection of HRP-conjugated secondary antibodies signals. The membranes were soaked in this ECL solution for 1 min then the image was taken into the chemiDoc device (C300 Biosystems, Azure) at a minimum of 10 sec and a maximum of 2 min 30 sec respectively. The statistical analysis of the band thickness was measured with ImageJ software and the calculation was done with Excel.

2.12. STATISTICAL ANALYSIS

GraphPad Prism 8 software was utilized for statistical analysis. The standard deviation +/- (SD) values were added to the graphs resulting in a statistically significant test two-way ANOVA or Student-t test. The significant value was considered according to a p-value less than 0.05 and 0.0001. The immunoblotting analysis was performed with ImageJ software. The results of all experiments were replicated at least three times.

3. RESULTS

3.1 TAMOXIFEN IN COMBINATION WITH EPIBRASSINOLIDE INDUCED CELL VIABILITY LOSS IN MCF-7/TAMR CELL LINE

The first step of this study was to determine whether MCF-7/TAMR cell line was resistant to TAM and the dose of TAM to which the cell line is resistant. For this purpose, the MTT assay was first performed at certain interval doses of TAM at 24 h. The TAM was administered to MCF-7/TAMR cell line at 0, 10, 15, and 20μM doses for 24 h. The result revealed that the doses of TAM given were not statistically significant when compared to the control, and TAM resistance properties of MCF-7/TAMR cell line were revealed at these doses. Subsequently, the effect of EBR alone and in combination with TAM on cell viability was evaluated. The conditions of MTT were as follows: control, 30μM EBR, 10μM TAM, 30μM EBR + 10μM TAM, 20μM TAM, 30μM EBR + 20μM TAM. According to the findings, it was shown that EBR had a statistically decreasing effect on cell viability. Additionally, a statistical decrease was observed in the combination of both 30μM EBR +10μM TAM and 30μM EBR+ 20μM TAM, compared to conditions where only 10μM or 20μM TAM was given. This data was obtained from at least 3 replications. Based on these data the graphs were evaluated (Figure 9).

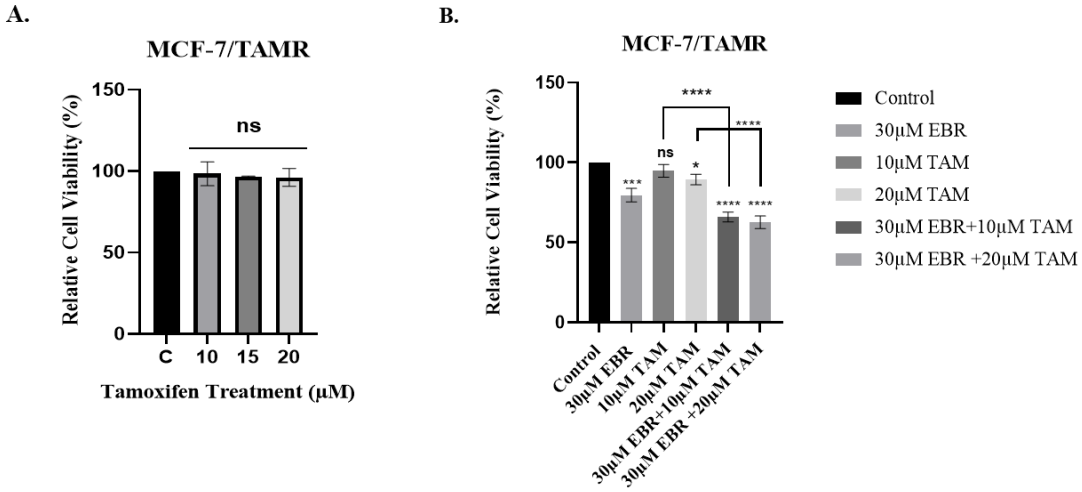

Figure 9. EBR and TAM administration declined cell viability on MCF-7/TAMR. **A**. Cells were incubated with different concentrations of TAM (0-10-15-20µM) for 24 h and then analyzed with MTT assay. **B**. Cells were treated with the 30µM EBR with the different concentrations of TAM for 24hr after then analyzed with MTT assay. Statistical differences were given with a one-way ANOVA test. (ns: no significant, *p<0.05, ***p < 0.001, ****p<0.0001)

Trypan blue dye exclusion assay was performed to evaluate the effectiveness of EBR on cell viability depending on time interval. Cells were treated with selected doses which were 30µM EBR and 10µM TAM for 24, 48, and 72 h. Then, the living cells that had not received dye were counted and the graph in Figure 9 was plotted with at least three biological replications with the help of GraphPad. The green, red, blue, and purple lines in the graphs represent the control, 30µM EBR, 10µM TAM, and 30µM EBR +10µM TAM conditions respectively. According to the data, a cytotoxic effect of EBR and EBR+TAM was observed significantly at 24 h. There were no significant changes in 10µM TAM at 24h. At 48 and 72 h the cytostatic effect was detected.

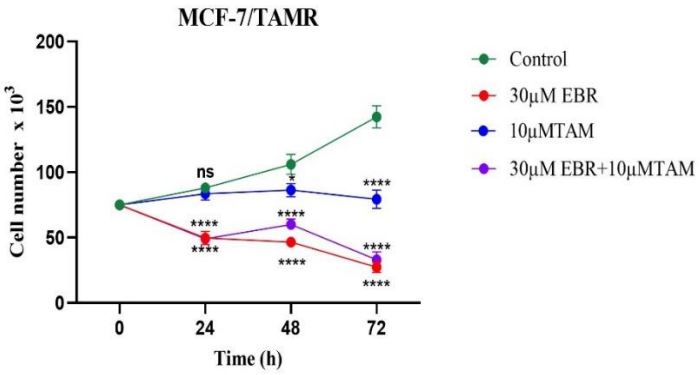

Figure 10. EBR in combination with TAM decreased cell survival in a time-dependent manner MCF-7/TAMR.
Trypan blue dye exclusion assay was performed in MCF-7/TAMR cells. Selected doses of EBR and TAM were administered either alone or in combination in a time-dependent manner (0-72 h). The cytotoxic effect of EBR and EBR+TAM was detected at 24 h. All results represented the average of three independent experiments. This graph was plotted with GraphPad software. (ns: no significant, *p<0.05, ****p<0.0001)

3.2. THE EPIBRASSINOLIDE COMBINED WITH TAMOXIFEN DECLINED THE 2-DIMENSIONAL COLONY-FORMING ABILITY OF MCF-7/TAMR CELLS

The 2D colony formation potential of MCF-7/TAMR cell line was analyzed based on the selected dose of drugs obtained from the previous experiment. During the experiment, MCF-7/TAMR cells were treated as follows; control,30µM EBR, 10µM TAM, 20µM TAM, 30µM EBR+10µM TAM, and 30µM EBR+20µM TAM (Figure 11 A). The colony formation potential was drastically reduced because of combinations of 30µM EBR+10µM TAM compared to the administration of 10µM TAM only. The number of colonies was counted with the help of Image J software and the graph was plotted depending on the percentage of colony numbers via GraphPad (Figure 11 B). A significant decrease in the number of colonies was observed when the control and combined treatments were compared in MCF-7/TAMR cell line.

A.

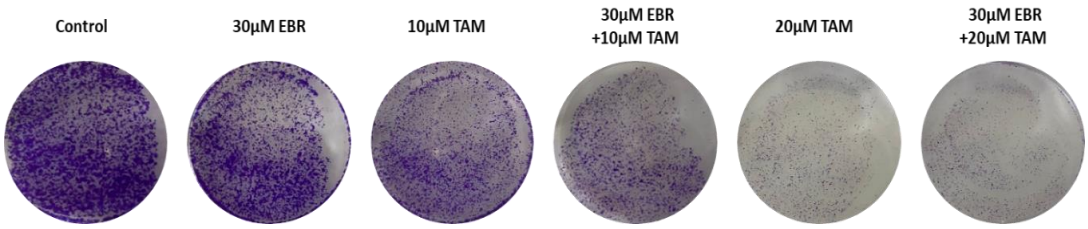

B.

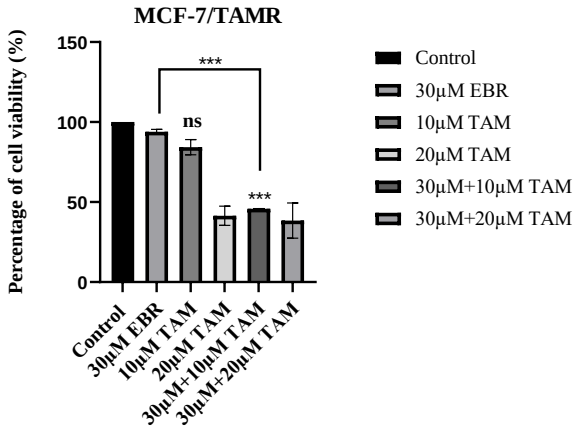

Figure 11. EBR combined with TAM decreased the two-dimensional colony formation potential of MCF-7/TAMR cells.

A. A colony formation potential was evaluated. **B.** The number of colonies was counted with the Image J program and then analyzed in GraphPad. The number of colonies was significantly decreased in combined treatment. (ns: no significant, *p<0.05, ***p<0.001)

3.3. THE EPIBRASSINOLIDE COMBINED WITH TAMOXIFEN RESTRICTED THE THREE-DIMENSIONAL COLONY-FORMING POTENTIAL OF MCF-7/TAMR CELLS

To evaluate the three-dimensional colony-forming potential, hanging drop analysis was performed with the appropriate time intervals (24,48 and 72 h). The image of each drop for each time interval was taken under the microscope at 4X magnitude (500μm) (Figure 12 A). When compared to the drop of control, a decrease in colony formation potential was detected in EBR+TAM conditions after 24 h of treatment. This was demonstrated by the increasing cavities in treated conditions. At the same time, no change was detected in the sphere form after the exposure of TAM alone at 24 h. Later

24 h, an increase in the number of drug-exposed cells was observed in 48 h and 72 h time intervals. The cells that underwent death due to accumulation were detected in dark brown or black color. The diameters of the sphere of cells were quantified using ImageJ software and the graph was plotted via GraphPad (Figure 12 B).

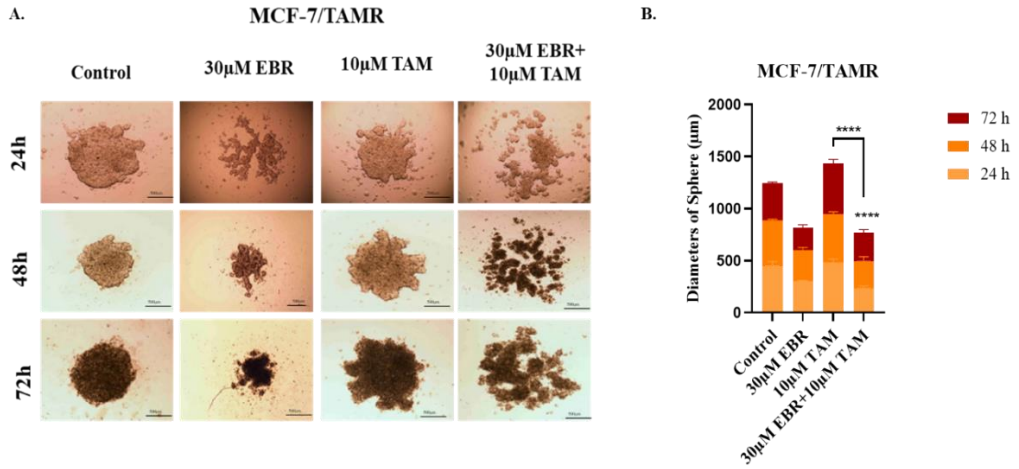

Figure 12. Hanging drop analysis demonstrated the decreasing three-dimensional colony formation potential of MCF-7/TAMR cells via EBR combination with TAM.
A. The 3D colony formation potential for each drug was evaluated by imaging the droplet of each condition in a certain time interval (24 h/48 h/72 h). The images were taken at 4X magnitude. **B.** Cell sphere area quantification was performed using ImageJ analysis. The graph was plotted with the GraphPad software. (****p<0.0001)

3.4. THE NUMBER OF DEAD CELLS WAS INCREASED IN MCF 7/TAMR CELL LINE AFTER EXPOSURE OF EPIBRASSINOLIDE COMBINED WITH TAMOXIFEN VIA PROPIDIUM IODIDE STAINING

PI staining was applied to assess the cell viability of MCF-7/TAMR cells. Figure 13. A demonstrates both light microscope (LM) and fluorescence microscope images, which were marked according to the type of given fluorescence dye, for the selected conditions. In these results, as a fluorescence dye, the PI stain which binds to the nucleic acids of the cells was used and seen as red dots. The light microscope image indicated that the number of cells was diminished due to the exposure to drugs compared to the control group (Figure 13 A). The number of dead cells was not present in the control group in Figure 13 A, the number of PI-stained cells was counted, and the graphs were plotted and given in Figure 13 B. Whereas the number of non-living cells was evaluated after the exposure to EBR treatment alone. Furthermore, the

number of dead cells was also significantly increased when the exposure of EBR+TAM compared to the administration of TAM only (Figure 13 B). When comparing the EBR and 30µM EBR +10µM TAM also EBR and 30µM EBR +20µM TAM statistical significance was identified and detected in the graph (Figure 13 B).

A.

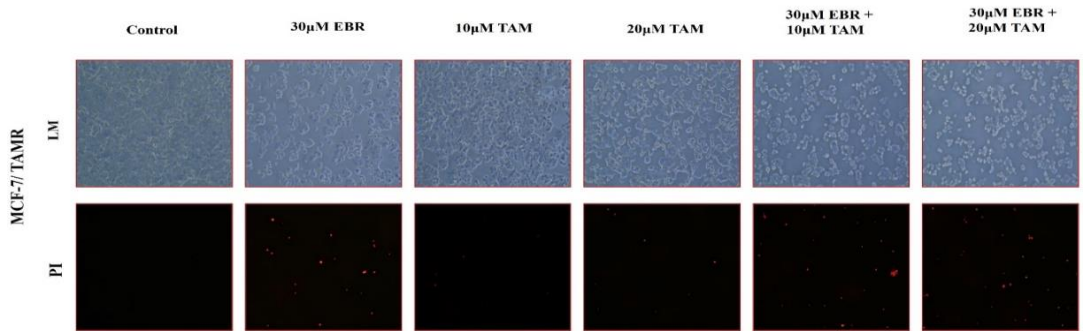

B.

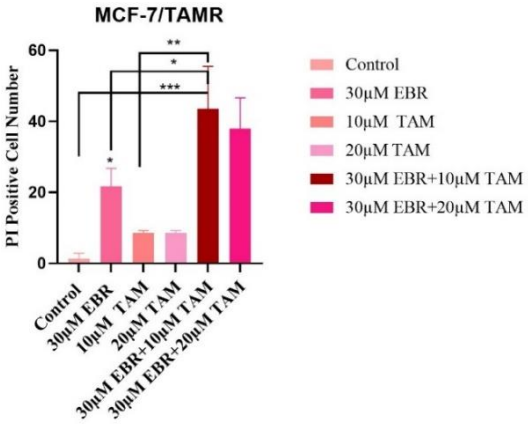

Figure 13. Propidium iodide-stained cells were increased after the ERB combination with TAM on MCF-7 TAMR cells.
A. The figure consists of the light microscope (LM) images also Propidium iodide (PI)-stained which are red fluorescence images for all conditions. The number of cells was diminished after the exposure to drugs in comparison with the control group in LM images. Moreover, in the PI-stained parts of the figure, the increasing number of dead cells was evaluated with the combination of 30µM EBR and 10µM TAM**. B.** PI positive cell numbers were counted from independent experiments, and the graph was plotted in GraphPad software. (*p<0.05, **p<0.01, ***p<0.001)

3.5. THE CELL VIABILITY LOSS OF MCF-7/TAMR CELLS WAS INCREASED BY TAMOXIFEN IN COMBINATION WITH EPIBRASSINOLIDE IN DAPI AND DiOC6 STAINING

For evaluating drug treatment effects on DNA fragmentation and mitochondrial membrane potential, alone or in combination, fluorescent dyes were used including DAPI and DiOC6 respectively in MCF-7/TAMR cell line. Fragmented DNA in the cells, also named DAPI-positive cells, was detected as bright blue dots in the nuclei (Figure 14). The number of DAPI-positive cells increased significantly with the treatment of EBR and TAM **c**ombination compared to exposure to drugs alone in MCF-7/TAMR cells. According to DiOC6 staining results, a control group was evaluated with the higher number of DiOc6-stained cells with healthy mitochondria. The number of viable cells was significantly reduced when the 30µM EBR +10µM TAM was administered There were not any significant differences between the control and 10µM TAM treated groups when the DiOC6 was given. The graphs seen in Figure 14 were plotted via GraphPad when they counter the dead cells for evaluating DAPI, as well as live cells for assessing DiOC6 with the help of ImageJ software.

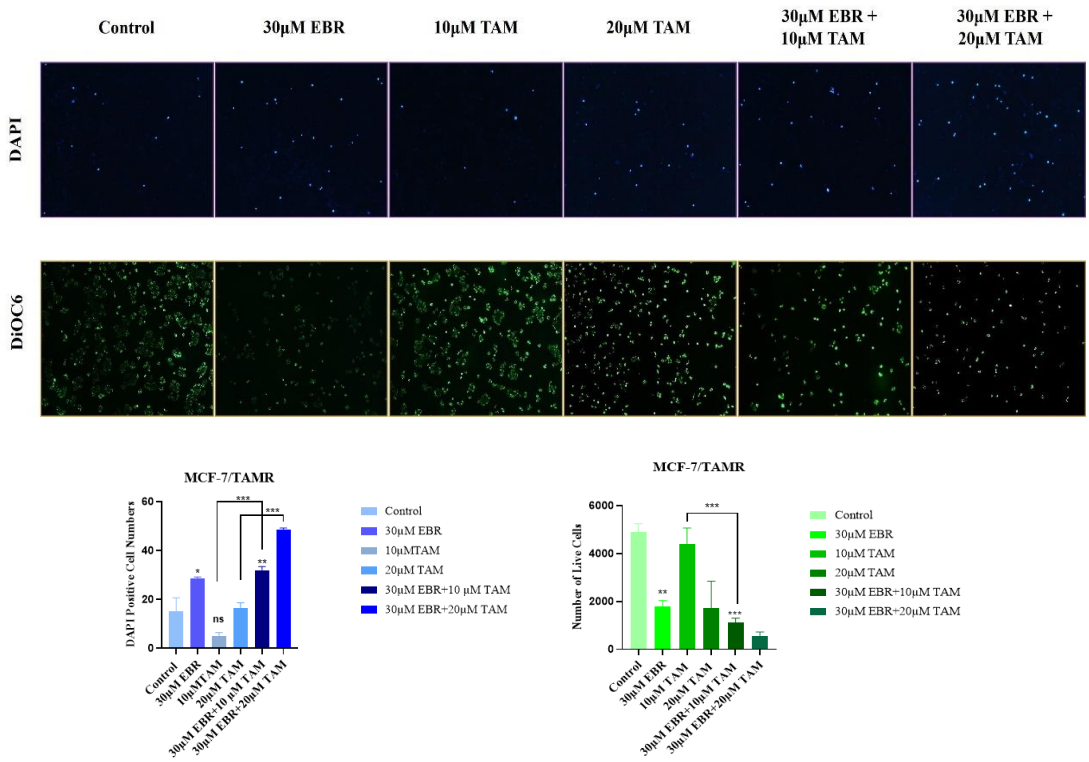

Figure 14. Fragmentation of DNA was increased, whereas the mitochondrial membrane potential was decreased in MCF-7/TAMR cells.

Increasing fragmentation of DNA was detected in the 30µM EBR and 30µM EBR+10µM TAM combinations via DAPI staining. Also, mitochondrial membrane potential was diminished after exposure to 30µM EBR and 30µM EBR+10µM TAM and this decrease was detected in DiOC6 staining. The graphs were plotted from at least 3 independent experiments with the help of the GraphPad software. (ns: no significant *p<0.05, **p<0.01, ***p<0.001)

3.6. THE EPIBRASSINOLIDE COMBINATION WITH TAMOXIFEN AFFECTED THE G1 PERCENTAGE IN MCF-7/TAMR CELL LINE

A flow cytometer approach was performed to observe the distribution of the cell cycle phases after drug treatments alone or in combination. It was also examined whether apoptotic cell death is present, and the cell population density in SubG1. Our results displayed that there was upregulation of G1 percentage in the 30µM EBR+10µM TAM conditions compared to control as well as 10µM TAM. This upregulation was statistically significant indicated in the graphs which were plotted based on all repeated experiments in GraphPad software.

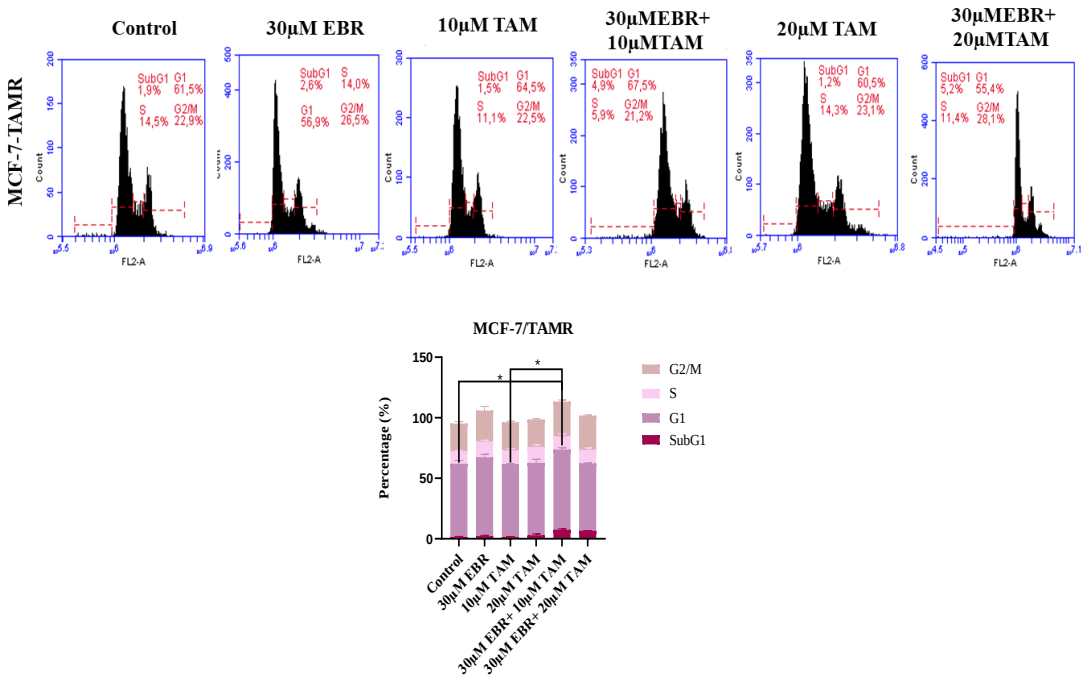

Figure 15. G1 arrest was detected in MCF-7/TAMR cells after the cells were treated with the EBR and TAM combinations.
Following the treatment, the PI staining was performed. Then flow cytometry was utilized to assess the distribution of cells across the cell cycle including G1, S, G2/M, and subG1. The percentage of G1 was augmented in 30µM EBR+10µM TAM conditions compared to 10µM TAM administered alone. Each experiment was conducted thrice, and graphs displayed the mean values along with the ± standard deviation. (*p<0.05)

3.7. THE ELEVATED EXPRESSION OF THE ENDOPLASMIC RETICULUM STRESS MARKERS WAS DETECTED AFTER EXPOSURE TO THE EPIBRASSIONOLIDE COMBINATION WITH THE TAMOXIFEN

For analyzing the expression changes of ER stress markers, immunoblotting was performed. Tun, which is an ER stress inducer, was used as a positive control (Luhr et al., 2019). Before the usage of Tun, the dose of Tun for MCF-7/TAMR was evaluated via MTT assay. According to data obtained from MTT, between the two selected concentrations of Tun treatment, no significant change was observed **(**Figure 16 A). Therefore, 5µM Tun was selected as a positive ER stress inducer. The expression of ER stress chaperons which are CALR, CANX, PDI, and BiP also three ER stress sensors including PERK, IRE1α, and ATF6 were investigated according to expression changes in MCF-7/TAMR cell line (Figure 16 B). Increased expression of ER stress markers was determined after the exposure of selected doses of EBR+TAM and Tun conditions compared to the EBR alone. When we look at the three ER stress sensors that harbor IRE1α, PERK, and ATF6, their expressions were increased after exposing the EBR+TAM. The GAPDH was used as a loading control.

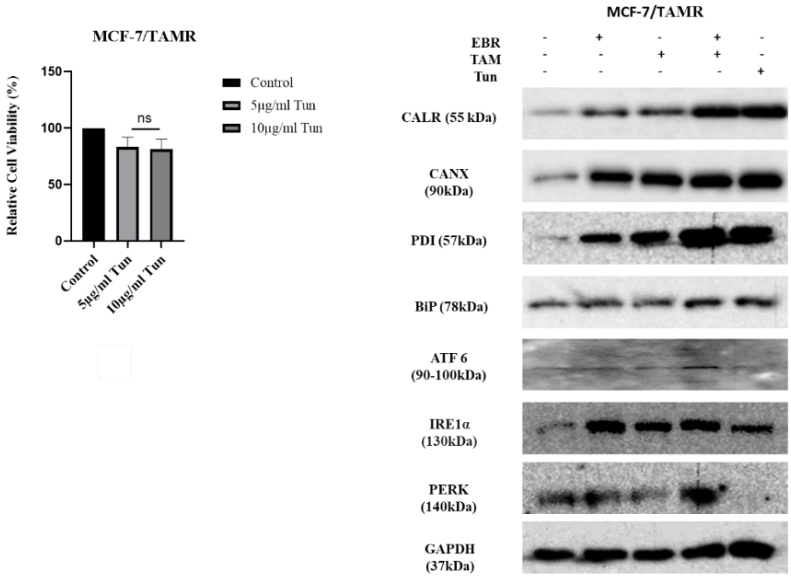

Figure 16. The expression of the ER stress markers augmented after exposing EBR combination with TAM on MCF-7/TAMR cell line.
A. The dose of the Tun for MCF-7/TAMR was determined via MTT assay. The graph was plotted based on the means of three replicates of experiments. The standard deviation was indicated ±. No significant change was observed between each dose of Tun **B.** ER stress marker expressions was detected via immunoblotting techniques. The cell lysate (25µg) was

loaded in 12% SDS-PAGE gels and propped with the CALR, CANX, PDI, BiP, ATF6, IRE1α, and PERK antibodies. Their expression augmented after the EBR combination with TAM. Tun was utilized as a positive control for ER stress. As a loading control, GAPDH was used.

3.8. AUTOPHAGY INDUCTION WAS DETECTED WITH EPIBRASSINOLIDE IN COMBINATION WITH TAMOXIFEN AND REVERSED WITH THE 3-METHYLADENINE IN ALL BREAST CANCER CELL LINES

For evaluating whether the decrease in cell viability occurs through autophagy, we used 3-MA, one of the autophagy inhibitors. Firstly, the dose of 3-MA was determined via MTT assay for each cell line (Figure 17 A). There were no significant changes between 5 and 10µM 3-MA in the MCF-7 and MCF-7/TAMR cell lines, whereas the significant changes were detected in 10µM 3-MA conditions in MDA-MB-231 cell line (Figure 17 A). The decreased cell viability following EBR alone or combined with TAM was reversed by the addition of 10µM 3-MA to the combination, which was detected by MTT assay (Figure 17 B). The administration of EBR+TAM has reduced the cell viability in all breast cancer cell lines. The cell viability was increased significantly in 3-MA combination with EBR+TAM in all breast cancer cell lines.

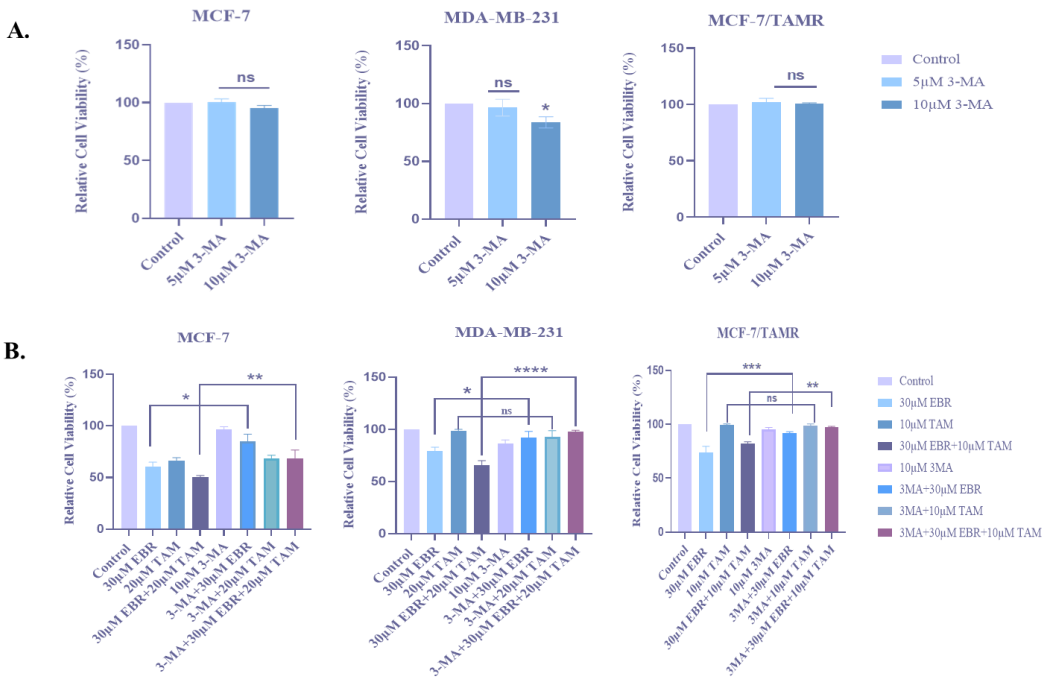

Figure 17. 3-MA and combination treatment of EBR and TAM reversed the loss of cell viability in MCF-7, MDA-MB-231, and MCF-7/TAMR cell lines.
A. Appropriate dose of 3-MA was determined via MTT assay. The 10µM 3-MA was significant for the MDA-MB-231 cell line. There were no significant changes after administration of 5 and 10µM 3-MA in MCF-7/TAMR and MCF-7 cell lines. **B.** 3-MA combination with EBR+TAM increased the cell viability compared to EBR+TAM treatment in all cell lines. The graphs were plotted from at least 3 independent experiments by using GraphPad software**.** (ns: no significant *p<0.05, **p<0.01, ***p<0.001)

To analyze the effect of 3-MA on 3D colony formation potential, hanging drop analysis was performed (Figure 18 A-C). The diameters of spheres were decreased significantly after exposure to EBR+TAM in all breast cancer cell lines. The administration of 3-MA reversed EBR and TAM combination's effect on the 3D colony formation ability in MCF-7 and MDA-MB-231 cell lines but not in MCF-7/TAMR cells. The sphere diameters were measured with the help of the ImageJ software and graphs were plotted via GraphPad software (Figure 18 D).

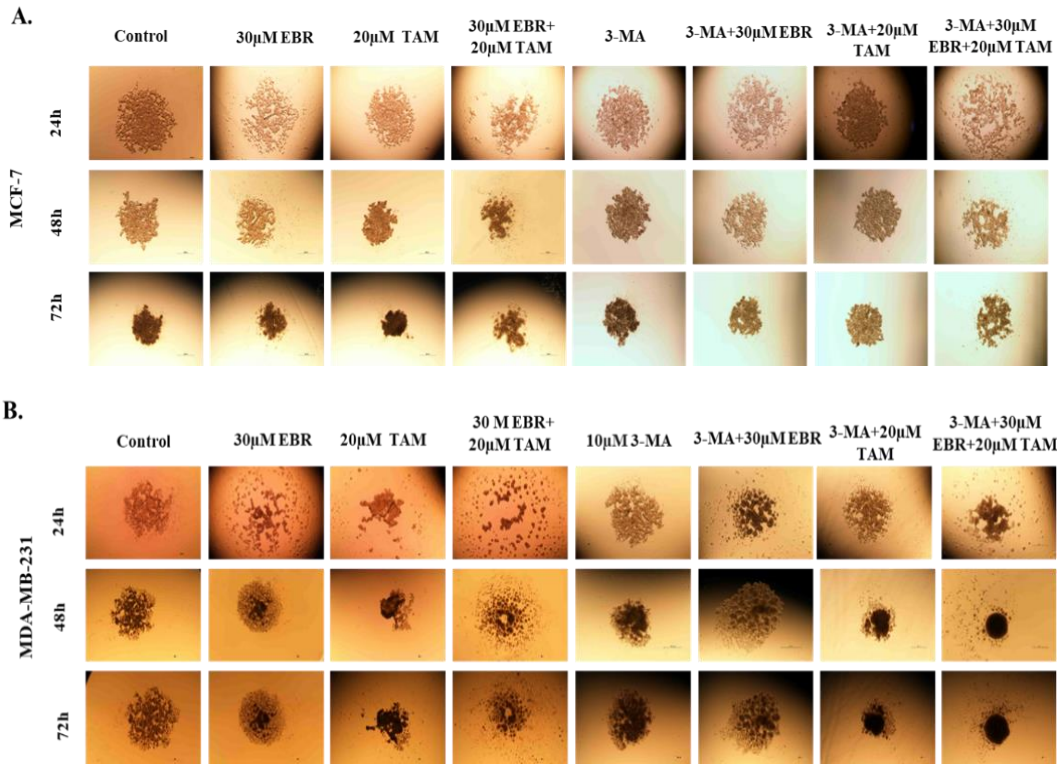

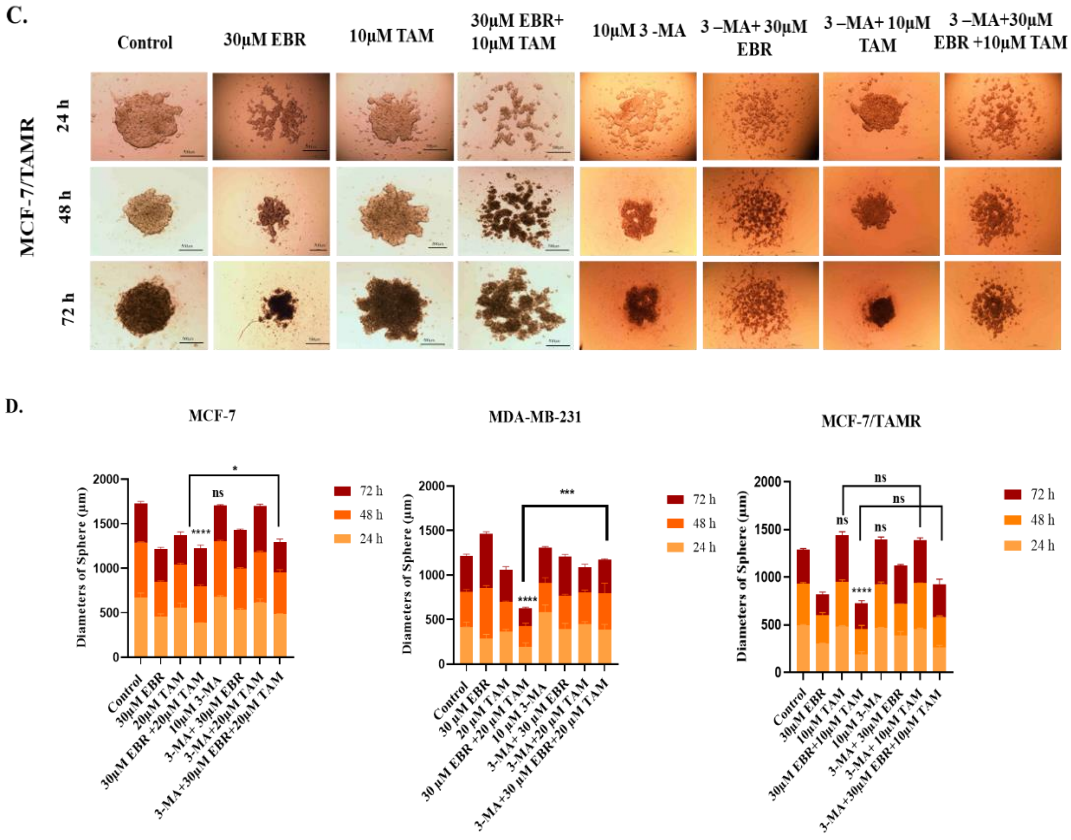

Figure 18. Diameters of the sphere were declined following the EBR+TAM condition reversed with the addition of 3-MA significantly in MCF-7, MDA-MB-231, and MCF-7 TAMR cell lines. **A-C.** The images of each condition were taken in a certain time interval 24 h/48 h/72 h at 4X magnitude (500µm) for each cell line. **D.** Diameters of cell sphere quantification were performed utilizing ImageJ analysis. The graph was plotted with the GraphPad software. (ns: no significant, *p<0.05, ****p<0.0001)

MDC staining was performed to indicate autophagic vacuole formation in MCF-7, MDA-MB-231, and MCF-7/TAMR cell lines respectively. Following the administration of selected doses of EBR and TAM, the addition of 3-MA to the combined treatment for 24 h, induced autophagic vacuole formation as seen in green dots under the fluorescence microscopy Figure 20. MDC-stained vacuole formation increased prominently by the induction of EBR and EBR+TAM combination as well as reduced cell density (Figure 19 A-C and IV). Whereas after the exposure of 3-MA serves as a negative control the autophagic vacuole formation decreased in MCF-7, MDA-MB-231, and MCF-7/TAMR cell lines. Also, cell density of each cell line was increased in the presence of 3-MA (Figure 19 A-C and VII).

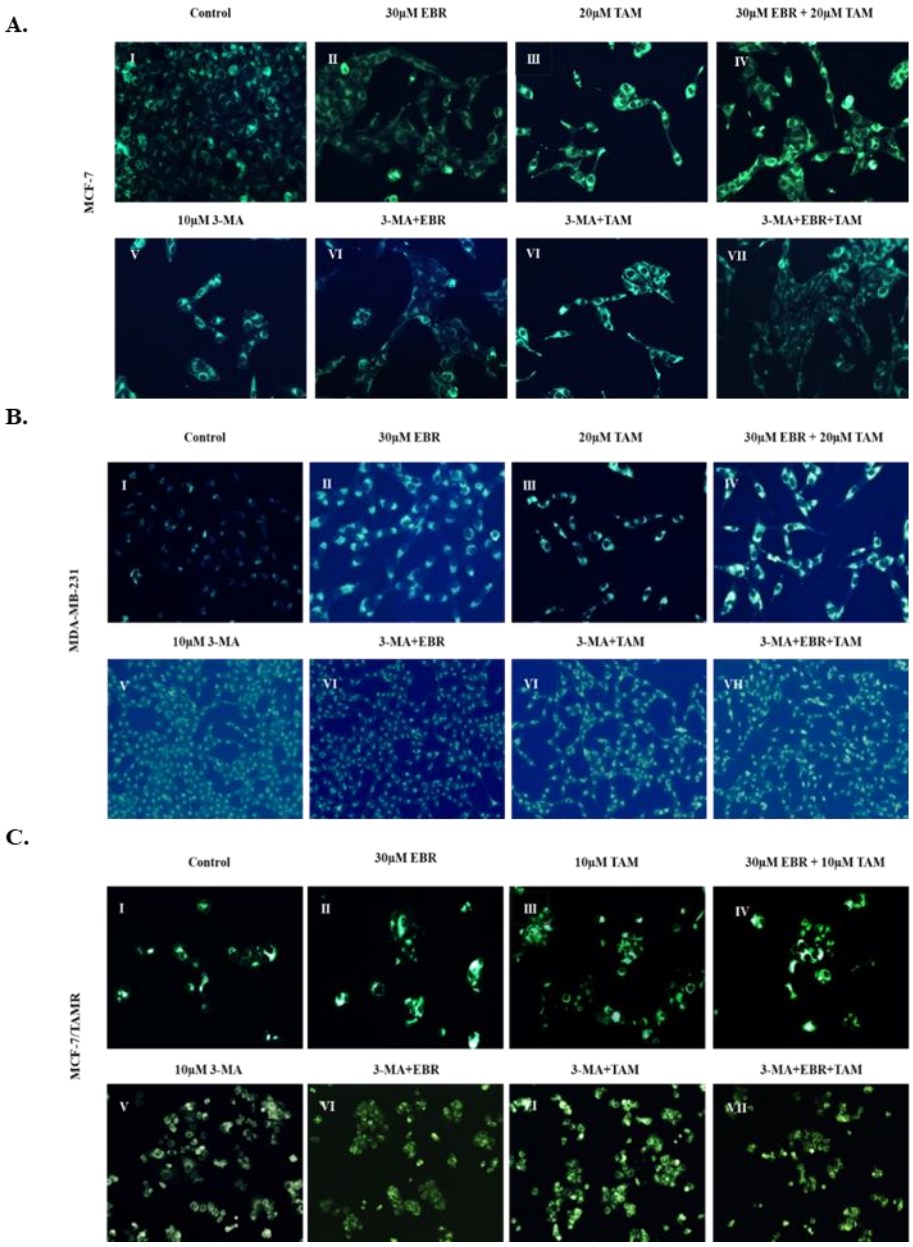

Figure 19. The autophagic vacuole formation was shown following treatment of EBR and TAM combination and reversed with the 3-MA in MCF-7, MDA-MB-231, and MCF-7/TAMR cell lines.
Cells were stained with the MDC following 24 h drug exposure The figures of MCF-7, MDA-MB-231, and MCF-7/TAMR were obtained via confocal microscopy. The results were listed as A-C belonging to MCF-7, MDA-MB-23 MCF-7/TAMR respectively.

The GFP-LC3 transfection was performed to detect the autophagy induction. MCF-7, MCF-7/TAMR, and MDA-MB-231 cells were treated with EBR, TAM, and EBR+TAM, as well as a 3-MA combination version for all these drugs over 24 h. Starvation conditions were applied as a positive control for all cell lines at 24 hr. The LC3 puncta formation was detected in each cell line. In the control conditions which

were taken only GFP-LC3 plasmid was used as a negative control for all cell lines. The LC3 puncta formation was detected slightly in control conditions of MCF-7 cell line compared to control conditions of other cell lines. The combined treatment of EBR and TAM was shown to induce autophagy and further increase the LC3 puncta formation compared to drugs administered alone in all cell lines. Moreover, the cells exposed to EBR+TAM combination with 3-MA indicated reduced puncta formation of LC3 when compared to only the administration of EBR+TAM in all cell lines (Figure 20).

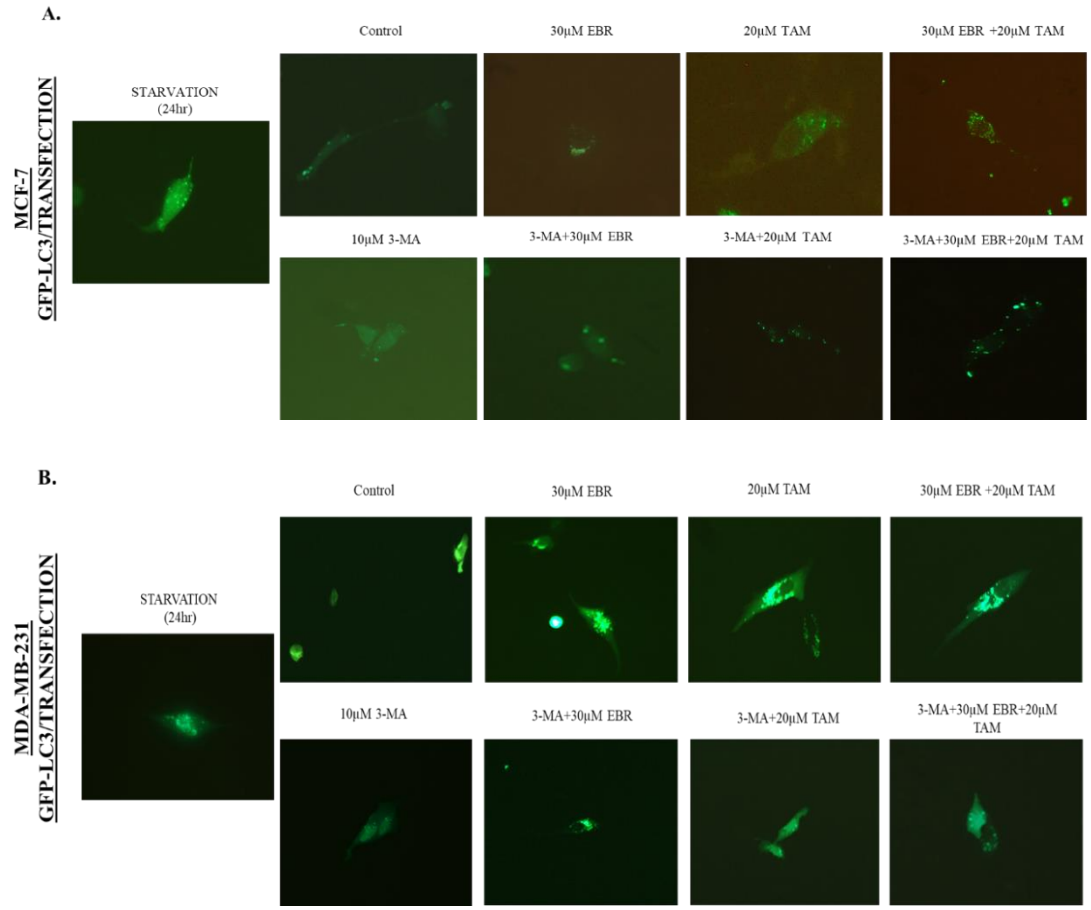

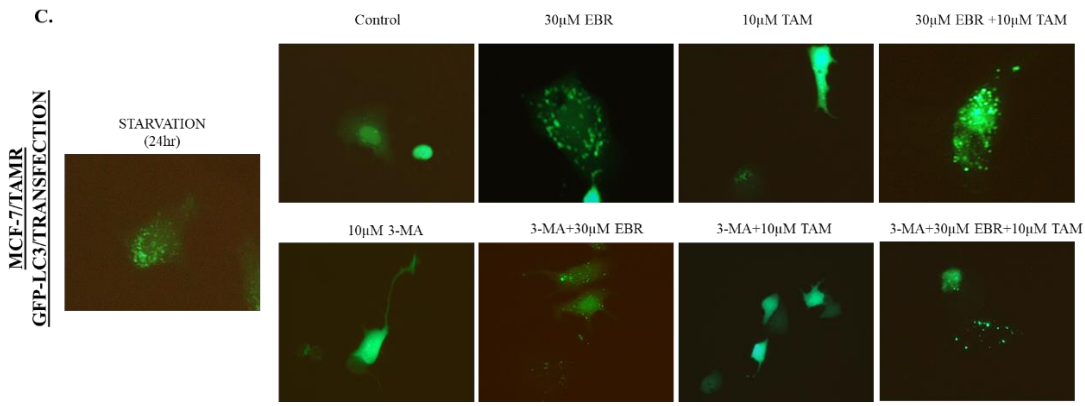

Figure 20. The GFP-LC3 puncta formation was augmented after exposure to EBR+TAM and the puncta formation was decreased in the addition of 3-MA to the combination of EBR+TAM in MCF-7, MDA-MB-231, and MCF-7/TAMR cell lines.
The cells were subjected to 24 h with EBR, TAM, and EBR+TAM. Also, the 3-MA alone or a combination version was administered. Moreover, the starvation media was given to all cell lines for 24 h. After the incubation period was completed, the images of each condition were obtained by confocal microscopy for all cell lines (A-C). The green dots represent the LC3 puncta formation.

3.9. THE EXPRESSIONS OF AUTOPHAGY-RELATED GENES AFTER THE ADMINISTRATION OF EPIBRASSINOLIDE IN COMBINATION WITH TAMOXIFEN WERE EVALUATED IN ALL BREAST CANCER CELL LINES

The effect of EBR, TAM, and EBR in combination with TAM on the expression of the autophagy-related genes was identified via immunoblotting in MCF-7, MDA-MB-231, and MCF-7/TAMR cell lines. These genes harbor Beclin-1, Atg5, and p62. GAPDH was used as a loading control for all cell lines. The Beclin-1 expression was increased with the administration of EBR+TAM in both MCF-7 and MDA-MB-231 cells. The Beclin-1 expression was decreased in MCF-7/TAMR cell lines after the combined treatment. The expression of the Atg5 was upregulated after treatments with EBR+TAM in MCF-7 and MDA-MB-231 cell lines. However, the expression of Atg5 was decreased after EBR+TAM treatment in MCF-7/TAMR cell line. The p62 expression was downregulated with EBR+TAM treatment both in MCF-7 and MDA-MB-231 cell lines. However, the expression of p62 was upregulated with EBR+TAM administration compared to the drug administered alone. The GAPDH was used as housekeeping control.

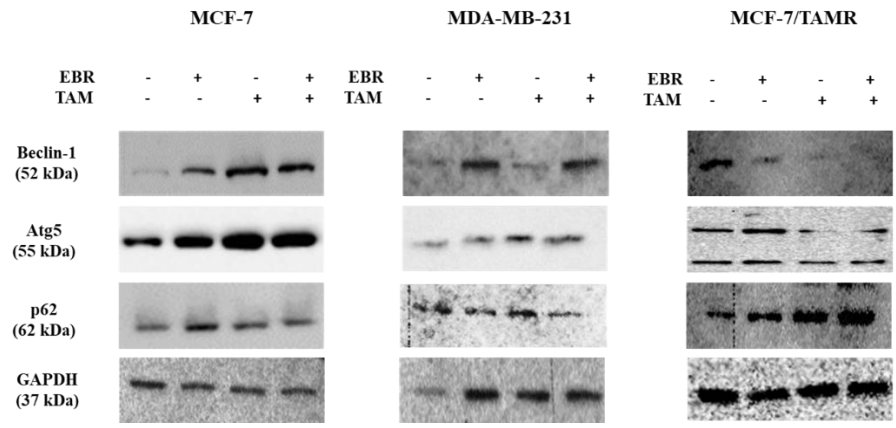

Figure 21. The effect of EBR, TAM, and their combination on the autophagy-related gene markers' expression was investigated on MCF-7, MDA-MB-231, and MCF-7/TAMR cell lines.
Expression of the autophagy-related gene markers including, Beclin-1, Atg5, and p62 were evaluated after the exposure of control, EBR, TAM, and EBR+TAM. GAPDH was used as a loading control. The proteins (25 ug) were loaded onto 12% SDS-PAGE gels.

3.10. THE EPIBRASSINOLIDE AND COMBINED TREATMENT WITH TAMOXIFEN-INDUCED AUTOPHAGY WAS PREVENTED VIA ADDITION OF 3-METHYLADENINE

The expression profiles of autophagy-related markers were evaluated by immunoblotting in all breast cancer cell lines. The expression of Beclin-1 was increased after the exposure of EBR+TAM whereas when the EBR+TAM combined with 3-MA the expression of Beclin-1 was diminished strikingly in both MCF-7 and MDA-MB-231 cell lines. The expression of the Atg5 upregulated in EBR+TAM treatment conditions in MCF-7 but not in MDA-MB-231. EBR+TAM treatment in the presence of 3-MA downregulated the expression of Atg5 in MCF-7 but not in MDA-MB-231. The lipidation of LC3 was detected in the presence of EBR and EBR+TAM conditions of the MCF-7 cell line. Also, the same treatment condition triggered the lipidation of LC3 in MDA-MB-231 cell line. Moreover, when the 3-MA+EBR+TAM treatment was performed, recovery of LC3 was not detected in MCF-7 cell line. However, in the same treatment condition, the expression of LC3I and LC3II was observed nearly the same in MDA-MB-231 cell line. The expression of the p62 downregulated following EBR+TAM treatment in MCF-7 and MDA-MB-231 cell lines. When the 3-MA combined with EBR+TAM the expression of p62 was decreased in MCF-7 cell line. However, p62 expression was increased after administration of the

same condition in MDA-MB-231 cell line. The same autophagic markers will be examined for MCF-7 TAMR. GAPDH was utilized as a loading control.

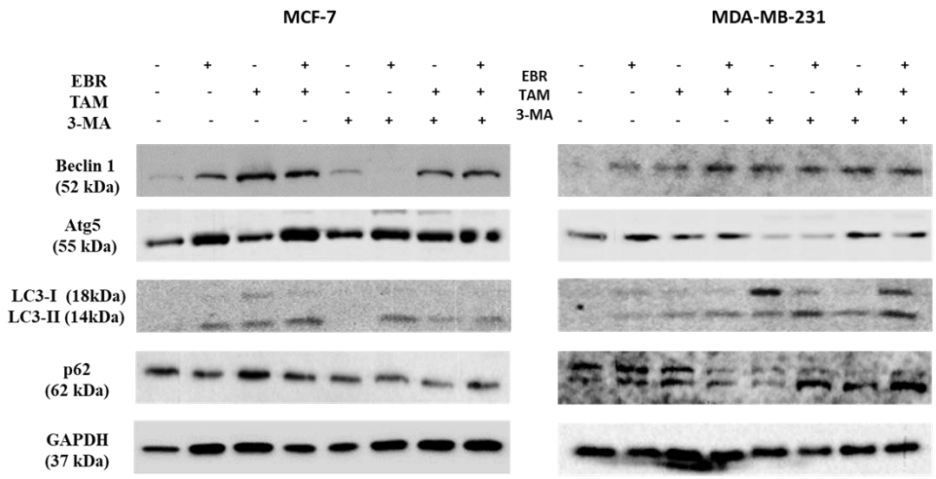

Figure 17. The effect of EBR, TAM, and 3-MA alone or their combination on autophagy-related gene expression was analyzed by immunoblotting. in MCF-7, and MDA-MB-231cell lines.
A total of 25µg cell lysate was loaded in 12% SDS-PAGE gels and probed with Beclin-1, Atg-5, LC3 I/II, and p62 antibodies. GAPDH was used as a loading control.

3.11. THE EXPRESSION CHANGES OF ENDOPLASMIC RETICULUM STRESS MARKERS WERE EVALUATED AFTER THE ADMINISTRATION OF EPIBRASSINOLIDE AND TAMOXIFEN IN THE PRESENCE OF 3-MA IN ALL BREAST CANCER CELL LINES

To analyze the changes in the expression of the ER stress markers, CALR, PDI, and BiP, in the presence of the 3-MA, the immunoblotting technique was performed in MCF-7, MDA-MB-231, and MCF-7/TAMR cell lines. The expression of the CALR was downregulated after the administration of EBR+TAM in both MCF-7 and MCF-7/TAMR cell lines. Whereas in the same condition, the expression of CALR was upregulated in MDA-MB-231 cell line. The presence of 3-MA combination with EBR+TAM increased the expression of CALR in MCF-7 cell line. However, in the same conditions, there was no change in the expression of CALR in MDA-MB-231 cell line compared to EBR+TAM treatment. The CALR expression profiling was decreased after exposure to 3-MA+EBR+TAM in MCF-7/TAMR cell line. Moreover,

the expression of PI was increased following EBR+TAM treatment in all breast cancer cell lines. The PI expression was decreased in EBR+TAM plus 3-MA treatment in all cell lines. The expression of BiP upregulated following EBR+TAM treatment in all cell lines. There was a slight increase in the BiP expression in the presence of 3-MA with EBR+TAM in MCF-7 and MDA-MB-231 cell lines. However, in the same treatment condition, the expression of the BiP was not changed compared to EBR+TAM administration alone in MCF-7/TAMR cell line.

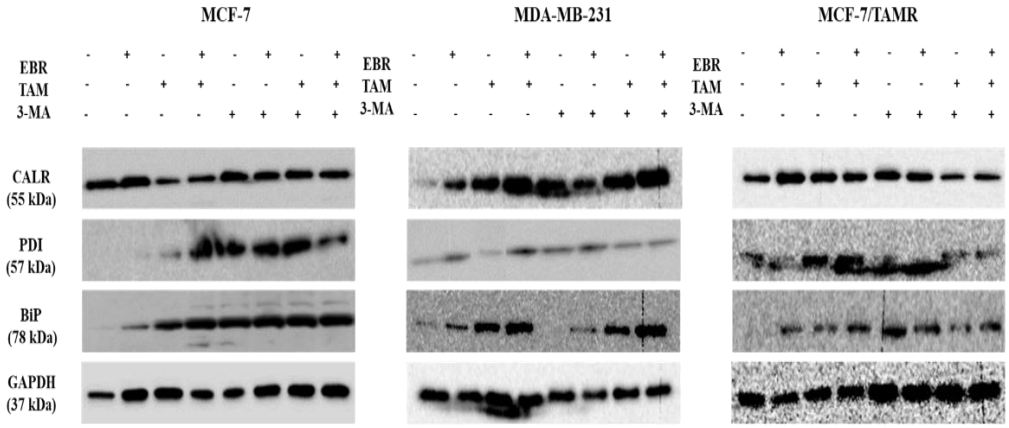

Figure 18. The effect of EBR, TAM, and 3-MA and their combination on the expression of ER stress markers was evaluated in MCF-7, MDA-MB-231, and MCF-7/TAMR cell lines. The expression profiling of CALR, PDI, and BiP were investigated via immunoblotting assay. The GAPDH was used as a loading control.

3.12. THE EXPRESSION CHANGES OF APOPTOSIS MARKERS WERE EVALUATED AFTER EXPOSURE TO EBR AND TAM IN THE PRESENCE OR ABSENCE OF 3-MA

We aimed to determine the expression changes of apoptotic markers including cleaved PARP (c-PARP), caspase 9, and cleaved caspase 3 (c-caspase3) by immunoblotting technique. We exposed selective doses of drugs for EBR and TAM in the presence or absence of the 3-MA. The expression of c-PARP was decreased following the administration of 3-MA+EBR+TAM compared to the administration of EBR+TAM in the MCF-7 cell line. The c-PARP expression was increased in EBR+TAM treatment compared to the administration of EBR and TAM alone in the MDA-MB-231 cell. The immunoblotting analysis indicated that EBR, TAM, and their combination did not affect the expression of c-PARP in the MCF-7/TAMR cell line. The cleaved caspase

9 expression was shown in 3-MA+EBR+TAM condition in MCF-7 cell line. The cleaved caspase 9 expression was decreased slightly when exposed to 3-MA+EBR+TAM condition compared to EBR+TAM condition in MDA-MB-231 cell line. Cleaved caspase 9 expression was upregulated after the exposure of 3-MA+EBR+TAM compared to EBR+TAM treatment in the MCF-7/TAMR cell line. The caspase 3 deficiency was detected in the MCF-7 and MCF-7/TAMR cell lines (Guo et al., 2016). Whereas expression of c-caspase 3 was upregulated in the presence of 3-MA and its combination with EBR, TAM, or EBR+TAM conditions in comparison to the absence of 3-MA conditions in MDA-MB-231 cell line.

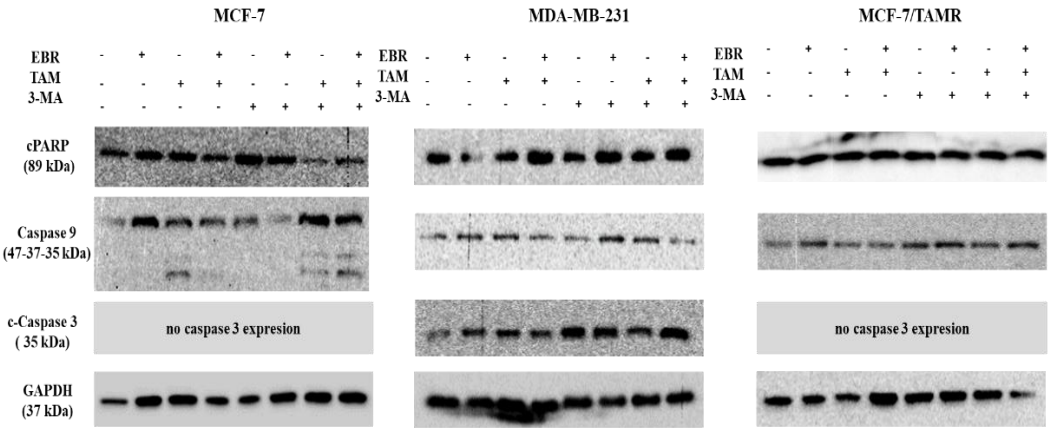

Figure 19. The expression of the apoptotic marker's presence of EBR, TAM, and 3-MA and their combination were analyzed in MCF-7, MDA-MB-231, and MCF-7/TAMR cell lines. Expression changes of c-PARP, caspase 9, and c-caspase 3 were evaluated in the presence of 3-MA. The caspase 3 expression was only detected in MDA-MB-231 cell lines. GAPDH was utilized as a housekeeping marker.

3.13. THE EPIBRASSINOLIDE AND COMBINED TREATMENT WITH TAMOXIFEN DECREASED DRUG RESISTANCE

To evaluate the effect of EBR and / or TAM in terms of the correlation between drug resistance mechanism and autophagy, MRPI (ABCC1), one of the MDR markers, was analyzed in the presence of 3-MA. As seen in Figure 25, after the exposure of EBR + TAM, the expression of the MRP1 was downregulated compared to the administration of EBR and TAM alone in all breast cancer cell lines. The expression of the MRP1 was increased in the presence of 3-MA combined with EBR + TAM conditions in all breast cancer cell lines.

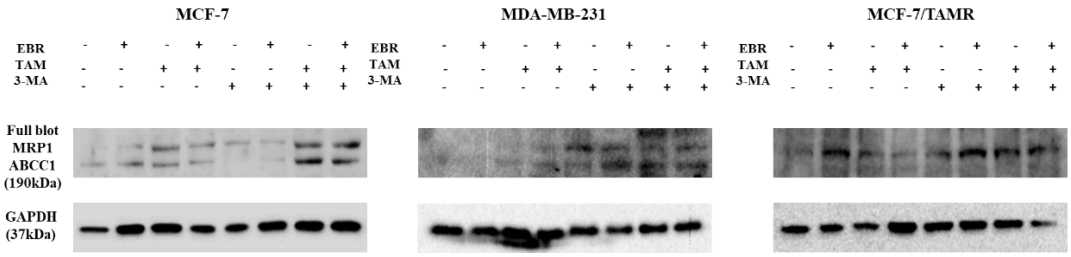

Figure 20. The expression of the MRP1 was decreased following administration of EBR+ TAM and was increased following 3-MA.EBR+TAM treatment in MCF-7, MDA-MB-231, and MCF-7/TAMR cell lines.
Expression changes of the MRP1 (ABCC1) cassette protein were investigated within the EBR, TAM, and 3-MA. The protein was loaded 25 ug on 12% SDS-PAGE. The GAPDH was used as a housekeeping marker.

4. DISCUSSION

BC is the most common type of cancer in women. Based on the molecular characterization 4 main classes for BC are Luminal A and B, HER2 +, and triple-negative BC cells. The most common prevalent BC subtype is estrogen-positive BC. Many treatment approaches for BC have been developed because of its heterogeneous structure (Winters et al., 2017). Some hormonal therapy approaches that either restrict estrogen synthesis or inhibit estrogen binding to its receptors have been developed to prevent progression of the estrogen-positive breast tumors. TAM is the most known SERM-utilized drug in the clinic in both premenopausal and postmenopausal cases. Additionally, its effects on estrogen receptor-negative patients have also been demonstrated in the literature (Croxtall et al., 1997) . However long-term usage of TAM results in disease relapse after a certain period or the development of intrinsic or acquired drug resistance because of the various complex changes that are taking place in the tumor microenvironment. The MDR is one of the main obstacles in current therapy approaches. The seven mechanisms contribute to the MDR. These mechanisms are listed as follows: reduced drug uptake also increased efflux of the drug, modified drug target, activated the detoxification mechanism, provided epigenetic regulation, blocked cell death mechanism, and changed in tumor microenvironment (Qing et al., 2023).

One of the corresponding mechanisms for drug resistance is ER stress (Qing et al., 2023). Any perturbation in the function of the ER results in ER stress. UPR which acts as an adaptive mechanism of the ER stress takes a role in restoring the protein homeostasis in the ER. Three membrane-localized receptors IRE1alpha, PERK, and ATF6 govern these UPR signaling. These proteins transmit UPR signals to the nucleus

via specific pathways, either preventing or promoting ER-stress-related cell death (Sano and Reed, 2013). While at rest, BiP (GRP78) interacts with all these stress sensors in the ER membrane. However, the accumulated misfolded or unfolded proteins remove the BiP from these sensors. This event causes IRE1α and PERK signaling and oligomerization, and transportation of ATF6 to Golgi for activation via proteases S1 and S2 (Bonsignore et al., 2023). These three signaling paths induce the ER chaperons including CALR, CALNX, and PDI to provide proper folding to rescue the cells. These chaperone proteins are also related to the induction of tumor progression (Yadav et al., 2014). Therefore, the targeting of ER stress mechanisms has been seen as a potential therapeutic approach for cancer therapy.

Many approaches have been found to cope with drug resistance besides the ER stress in literature. Autophagy is one of the other corresponding strategies for drug resistance mechanisms (İsaoğlu et al., 2020). Autophagy is vital for maintaining cellular homeostasis by eliminating damaged or unnecessary components that harbor proteins and organelles through controlled degradation. It can be triggered via various stimuli such as stress, nutrition deprivation, low oxygen levels, and energy deficits. The Pı3K/Akt/mTOR signaling paths are highly correlated with ER stress according to previous research (Y. Lin et al., 2019). This stress stimulus inhibits the mTOR signaling, this way, it leads to the activation of autophagy-promoting synthesis proteins needed for autophagy and produces autophagosomes. As a result of the formation of autophagosomes this fuse with the lysosomes to form autophagolysosomes complex for the degradation of unnecessary cellular components for recycling them. The effect of autophagy on cancer is double-edged. Whereas the basal level of autophagy seems in cytoprotective role for cancer cells, sustained autophagy can lead to cell death via self-degradation of tumor cells. Intercalary, a multifaceted relationship has been found between autophagy and drug resistance in cancer. Autophagy contributes to resistance by promoting cancer cells to survive against chemotherapy or targeted therapy. It also sensitizes them to treatment-induced stress via increasing drug effectiveness. This interaction varies depending on factors such as the type of cancer, specific drugs, and cellular conditions, highlighting the importance of understanding it for improving cancer treatment (Sameiyan et al., 2019).

Recent years have seen a significant increase in interest in the use of natural product components for cancer prevention and therapy. Brassinosteroids (BRs) which are plant steroid hormones take a critical role in plant development. Currently, studies on these hormones are being conducted because of the finding of anti-cancer effects without affecting normal cells in research (Kaur Kohli et al., 2020). Two of these have been found the most current and promising anti-cancer properties, 24- homocastasterone and EBR. In Malikova's study, which was the first study of these hormones, the anti-cancer and anti-proliferative effects of these BRs have been indicated. In this investigation, they put forward that the inhibitory effect of BRs at micromolar concentrations in prostate and BC cell lines including LNCaP/DU-145, and MCF-7/MDA-MB-468 cells in order with the minimal effects on normal cell lines (Malíková et al., 2008). BRs' similarity to steroid-like composition led to the first assumption that they exclusively affected hormones, such as NHR inhibitors. However, much research indicated that EBR leads to cell death in both NHR-expressing and non-expressing cancer cells (Huskova et al., 2020; Malíková et al., 2008; Steigerová et al., 2010, 2012). Furthermore, our earlier research showed that there was no change in cell viability in mouse embryonic fibroblast cells (MEF) following the EBR therapy (Adacan and Obakan-Yerlikaya, 2020a). This shows that natural BRs cause different reactions in cancer and normal cells, showing a high therapeutic index due to their selective cytotoxicity on cancer cell lines rather than untransformed human fibroblasts (Huskova et al., 2020).

In our study, we used the three different BC cell lines including MCF-7/TAMR, MCF-7, and MDA-MB-231 cells for the investigation of the effect of EBR in terms of autophagy induction via overcoming resistance through the ER stress. Our lab already demonstrated that EBR and TAM combined treatment decreased cell viability significantly compared to drug-alone conditions in hormone-sensitive/insensitive cell lines, MCF-7 and MDA-MB-231 respectively. At the beginning of this study, we evaluated the anti-proliferative effect of EBR in combination with TAM on the MCF-7/TAMR cell line. Firstly, the TAM-resistant dose for MCF-7/TAMR cells was determined by the MTT assay which is one of the cell viability assays. In the literature, different TAM-resistant doses were detected (Actis et al., 2021). Our results showed no significant changes in cell viability after exposure to the different doses of TAM

(10,15 and 20μM). This result represents acquired drug resistance in MCF-7/TAMR cells to TAM. As a further step, the 30μM dose of EBR which was determined based on our previous study was administered individually and in combination with TAM on the MCF-7/TAMR cell line (Adacan and Obakan Yerlikaya, 2020b). These results showed that the resistance developed against TAM drastically reduced in 30μM EBR combination with 10μM TAM in 24 h due to increases in the loss of cell viability. It means that the antiproliferative effect of the TAM was increased with the combination of the EBR. In literature as a natural compound, the synergistic effect of TAM with sulforaphane or erucin which are the members of isothiocyanates (ITC) that are phytochemicals found naturally in cruciferous plants also detected in MCF-7/TAMR cells (Pawlik et al., 2016). Furthermore, in the literature, *Antrodia cinnamomea* extract combined treatment with TAM demonstrated cell proliferation inhibition in MCF-7/TAMR cells (Y.-S. Lin et al., 2018). Also, the synergistic effect of EBR was detected by Yerlikaya et al., (2022). The EBR enhances the apoptotic effect of gemcitabine in pancreatic cancer cell lines (Yerlikaya and Naxmedova, 2022). Furthermore, in our study, the effect of the EBR+TAM on survival was evaluated in a time-dependent manner. The cytotoxic effect of EBR in combination with TAM was detected in 24 h. Also, the cytostatic effect was detected at 48 h and 72 h. In previous experiments, combining TAM with persin, one of the plant toxins, indicated cytotoxic synergy in the MCF-7/TAMR cell line (McCloy et al., 2013).

The effect of EBR through the inhibition of cell proliferation has been shown in various types of cancer including prostate, pancreatic, lung, colon, and BC (Coskun et al., 2015; Huskova et al., 2020; Malíková et al., 2008; Sadava and Chen, 2023; Steigerová et al., 2010, 2012; Yerlikaya and Naxmedova, 2022). In this research response of the EBR slightly differs for each type of cancer. Moreover, the inhibition of cell proliferation after TAM administration has been detected in several cancer types such as breast, liver, and ovaries (Sanaei et al., 2017). Besides the cell proliferation inhibition, the effect of colony formation potential of EBR and TAM was analyzed in MCF-7/TAMR cells with both 2D and 3D cell culture techniques. In a previous study, colony numbers were reduced after exposure to the EBR in PANC-1 and MIA PaCa-2 cell lines (Yerlikaya et al., 2022). Moreover, colony formation potential declined after TAM was administered in MCF-7 cell line (Abdallah et al., 2020). In our

investigation, we found that cotreatment EBR with TAM significantly decreased the colony numbers in MCF-7/TAMR cell line. In literature TAM combination with other natural drugs also decreased the colony formation ability, particularly in breast cancer cell lines (Mandal et al., 2023; Wang et al., 2021). For instance, TAM combined with D-limonene resulted in the decreasing colony formation ability of MCF-7 cells (Mandal et al., 2023). Furthermore, to mimic the 3D form of the tumors in cell culture, the hanging drop analysis was performed (Foty, 2011). In the literature, spheroid diameters were decreased after the exposure of the 30μM EBR in SW480 and DLD-1 cells (Obakan Yerlikaya et al., 2023). In our investigation, we found that the sphere forms of a control group and TAM-given only groups were the same, whereas sphere formation was disrupted after the exposure of EBR in combination with TAM in MCF-7/TAMR cell lines.

The diminishing of the MMP is generally observed during the apoptotic process (Métivier et al., 1998)**.** In literature, the decreasing MMP was detected after exposing EBR to pancreatic cells (Yerlikaya et al., 2022). Similar results were obtained in our study indicating that the EBR combined with TAM exposure after 24 h diminished the numbers of DiOC6 cells significantly in MCF-7/TAMR. Moreover, in the literature, TAM combined with D-limonene enhanced DNA fragmentation in MCF-7 cells compared to drug exposure alone (Mandal et al., 2023). Our study also indicated that combination therapy increased cell death numbers compared to EBR and TAM administration alone in MCF-7/TAMR cells.

The cell cycle represents a sequence of events within a cell that orchestrates a cell progression facilitating division and replication. According to the literature, the G1 to S transition in the cell cycle was increased in MCF-7 /TAMR cells in contrast to MCF-7 cells (Moon et al., 2021). In our investigation, we want to evaluate the effect of EBR+TAM combination through the cell cycle progression in MCF-/TAMR cells. Previous studies highlighted the role of EBR in cancer therapy via triggering cell cycle arrest at G1 stages (Steigerová et al., 2010). Similarly, research regarding TAM has been indicated to have G1 cell cycle arrest in various cancer cells (Mandal et al., 2023; Sanaei et al., 2017). Moreover, combining TAM with naringenin caused cell cycle blocking at G2 /M stages in the MCF-7 cell line (Z. Xu et al., 2018). In other studies, combined treatment of TAM with celastrol leads to cell cycle arrest at the G1 phase in

the MCF-7 cell line (Wang et al., 2021). Our findings revealed that the EBR+TAM combination caused the G1 arrest in the MCF-/TAMR cell line. These results suggested that EBR and TAM in combination may have a considerable effect on the suppression of cancer cell proliferation.

ER stress has been implicated in several stages of tumor formation. Extensive research indicates that UPR plays an essential role in the cancer cell's ability to maintain their malignancy and resistance to therapy (Bonsignore et al., 2023). For instance, TAM can activate UPR proteins harboring BiP and LAMP3, this makes cells more resistant to TAM (Nagelkerke et al., 2014). Furthermore, in earlier research, key elements of the ER stress pathway have been connected to endocrine response (McCloy et al., 2013). Recent investigations have found that alterations in BiP and CHOP are linked to the response of TAM, harboring reversing resistance (Brüning et al., 2010; Tiwary et al., 2011). EBR is triggering the ER stress mechanism was evaluated in the previous studies via SILAC and mass spectrometry approaches. In a study, the increased expression of CALR and CALNX was detected when the pancreatic cancer cells were exposed to EBR (Yerlikaya et al., 2022). Moreover, in a research, TAM, and combination with persin increased the expression of the ER stress response by upregulating ER stress markers which are BiP, CHOP, and XBP-1 in the MCF-7/TAMR cell line (McCloy et al., 2013). In our study, we evaluated the effect of EBR in combination with TAM on expression changes in ER stress markers in MCF-7/TAMR cells. As a result of immunoblotting, EBR in combination with TAM increased the expression of the UPR sensors (PERK, IRE1α, and ATF6), chaperons' proteins (CALR and PDI) also BiP compared to drugs administration alone. Tun was found a positive control for ER stress induction (Luhr et al., 2019). These results indicated that EBR+TAM contributes to the ER stress mechanism in MCF-7/TAMR cells. This upregulation of ER stress markers might be associated with the developing resistance mechanisms against the chemotherapeutic drugs. In this case, targeting UPR components or the related signaling mechanism has been seen as one of the treatment strategies nowadays (Bonsignore et al., 2023).

Within the tumor microenvironment, cancer cells proliferate in a persistent environment of stress. Metabolic and pharmacological stress triggers several processes for maintaining cell homeostasis such as autophagy. Previous studies put forward that

one of the contributing mechanisms of autophagy is ER stress (Amaravadi et al., 2019). Each of the UPR arms contributes to the induction of autophagy (Song et al., 2018). Our next step was to examine whether ER stress activation contributes to the induction of autophagy in BC cells treated with EBR+TAM. For this purpose, we investigated the effect of EBR in combination with TAM combined with the 3-MA, which is one of the early-stage autophagy inhibitors, on ER stress markers (Tran et al., 2015). To detect the ER stress contributing to autophagy in distinct BC cell lines including MDA-MB-231 and MCF-7 hormone-insensitive/sensitive cells besides the MCF-7/TAMR resistance cell line.

Before revealing the relationship between ER stress and autophagy, autophagy was first intended to be demonstrated. To assess whether autophagy triggered by EBR+TAM promotes survival or death, as a first step, an MTT assay was done for all cell lines to select the dose of 3-MA either alone or in combination with EBR and TAM. The dose of EBR was the same as 30μM for the all-cell line for co-treatment, however, the dose of TAM differed compared to MCF-7/TAMR and the other two cell lines. Our previous studies indicated the synergistic effect of TAM and EBR was determined at 20μM and 30μM respectively for both MCF-7 and MDA-MB-231 cell lines. At the same time, the MCF-7/TAMR cell line exhibited drug resistance even for a similar dose. Therefore, TAM concentrations were selected as 10μM for the MCF-7/TAMR cell line. in the literature, cytotoxicity of TAM in MCF-7 cells was suppressed with the addition of 3-MA (Kanematsu et al., 2010). Similarly, our results demonstrated that the reconstructed cell viability was detected when the 10μM 3-MA was combined with EBR+TAM in all cell lines.

Autophagy has a paradoxical role in tumor progression The cytoprotective and cytotoxic properties change regarding the duration of stress stimulus. Moreover, the nature of the cancer cells also affects the tendency of autophagy. The tendency of autophagy is distinct based on the different natures of BC cells. MCF-7/TAMR cell lines are more potent in demonstrating autophagy induction (Actis et al., 2021; Finnegan et al., 2022). Therefore, previous research identified that suppressing autophagy might be used to re-sensitize TAM-resistant BC cell lines (Wen et al., 2020). On the other hand, one study demonstrated that induction of autophagy was seen as a potential therapeutic approach to preventing tumor progression in TNBC

cells (Zhao et al., 2024). In this study, the effect of EBR+TAM on autophagy was investigated using MDC and GFP-LC3 methods (Klionsky et al., 2016; Verwey et al., 2016). One of the previous studies demonstrated that induction of autophagy was mediated by the EBR administration detecting autophagosome formation in colon cancer cell lines (Adacan and Obakan Yerlikaya, 2020b). Moreover, after exposure to TAM in MDA-MB-231 cell line observed that the number of autophagic vacuoles increased (SWu et al., 2016). Moreover Qadir et al., study indicated that following TAM treatment increased punctate staining cells which were stained with MDC in MCF-7 cell line (Qadir et al., 2008). In our research, MCF-7, MDA-MB-231, and MCF-7/TAMR cells treated with EBR combined with a selected dose of TAM over 24 h indicated increased autophagic vacuole formation. After the addition of 3-MA in EBR+TAM combination vacuoles number decreased but was not eliminated completely. This may be due to the off-target effects of 3-MA (Qadir et al., 2008).

Previous studies indicated that induction of ER stress leads to activation of LC3 lipidation in MEF cells after exposure to EBR (Adacan and Obakan-Yerlikaya, 2020b). In the literature, the quantity of LC3 puncta augmented following TAM treatment in both MCF-7 and MCF-7/TAMR cells but declined following the 3-MA combination (Li et al., 2022). In contrast, another investigation revealed that LC3 puncta formation raised after exposing bafilomycin, which is one type of autophagy inhibitor, with tamoxifen in both MCF-7 and MCF-7/TAMR cell lines (Lee et al., 2018). Deprivation of serum increased the autophagy detected in various cell lines such as MDA-MB-231, MCF-7, and LNCaP cells (De et al., 2019). Similarly in our investigation puncta formation was shown in the starvation conditions of autophagy in all breast cancer cell lines. Moreover, a notable rise in the LC3 puncta formation resulted following EBR+TAM administration in all breast cancer cells. However, the synergistic effect of these drugs was reversed in all cell lines.

Previous research revealed that ER stress is one of the triggering mechanisms for autophagy (Oh and Lim, 2009). One of the studies indicated that LC3 conversion was mediated via activation of the PERK/eIF2α pathway (Kouroku et al., 2007). Moreover, Ogata et al., (2006) study demonstrated that autophagosome formation was observed both in starvation and ER stressors in MDA-MB-231 cell line (Ogata et al., 2006). Moreover, one study indicated that TAM resistance was mediated with BiP via

triggering autophagy (Cook et al., 2012). The induction of autophagy by EBR through the ER stress was identified in the SCID mouse xenograft model, inhibiting the growth of colon cancer (Obakan Yerlikaya et al., 2023). Moreover, in other studies, the TAM induced ER stress by activating the AMPK/mTOR pathway which is the master regulator of the autophagy process in the TNBC cell line (Wu et al., 2016). Our study evaluated the expression of the ER stress markers in all cell lines following administration of solely EBR, TAM, and 3-MA or in combination. Previous studies found that CALR, ER stress-related chaperone, was a principal target of EBR-mediated apoptosis. The decreasing or increasing CALR expression was also detected after the administration of EBR in different colon cancer patients. However, the same study revealed that there was an increase in the expression level of most of the ER stress markers (Obakan et al., 2015). In our research, the expression of CALR was decreased after exposure to EBR+TAM in estrogen-sensitive cell lines, however, upregulated expression of CALR was detected in MDA-MB-231 cell line. When 3-MA was administered with EBR and TAM, it was observed that CALR expression was completely reversed compared to drug exposure alone. This different response may be due to the heterogenic nature of breast cancer cells. Moreover, the level of BiP expression was augmented following EBR+TAM exposure in our study. In terms of mechanism, BiP signaling might suppress apoptosis and trigger autophagy to assist cells in coping with stress by inhibiting mTOR function and indirectly fostering activation of Bec1in-1 within breast cancer cell lines (Q. Wu et al., 2023). The double-sided effect of PDI and autophagy was detected in the literature (Wang et al., 2022). In our study, the expression of PDI was upregulated after exposure to EBR+TAM and reversed in the presence of 3-MA. In this context, it can be said that it takes a role in mediating of autophagy process.

Our experiment also continued by analyzing the effect of EBR+TAM on autophagy markers. Previous studies demonstrated the EBR-induced autophagy effect (Adacan and Obakan Yerlikaya, 2020b). TAM is seen as an autophagy inducer affecting several autophagy-related genes (Actis et al., 2021; Boretto et al., 2023). For instance, the effect of TAM through autophagy induction was evaluated in the MDA-MB-231 cell line (S.T. Wu et al., 2016). According to the literature, the increasing expression of Beclin-1, Atg-related genes, LC3-II, and decreasing expression of p62 seem to be core

markers for the detection of autophagy. In our study, we performed immunoblotting analysis with those markers within the presence of 3-MA. The presence of the 3-MA results in the decreasing expression of those markers compared to 3-MA absence version. For instance, the TAM in combination with 3-MA decreases the LC3-II expression compared to TAM given alone (Samaddar et al., 2008). A study supporting our results indicated that inhibition of autophagy was carried out via 3-MA in this way increasing cell survival in both MCF-7 and MDA-MB-231 cell lines were detected (Lee et al., 2012; Verwey et al., 2016).In the literature, a combination of TAM and ITC resulted in lipidation of LC3 (Pawlik et al., 2016). Moreover, TAM combined with celastrol demonstrated a synergistic effect on autophagy through lipidation of LC3 and decreased the p62 expression in the MCF-7 cell line Wang et al., 2021). In our study, after EBR combination with TAM, the LC3-II expression, which is one of the characteristic markers for the autophagy process, was increased in MCF-7 and MDA-MB-231 cell lines. However, the lipidation of LC3 was decreased after the addition of 3-MA within EBR +TAM condition in MDA-MB-231 cell line whereas not in the MCF-7 cell line. This means the recovery of autophagy was not detected in MCF-7 cells compared to MDA-MB-231 cells. Sequestration of the p62, which is a critical autophagy receptor, was detected in both MCF-7 and MDA-MB-231 cell lines following EBR+TAM exposure. However, the expression of the p62 elevated after exposure to the 3-MA plus EBR in combination with TAM in MDA-MB-231 cell line. Also, the expression of p62 was elevated after EBR+TAM administration in MCF-7/TAMR cells. According to the literature, accumulation of p62 was detected in the inhibition of autophagy. (Liu et al., 2019). Expression of Beclin-1 was increased following EBR +TAM conditions in MCF-7 and MDA-MB-231 cell lines. Whereas in the presence of 3-MA with the same conditions, Beclin-1 expression was slightly decreased both in two cell lines. However, the expression of Beclin-1 in EBR+TAM condition was downregulated in MCF-7/TAMR cells. This result is contrary to the literature. However, in the literature, the highest expression of Beclin-1 was detected after the administration of TAM in MCF-7/TAMR cells compared to MCF-7 (Liu et al., 2019). The expression of Atg5 was upregulated after exposure to the EBR and TAM in MCF-7 cells. However, no change in the expression of Atg5 was seen in MDA-MB-231 cell line following the same treatment conditions. On the one hand, the

Atg5 expression in Mcf-7/TAMR was decreased with EBR+TAM treatment. These may be due to Atg5/7-independent induction of autophagy. In the literature, Atg5/7 independent macroautophagy has been detected in mice (Nishida et al., 2009). In addition, it has been shown in the literature, that EBR-induced autophagy was independent of Atg5/7 (Adacan and Obakan-Yerlikaya, 2020a). On the other hand, the expression of another autophagy marker could not be measured in the MCF-7/TAMR cell line. The analysis of this marker will be performed in the future both in combination with 3-MA or alone treatment conditions.

Autophagy is one of the critical mechanisms contributing to drug resistance (Chang and Zou, 2020). Nowadays much research indicates that autophagy induction has been seen as one of the contributors to therapy resistance in breast cancer cells (Liu et al., 2019). In a further step of these experiments, we focused on autophagy and drug resistance mechanism relationships. Elevated expression of the ABC transporters' proteins harbor MRP1 (ABCC1), ABCB1, and ABCB2 accompanied the TAM resistance (Guney Eskiler et al., 2016). In the literature, many studies focused on TAM resistance mechanisms and autophagy (Finnegan et al., 2022). According to an investigation, ER stress-triggered autophagy increased intracellular drug efflux via upregulation expression of MRP1 (Chang and Zou., 2020). MCF-7 TAMR cell lines are prone to autophagy to contribute to the resistance mechanism (Boretto et al., 2023). Nowadays, to combat drug resistance against TAM, combination therapy approaches to increase the sensitivity of TAM have been the subject of research articles. One of them is that BreastDefend (BD), is a dietary supplement, and TAM reduces the proliferation of MCF-7 cells in *vitro* and tumor progression in *vivo*, leading to cell death through apoptosis and/or modulation of TAM resistance proteins (Cheng et al., 2017). Our study has been presented similarly to these studies. In this research, we aimed to overcome TAM resistance by increasing the effectiveness of TAM via EBR and TAM combined treatment. Our immunoblotting assay indicated that 3-MA addition restored the expression of MRP1 which was downregulated after exposure to EBR+TAM conditions. These results revealed that EBR and TAM act synergistically against the resistance of breast cancer cells by suppressing the expression of the MRP1. We also showed that this suppression occurs through the triggering of autophagy.

The relationship between autophagy and apoptosis is unclear. There are three types of interactions between autophagy and apoptosis: (a) synergistic or collaborative effect, where both promote cell death; (b) promoting effect, where autophagy induces apoptosis; and (c) antagonistic effect, where autophagy inhibits apoptosis-induced cell death (Das et al., 2021). For instance, celastrol is one of the traditional Chinese Medicines that heightened the sensitivity of TAM by triggering apoptosis and autophagy (Wang et al., 2021). In the current study, the apoptotic biomarkers including PARP, caspase-9, and caspase-3 were investigated within the presence and absence of 3-MA and drug combinations to explore the possible correlation of EBR+TAM-induced autophagy with apoptosis. The addition of 3-MA partially reduced the cleaved PARP expression in MCF-7 cell lines compared to EBR+TAM administered alone. Similarly in the literature inhibition of autophagy partially decreased the cleavage of caspase 3 and PARP in C42 cell line (Zhang et al., 2011). No significant changes were observed in PARP expression for TAMR, which is controversial in the literature.

In literature, caffeic acid phenethyl ester (CAPE) and TAM combination enhances the cleaved caspase 9 expression which is the marker for the apoptosis in the MCF-7 cell line. On the controversy, this combination did not affect the lipidation of LC3 (Motawi et al., 2016). However, in literature inhibition of autophagy leads to apoptosis (Kanematsu et al., 2010). In our study when we look at the caspase 9 expression, TAM combination with EBR suppresses the apoptosis and leads to autophagy in all breast cancer cell lines. When the autophagy was inhibited with 3-MA within these conditions the expression of cleavage caspase-9 increased in MCF-7. Moreover, caspase 9 expression was decreased in both MDA-MB-231 and MCF-7/TAMR cell lines. The caspase-3 expression was not detected in the literature in MCF-7 and MCF-7/TAMR cell lines (Guo et al., 2016). In our study, cleaved caspase-3 detection was only observed in the MDA-MB-231cell line. The cleaved caspase-3 expression decreased in EBR in combination with TAM, whereas when the 3-MA was added to drugs the cleaved caspase-3 expression augmented. Our results indicated that autophagy inhibition leads to caspase-dependent apoptosis.

The development of TAM resistance is virtually unavoidable caussing significant therapeutic concern. ER stress is an important driver of a resistance mechanism. It takes a critical role in the decision of cell death either survival or death triggering

apoptosis or autophagy based on the stress level. Combination therapy with synthetic and natural medicines has been proposed to alleviate tamoxifen's side effects and drug resistance (Wang et al., 2021). In conclusion, our investigation indicated the synergistic effect of EBR with TAM can lead to stress-mediated autophagy induction to cope with drug resistance.

5. REFERENCES

Abdallah, M. E., El-Readi, M. Z., Althubiti, M. A., Almaimani, R. A., Ismail, A. M., Idris, S., Refaat, B., Almalki, W. H., Babakr, A. T., Mukhtar, M. H., Abdalla, A. N., & Idris, O. F. (2020). Tamoxifen and the PI3K Inhibitor: LY294002 Synergistically Induce Apoptosis and Cell Cycle Arrest in Breast Cancer MCF-7 Cells. *Molecules*, *25*(15), 3355. doi: 10.3390/molecules25153355

Actis, C., Muzio, G., & Autelli, R. (2021). Autophagy Triggers Tamoxifen Resistance in Human Breast Cancer Cells by Preventing Drug-Induced Lysosomal Damage. *Cancers*, *13*(6), 1252. doi: 10.3390/cancers13061252

Adacan, K., Obakan-Yerlikaya, P., Arisan, E. D., Coker-Gurkan, A., Kaya, R. I., & Palavan-Unsal, N. (2020a). Epibrassinolide-induced autophagy occurs in an Atg5-independent manner due to endoplasmic stress induction in MEF cells. *Amino Acids*, *52*(6–7), 871–891. doi: 10.1007/s00726-020-02857-w

Adacan, K., & Obakan Yerlİkaya, P. (2020b). Epibrassinolide activates AKT to trigger autophagy with polyamine metabolism in SW480 and DLD-1 colon cancer cell lines. *Turkish Journal of Biology = Turk Biyoloji Dergisi*, *44*(6), 417–426. doi: 10.3906/biy-2005-37

Ahmed, N. S., Samec, M., Liskova, A., Kubatka, P., & Saso, L. (2021). Tamoxifen and oxidative stress: an overlooked connection. *Discover Oncology*, *12*(1), 17. doi: 10.1007/s12672-021-00411-y

Alvarez-Meythaler, J. G., Garcia-Mayea, Y., Mir, C., Kondoh, H., & LLeonart, M. E. (2020). Autophagy Takes Center Stage as a Possible Cancer Hallmark. In Frontiers in Oncology (Vol. 10). Frontiers Media S.A. doi: 10.3389/fonc.2020.586069

Amaravadi, R. K., Kimmelman, A. C., & Debnath, J. (2019). Targeting Autophagy in Cancer: Recent Advances and Future Directions. *Cancer Discovery*, *9*(9), 1167–1181. doi: 10.1158/2159-8290.CD-19-0292

Auzmendi-Iriarte, J., & Matheu, A. (2021). Impact of Chaperone-Mediated Autophagy in Brain Aging: Neurodegenerative Diseases and Glioblastoma. *Frontiers in Aging Neuroscience*, *12*. doi: 10.3389/fnagi.2020.630743

Banerjee, I. A., Fath, K. R., Frayne, S. H., Hugo, M. M., & Cohen, B. (2019). Development of self-assembled phytosterol based nanoassemblies as vehicles for enhanced uptake of doxorubicin to HeLa cells. *Materials Science and Engineering: C*, *97*, 451–460. doi: 10.1016/j.msec.2018.12.037

Barazetti, J. F., Jucoski, T. S., Carvalho, T. M., Veiga, R. N., Kohler, A. F., Baig, J., Al Bizri, H., Gradia, D. F., Mader, S., & Carvalho de Oliveira, J. (2021). From Micro to Long: Non-Coding RNAs in Tamoxifen Resistance of Breast Cancer Cells. *Cancers*, *13*(15), 3688. doi: 10.3390/cancers13153688

Bekele, R. T., Venkatraman, G., Liu, R.-Z., Tang, X., Mi, S., Benesch, M. G. K., Mackey, J. R., Godbout, R., Curtis, J. M., McMullen, T. P. W., & Brindley, D. N. (2016). Oxidative stress contributes to the tamoxifen-induced killing of breast cancer cells: implications for tamoxifen therapy and resistance. *Scientific Reports*, *6*(1), 21164. doi: 10.1038/srep21164

BeLow, M., & Osipo, C. (2020). Notch Signaling in Breast Cancer: A Role in Drug Resistance. In Cells (Vol. 9, Issue 10). NLM (Medline). doi: 10.3390/cells9102204

Bonsignore, G., Martinotti, S., & Ranzato, E. (2023). Endoplasmic Reticulum Stress and Cancer: Could Unfolded Protein Response Be a Druggable Target for Cancer Therapy? *International Journal of Molecular Sciences*, *24*(2), 1566. doi: 10.3390/ijms24021566

Boretto, C., Actis, C., Faris, P., Cordero, F., Beccuti, M., Ferrero, G., Muzio, G., Moccia, F., & Autelli, R. (2023). Tamoxifen Activates Transcription Factor EB and Triggers Protective Autophagy in Breast Cancer Cells by Inducing Lysosomal Calcium Release: A Gateway to the Onset of Endocrine

Resistance. *International Journal of Molecular Sciences*, *25*(1), 458. doi: 10.3390/ijms25010458

Brüning, A., Friese, K., Burges, A., & Mylonas, I. (2010). Tamoxifen enhances the cytotoxic effects of nelfinavir in breast cancer cells. *Breast Cancer Research*, *12*(4), R45. doi: 10.1186/bcr2602

Chang, H., & Zou, Z. (2020). Targeting autophagy to overcome drug resistance: further developments. *Journal of Hematology & Oncology*, *13*(1), 159. doi: 10.1186/s13045-020-01000-2

Chavez-Dominguez, R., Perez-Medina, M., Lopez-Gonzalez, J. S., Galicia-Velasco, M., & Aguilar-Cazares, D. (2020). The Double-Edge Sword of Autophagy in Cancer: From Tumor Suppression to Pro-tumor Activity. *Frontiers in Oncology*, *10*. doi: 10.3389/fonc.2020.578418

Chen, X., & Cubillos-Ruiz, J. R. (2021). Endoplasmic reticulum stress signals in the tumour and its microenvironment. *Nature Reviews Cancer*, *21*(2), 71–88. doi: 10.1038/s41568-020-00312-2

Cheng, S., Castillo, V., Welty, M., Alvarado, M., Eliaz, I., Temm, C. J., Sandusky, G. E., & Sliva, D. (2017). BreastDefend enhances effect of tamoxifen in estrogen receptor-positive human breast cancer in vitro and in vivo. *BMC Complementary and Alternative Medicine*, *17*(1), 115. doi: 10.1186/s12906-017-1621-7

Clusan, L., Ferrière, F., Flouriot, G., & Pakdel, F. (2023). A Basic Review on Estrogen Receptor Signaling Pathways in Breast Cancer. In International Journal of Molecular Sciences (Vol. 24, Issue 7). Multidisciplinary Digital Publishing Institute (MDPI). doi: 10.3390/ijms24076834

Cocco, S., Leone, A., Piezzo, M., Caputo, R., Di Lauro, V., Di Rella, F., Fusco, G., Capozzi, M., Gioia, G. di, Budillon, A., & De Laurentiis, M. (2020). Targeting Autophagy in Breast Cancer. *International Journal of Molecular Sciences*, *21*(21), 7836. doi: 10.3390/ijms21217836

Cook, K. L., Shajahan, A. N., Wärri, A., Jin, L., Hilakivi-Clarke, L. A., & Clarke, R. (2012). Glucose-Regulated Protein 78 Controls Cross-talk between

Apoptosis and Autophagy to Determine Antiestrogen Responsiveness. *Cancer Research*, *72*(13), 3337–3349. doi: 10.1158/0008-5472.CAN-12-0269

Coskun, D., Obakan, P., Arisan, E. D., Çoker-Gürkan, A., & Palavan-Ünsal, N. (2015). Epibrassinolide alters PI3K/MAPK signaling axis via activating Foxo3a-induced mitochondria-mediated apoptosis in colon cancer cells. *Experimental Cell Research*, *338*(1), 10–21. doi: 10.1016/j.yexcr.2015.08.015

Croxtall, J. D., Choudhury, Q., White, J. O., & Flower, R. J. (1997). Tamoxifen inhibits the release of arachidonic acid stimulated by thapsigargin in estrogen receptor-negative A549 cells. In Biochimica et Biophysica Acta (Vol. 1349).

Crusio, W. E., Dong, H., & Radeke, H. H. (n.d.). Volume 1187 Series Editors. In Advances in Experimental Medicine and Biology. Retrieved from http://www.springer.com/series/5584

Das, S., Shukla, N., Singh, S. S., Kushwaha, S., & Shrivastava, R. (2021). Mechanism of interaction between autophagy and apoptosis in cancer. In Apoptosis (Vol. 26, Issues 9–10, pp. 512–533). Springer. doi: 10.1007/s10495-021-01687-9

de la Calle, C. M., Shee, K., Yang, H., Lonergan, P. E., & Nguyen, H. G. (2022). The endoplasmic reticulum stress response in prostate cancer. *Nature Reviews Urology*, *19*(12), 708–726. doi: 10.1038/s41585-022-00649-3

Feng, Y., Spezia, M., Huang, S., Yuan, C., Zeng, Z., Zhang, L., Ji, X., Liu, W., Huang, B., Luo, W., Liu, B., Lei, Y., Du, S., Vuppalapati, A., Luu, H. H., Haydon, R. C., He, T.-C., & Ren, G. (2018). Breast cancer development and progression: Risk factors, cancer stem cells, signaling pathways, genomics, and molecular pathogenesis. *Genes & Diseases*, *5*(2), 77–106. doi: 10.1016/j.gendis.2018.05.001

Ferlay J, Ervik M, Lam F, Laversanne M, Colombet M, Mery L, Piñeros M, Znaor A, Soerjomataram I, Bray F (2024). Global Cancer Observatory: Cancer

Today. Lyon, France: International Agency for Research on Cancer. Available from: https://gco.iarc.who.int/today, accessed [10.12.2023].

Finnegan, R. M., Elshazly, A. M., Schoenlein, P. V., & Gewirtz, D. A. (2022). Therapeutic Potential for Targeting Autophagy in ER+ Breast Cancer. *Cancers*, *14*(17), 4289. doi: 10.3390/cancers14174289

Foty, R. (2011). A Simple Hanging Drop Cell Culture Protocol for Generation of 3D Spheroids. *Journal of Visualized Experiments*, *51*. doi: 10.3791/2720

Fu, X., Cui, J., Meng, X., Jiang, P., Zheng, Q., Zhao, W., & Chen, X. (2021). Endoplasmic reticulum stress, cell death and tumor: Association between endoplasmic reticulum stress and the apoptosis pathway in tumors (Review). *Oncology Reports*, *45*(3), 801–808. doi: 10.3892/or.2021.7933

Fuentes, N., & Silveyra, P. (2019). *Estrogen receptor signaling mechanisms* (pp. 135–170). doi: 10.1016/bs.apcsb.2019.01.001

Galiè, M. (2019). RAS as Supporting Actor in Breast Cancer. *Frontiers in Oncology*, *9*. doi: 10.3389/fonc.2019.01199

Gimple, R. C., & Wang, X. (2019). RAS: Striking at the Core of the Oncogenic Circuitry. *Frontiers in Oncology*, *9*. doi: 10.3389/fonc.2019.00965

Girgert, R., Emons, G., & Gründker, C. (2019). Estrogen Signaling in ERα-Negative Breast Cancer: ERβ and GPER. *Frontiers in Endocrinology*, *9*. doi: 10.3389/fendo.2018.00781

Guney Eskiler, G., Cecener, G., Tunca, B., & Egeli, U. (2016). An in vitro model for the development of acquired tamoxifen resistance. *Cell Biology and Toxicology*, *32*(6), 563–581. doi: 10.1007/s10565-016-9355-8

Guo, W., Wang, Y., Wang, Z., Wang, Y., & Zheng, H. (2016). Inhibiting autophagy increases epirubicin's cytotoxicity in breast cancer cells. *Cancer Science*, *107*(11), 1610–1621. doi: 10.1111/cas.13059

Hanahan, D. (2022). Hallmarks of Cancer: New Dimensions. *Cancer Discovery*, *12*(1), 31–46. doi: 10.1158/2159-8290.CD-21-1059

Hanahan, D., & Weinberg, R. A. (2011). Hallmarks of cancer: The next generation. *Cell*, *144*(5), 646–674. doi: 10.1016/j.cell.2011.02.013

Hansen, M., Rubinsztein, D. C., & Walker, D. W. (2018). Autophagy as a promoter of longevity: insights from model organisms. In Nature Reviews Molecular Cell Biology (Vol. 19, Issue 9, pp. 579–593). Nature Publishing Group. doi: 10.1038/s41580-018-0033-y

Harbeck, N., Penault-Llorca, F., Cortes, J., Gnant, M., Houssami, N., Poortmans, P., Ruddy, K., Tsang, J., & Cardoso, F. (2019). Breast cancer. *Nature Reviews Disease Primers*, *5*(1). doi: 10.1038/s41572-019-0111-2

Hetz, C., Zhang, K., & Kaufman, R. J. (2020). Mechanisms, regulation and functions of the unfolded protein response. *Nature Reviews. Molecular Cell Biology*, *21*(8), 421–438. doi: 10.1038/s41580-020-0250-z

Hillary, R. F., & FitzGerald, U. (2018). A lifetime of stress: ATF6 in development and homeostasis. *Journal of Biomedical Science*, *25*(1), 48. doi: 10.1186/s12929-018-0453-1

Howell, A., & Howell, S. J. (2023). Tamoxifen evolution. *British Journal of Cancer*, *128*(3), 421–425. doi: 10.1038/s41416-023-02158-5

Huang, T., Song, X., Yang, Y., Wan, X., Alvarez, A. A., Sastry, N., Feng, H., Hu, B., & Cheng, S. Y. (2018). Autophagy and hallmarks of cancer. *Critical Reviews in Oncogenesis*, *23*(5–6), 247–267. doi: 10.1615/CritRevOncog.2018027913

Huang, W., Gong, Y., & Yan, L. (2023). ER Stress, the Unfolded Protein Response and Osteoclastogenesis: A Review. *Biomolecules*, *13*(7), 1050. doi: 10.3390/biom13071050

Huskova, Z., Steigerova, J., Oklestkova, J., Rarova, L., Kolar, Z., & Strnad, M. (2020). Molecular mechanisms of plant steroids and study of their interaction with nuclear receptors in prostate cancer cells. *Food and Chemical Toxicology*, *137*, 111164. doi: 10.1016/j.fct.2020.111164

İsaoğlu, M., Güllüce, M., & Karadayı, M. (n.d.). *Plant-Derived Natural Products as Multidrug Resistance Modulators in Cancer Therapy*.

Jan, R., & Chaudhry, G.-S. (2019). Understanding Apoptosis and Apoptotic Pathways Targeted Cancer Therapeutics. *Advanced Pharmaceutical Bulletin*, *9*(2), 205–218. doi: 10.15171/apb.2019.024

Jones, R. L., Constantinidou, A., & Reis-Filho, J. S. (2012). Molecular Classification of Breast Cancer. In Surgical Pathology Clinics (Vol. 5, Issue 3, pp. 701–717). doi: 10.1016/j.path.2012.06.008

Kanematsu, S., Uehara, N., Miki, H., Yoshizawa, K., Kawanaka, A., Yuri, T., & Tsubura, A. (n.d.). *Autophagy Inhibition Enhances Sulforaphane-induced Apoptosis in Human Breast Cancer Cells*.

Kara, M., & Oztas, E. (2020). Endoplasmic Reticulum Stress-Mediated Cell Death. In Programmed Cell Death. IntechOpen. doi: 10.5772/intechopen.85401

Kaur Kohli, S., Bhardwaj, A., Bhardwaj, V., Sharma, A., Kalia, N., Landi, M., & Bhardwaj, R. (2020). Therapeutic Potential of Brassinosteroids in Biomedical and Clinical Research. *Biomolecules*, *10*(4), 572. doi: 10.3390/biom10040572

Klionsky, D. J., Abdelmohsen, K., Abe, A., Abedin, M. J., Abeliovich, H., Acevedo Arozena, A., Adachi, H., Adams, C. M., Adams, P. D., Adeli, K., Adhihetty, P. J., Adler, S. G., Agam, G., Agarwal, R., Aghi, M. K., Agnello, M., Agostinis, P., Aguilar, P. V, Aguirre-Ghiso, J., … Zughaier, S. M. (2016). Guidelines for the use and interpretation of assays for monitoring autophagy (3rd edition). *Autophagy*, *12*(1), 1–222. doi: 10.1080/15548627.2015.1100356

Kocaturk, N. M., Akkoc, Y., Kig, C., Bayraktar, O., Gozuacik, D., & Kutlu, O. (2019a). Autophagy as a molecular target for cancer treatment. *European Journal of Pharmaceutical Sciences*, *134*, 116–137. doi: 10.1016/j.ejps.2019.04.011

Kouroku, Y., Fujita, E., Tanida, I., Ueno, T., Isoai, A., Kumagai, H., Ogawa, S., Kaufman, R. J., Kominami, E., & Momoi, T. (2007). ER stress (PERK/eIF2α phosphorylation) mediates the polyglutamine-induced LC3

conversion, an essential step for autophagy formation. *Cell Death & Differentiation*, *14*(2), 230–239. doi: 10.1038/sj.cdd.4401984

Kumar, A., & Jaitak, V. (2019). Natural products as multidrug resistance modulators in cancer. *European Journal of Medicinal Chemistry*, *176*, 268–291. doi: 10.1016/j.ejmech.2019.05.027

Kumar, H., Gupta, N. V., Jain, R., Madhunapantula, S. V., Babu, C. S., Kesharwani, S. S., Dey, S., & Jain, V. (2023). A review of biological targets and therapeutic approaches in the management of triple-negative breast cancer. *Journal of Advanced Research*, *54*, 271–292. doi: 10.1016/j.jare.2023.02.005

Kvasnica, M., Buchtova, K., Budesinsky, M., Beres, T., Rarova, L., & Strnad, M. (2019). Synthesis, characterization and antiproliferative activity of seco analogues of brassinosteroids. *Steroids*, *146*, 1–13. doi: 10.1016/j.steroids.2019.03.004

Lee, Y. J., Won, A. J., Lee, J., Jung, J. H., Yoon, S., Lee, B. M., & Kim, H. S. (2012). Molecular Mechanism of SAHA on Regulation of Autophagic Cell Death in Tamoxifen-Resistant MCF-7 Breast Cancer Cells. *International Journal of Medical Sciences*, *9*(10), 881–893. doi: 10.7150/ijms.5011

Li, M., Liu, J., Li, S., Feng, Y., Yi, F., Wang, L., Wei, S., & Cao, L. (2019). Autophagy-related 7 modulates tumor progression in triple-negative breast cancer. *Laboratory Investigation*, *99*(9), 1266–1274. doi: 10.1038/s41374-019-0249-2

Li, Y.-J., Lei, Y.-H., Yao, N., Wang, C.-R., Hu, N., Ye, W.-C., Zhang, D.-M., & Chen, Z.-S. (2017). Autophagy and multidrug resistance in cancer. *Chinese Journal of Cancer*, *36*(1), 52. doi: 10.1186/s40880-017-0219-2

Lin, Y., Jiang, M., Chen, W., Zhao, T., & Wei, Y. (2019). Cancer and ER stress: Mutual crosstalk between autophagy, oxidative stress and inflammatory response. In Biomedicine and Pharmacotherapy (Vol. 118). Elsevier Masson SAS. doi: 10.1016/j.biopha.2019.109249

Lin, Y.-S., Lin, Y.-Y., Yang, Y.-H., Lin, C.-L., Kuan, F.-C., Lu, C.-N., Chang, G.-H., Tsai, M.-S., Hsu, C.-M., Yeh, R.-A., Yang, P.-R., Lee, I.-Y., Shu, L.-H., Cheng, Y.-C., Liu, H.-T., Lee, K.-D., Chang, D.-C., & Wu, C.-Y. (2018). Antrodia cinnamomea extract inhibits the proliferation of tamoxifen-resistant breast cancer cells through apoptosis and skp2/microRNAs pathway. *BMC Complementary and Alternative Medicine*, *18*(1), 152. doi: 10.1186/s12906-018-2204-y

Liu, J., Yue, W., & Chen, H. (2019). The correlation between autophagy and tamoxifen resistance in breast cancer. *International Journal of Clinical and Experimental Pathology*, *12*(6), 2066–2074.

Luhr, M., Torgersen, M. L., Szalai, P., Hashim, A., Brech, A., Staerk, J., & Engedal, N. (2019). The kinase PERK and the transcription factor ATF4 play distinct and essential roles in autophagy resulting from tunicamycin-induced ER stress. *Journal of Biological Chemistry*, *294*(20), 8197–8217. doi: 10.1074/jbc.RA118.002829

Łukasiewicz, S., Czeczelewski, M., Forma, A., Baj, J., Sitarz, R., & Stanisławek, A. (2021). Breast cancer—epidemiology, risk factors, classification, prognostic markers, and current treatment strategies—An updated review. In Cancers (Vol. 13, Issue 17). MDPI. doi: 10.3390/cancers13174287

Makki, J. (2015). Diversity of Breast Carcinoma: Histological Subtypes and Clinical Relevance. *Clinical Medicine Insights: Pathology*, *8*, CPath.S31563. doi: 10.4137/CPath.S31563

Malíková, J., Swaczynová, J., Kolář, Z., & Strnad, M. (2008). Anticancer and antiproliferative activity of natural brassinosteroids. *Phytochemistry*, *69*(2), 418–426. doi: 10.1016/j.phytochem.2007.07.028

Mandal, D., Sahu, B. R., & Parija, T. (2023). Combination of tamoxifen and D-limonene enhances therapeutic efficacy in breast cancer cells. *Medical Oncology*, *40*(8), 216. doi: 10.1007/s12032-023-02081-y

Mayrovitz, H. N. (Ed.). (2022). *Breast Cancer*. Exon Publications. doi: 10.36255/exon-publications-breast-cancer

McCloy, R. A., Shelley, E. J., Roberts, C. G., Boslem, E., Biden, T. J., Nicholson, R. I., Gee, J. M., Sutherland, R. L., Musgrove, E. A., Burgess, A., & Butt, A. J. (2013). Role of endoplasmic reticulum stress induction by the plant toxin, persin, in overcoming resistance to the apoptotic effects of tamoxifen in human breast cancer cells. *British Journal of Cancer*, *109*(12), 3034–3041. doi: 10.1038/bjc.2013.693

McDonald, E. S., Clark, A. S., Tchou, J., Zhang, P., & Freedman, G. M. (2016). Clinical diagnosis and management of breast cancer. *Journal of Nuclear Medicine*, *57*, 9S-16S. doi: 10.2967/jnumed.115.157834

Mehdizadehtapeh, L., & Obakan Yerlikaya, P. (2021). Endoplasmic reticulum stress and oncomir-associated chemotherapeutic drug resistance mechanisms in breast cancer tumors. *TURKISH JOURNAL OF BIOLOGY*, *45*(1), 1–16. doi: 10.3906/biy-2010-62

Mele, L., del Vecchio, V., Liccardo, D., Prisco, C., Schwerdtfeger, M., Robinson, N., Desiderio, V., Tirino, V., Papaccio, G., & La Noce, M. (2020). The role of autophagy in resistance to targeted therapies. In Cancer Treatment Reviews (Vol. 88). W.B. Saunders Ltd. doi: 10.1016/j.ctrv.2020.102043

Métivier, D., Dallaporta, B., Zamzami, N., Larochette, N., Susin, S. A., Marzo, I., & Kroemer, G. (1998). Cytofluorometric detection of mitochondrial alterations in early CD95/Fas/APO-1-triggered apoptosis of Jurkat T lymphoma cells. Comparison of seven mitochondrion-specific fluorochromes. *Immunology Letters*, *61*(2–3), 157–163. doi: 10.1016/S0165-2478(98)00013-3

Moon, S. Y., Lee, H., Kim, S., Hong, J. H., Chun, S. H., Lee, H. Y., Kang, K., Kim, H. S., Won, H. S., & Ko, Y. H. (2021). Inhibition of STAT3 enhances sensitivity to tamoxifen in tamoxifen-resistant breast cancer cells. *BMC Cancer*, *21*(1), 931. doi: 10.1186/s12885-021-08641-7

Motawi, T. K., Abdelazim, S. A., Darwish, H. A., Elbaz, E. M., & Shouman, S. A. (2016). Modulation of Tamoxifen Cytotoxicity by Caffeic Acid Phenethyl Ester in MCF-7 Breast Cancer Cells. *Oxidative Medicine and Cellular Longevity*, *2016*, 1–13. doi: 10.1155/2016/3017108

Nagelkerke, A., Sieuwerts, A. M., Bussink, J., Sweep, F. C. G. J., Look, M. P., Foekens, J. A., Martens, J. W. M., & Span, P. N. (2014). LAMP3 is involved in tamoxifen resistance in breast cancer cells through the modulation of autophagy. *Endocrine-Related Cancer*, *21*(1), 101–112. doi: 10.1530/ERC-13-0183

Nishida, Y., Arakawa, S., Fujitani, K., Yamaguchi, H., Mizuta, T., Kanaseki, T., Komatsu, M., Otsu, K., Tsujimoto, Y., & Shimizu, S. (2009). Discovery of Atg5/Atg7-independent alternative macroautophagy. *Nature*, *461*(7264), 654–658. doi: 10.1038/nature08455

Oakes, S. A. (2020). Endoplasmic Reticulum Stress Signaling in Cancer Cells. In American Journal of Pathology (Vol. 190, Issue 5, pp. 934–946). Elsevier Inc. doi: 10.1016/j.ajpath.2020.01.010

Obakan, P., Arisan, E. D., Coker-Gurkan, A., & Palavan-Unsal, N. (2014). Epibrassinolide-induced apoptosis regardless of p53 expression via activating polyamine catabolic machinery, a common target for androgen sensitive and insensitive prostate cancer cells. *The Prostate*, *74*(16), 1622–1633. doi: 10.1002/pros.22879

Obakan, P., Barrero, C., Coker-Gurkan, A., Arisan, E. D., Merali, S., & Palavan-Unsal, N. (2015). SILAC-Based Mass Spectrometry Analysis Reveals That Epibrassinolide Induces Apoptosis via Activating Endoplasmic Reticulum Stress in Prostate Cancer Cells. *PLOS ONE*, *10*(9), e0135788. doi: 10.1371/journal.pone.0135788

Obakan Yerlikaya, P., Adacan, K., Karatug Kacar, A., Coker Gurkan, A., & Arisan, E. D. (2023). Epibrassinolide impaired colon tumor progression and induced autophagy in SCID mouse xenograft model via acting on cell cycle progression without affecting endoplasmic reticulum stress observed in vitro. *The International Journal of Biochemistry & Cell Biology*, *155*, 106360. doi: 10.1016/j.biocel.2022.106360

Obakan-Yerlikaya, P., Arisan, E. D., Coker-Gurkan, A., Adacan, K., Ozbey, U., Somuncu, B., Baran, D., & Palavan-Unsal, N. (2017). Calreticulin is a fine tuning molecule in epibrassinolide-induced apoptosis through activating

endoplasmic reticulum stress in colon cancer cells. *Molecular Carcinogenesis*, *56*(6), 1603–1619. doi: 10.1002/mc.22616

Ogata, M., Hino, S., Saito, A., Morikawa, K., Kondo, S., Kanemoto, S., Murakami, T., Taniguchi, M., Tanii, I., Yoshinaga, K., Shiosaka, S., Hammarback, J. A., Urano, F., & Imaizumi, K. (2006). Autophagy Is Activated for Cell Survival after Endoplasmic ReticulumStress. *Molecular and Cellular Biology*, *26*(24), 9220–9231. doi: 10.1128/MCB.01453-06

Oh, S.-H., & Lim, S.-C. (2009). Endoplasmic Reticulum Stress-Mediated Autophagy/Apoptosis Induced by Capsaicin (8-Methyl- *N* -vanillyl-6-nonenamide) and Dihydrocapsaicin is Regulated by the Extent of c-Jun NH_2 -Terminal Kinase/Extracellular Signal-Regulated Kinase Activation in WI38 Lung Epithelial Fibroblast Cells. *Journal of Pharmacology and Experimental Therapeutics*, *329*(1), 112–122. doi: 10.1124/jpet.108.144113

Ortega, M. A., Fraile-Martínez, O., Asúnsolo, Á., Buján, J., García-Honduvilla, N., & Coca, S. (2020). Signal Transduction Pathways in Breast Cancer: The Important Role of PI3K/Akt/mTOR. *Journal of Oncology*, *2020*, 1–11. doi: 10.1155/2020/9258396

Patra, A., Adhikary, A., & Ghosh, S. (2023). The unfolded protein response (UPR) pathway: the unsung hero in breast cancer management. *Apoptosis*, *28*(3–4), 263–276. doi: 10.1007/s10495-022-01803-3

Pawlik, A., Słomińska-Wojewódzka, M., & Herman-Antosiewicz, A. (2016). Sensitization of estrogen receptor-positive breast cancer cell lines to 4-hydroxytamoxifen by isothiocyanates present in cruciferous plants. *European Journal of Nutrition*, *55*(3), 1165–1180. doi: 10.1007/s00394-015-0930-1

Qadir, M. A., Kwok, B., Dragowska, W. H., To, K. H., Le, D., Bally, M. B., & Gorski, S. M. (2008). Macroautophagy inhibition sensitizes tamoxifen-resistant breast cancer cells and enhances mitochondrial depolarization. *Breast Cancer Research and Treatment*, *112*(3), 389–403. doi: 10.1007/s10549-007-9873-4

Qing, B., Wang, S., Du, Y., Liu, C., & Li, W. (2023). Crosstalk between endoplasmic reticulum stress and multidrug-resistant cancers: hope or frustration. *Frontiers in Pharmacology*, *14*. doi: 10.3389/fphar.2023.1273987

Radin, D. P., & Patel, P. (2016). Delineating the molecular mechanisms of tamoxifen's oncolytic actions in estrogen receptor-negative cancers. *European Journal of Pharmacology*, *781*, 173–180. doi: 10.1016/j.ejphar.2016.04.017

Rozpedek, W., Pytel, D., Mucha, B., Leszczynska, H., Diehl, J. A., & Majsterek, I. (2016). The Role of the PERK/eIF2α/ATF4/CHOP Signaling Pathway in Tumor Progression During Endoplasmic Reticulum Stress. *Current Molecular Medicine*, *16*(6), 533–544. doi: 10.2174/1566524016666160523143937

Rybstein, M. D., Bravo-San Pedro, J. M., Kroemer, G., & Galluzzi, L. (2018). The autophagic network and cancer. In Nature Cell Biology (Vol. 20, Issue 3, pp. 243–251). Nature Publishing Group. doi: 10.1038/s41556-018-0042-2

Sadava, D., & Chen, S. (2023). Castasterone, a Plant Steroid Hormone, Affects Human Small-Cell Lung Cancer Cells and Reverses Multi-Drug Resistance. *Pharmaceuticals*, *16*(2), 170. doi: 10.3390/ph16020170

Samaddar, J. S., Gaddy, V. T., Duplantier, J., Thandavan, S. P., Shah, M., Smith, M. J., Browning, D., Rawson, J., Smith, S. B., Barrett, J. T., & Schoenlein, P. V. (2008). A role for macroautophagy in protection against 4-hydroxytamoxifen–induced cell death and the development of antiestrogen resistance. *Molecular Cancer Therapeutics*, *7*(9), 2977–2987. doi: 10.1158/1535-7163.MCT-08-0447

Sameiyan, E., Hayes, A. W., & Karimi, G. (2019). The effect of medicinal plants on multiple drug resistance through autophagy: A review of in vitro studies. *European Journal of Pharmacology*, *852*, 244–253. doi: 10.1016/j.ejphar.2019.04.001

Sanaei, M., Kavoosi, F., Atashpour, S., & Haghighat, S. (2017). Effects of Genistein and Synergistic Action in Combination with Tamoxifen on the HepG2 Human Hepatocellular Carcinoma Cell Line. *Asian Pacific Journal of Cancer Prevention : APJCP*, *18*(9), 2381–2385. doi: 10.22034/APJCP.2017.18.9.2381

Sano, R., & Reed, J. C. (2013). ER stress-induced cell death mechanisms. *Biochimica et Biophysica Acta (BBA) - Molecular Cell Research*, *1833*(12), 3460–3470. doi: 10.1016/j.bbamcr.2013.06.028

Sarhangi, N., Hajjari, S., Heydari, S. F., Ganjizadeh, M., Rouhollah, F., & Hasanzad, M. (2022). Breast cancer in the era of precision medicine. In Molecular Biology Reports (Vol. 49, Issue 10, pp. 10023–10037). Springer Science and Business Media B.V. doi: 10.1007/s11033-022-07571-2

Schuur, E. R., & DeAndrade, J. P. (2015a). Breast Cancer: Molecular Mechanisms, Diagnosis, and Treatment. In International Manual of Oncology Practice (pp. 155–200). Springer International Publishing. doi: 10.1007/978-3-319-21683-6_9

Schuur, E. R., & DeAndrade, J. P. (2015b). Breast Cancer: Molecular Mechanisms, Diagnosis, and Treatment. In International Manual of Oncology Practice (pp. 155–200). Cham: Springer International Publishing. doi: 10.1007/978-3-319-21683-6_9

Scull, C. M., & Tabas, I. (2011). Mechanisms of ER Stress-Induced Apoptosis in Atherosclerosis. *Arteriosclerosis, Thrombosis, and Vascular Biology*, *31*(12), 2792–2797. doi: 10.1161/ATVBAHA.111.224881

Shagufta, & Ahmad, I. (2018). Tamoxifen a pioneering drug: An update on the therapeutic potential of tamoxifen derivatives. *European Journal of Medicinal Chemistry*, *143*, 515–531. doi: 10.1016/j.ejmech.2017.11.056

Shaikh, S. S., & Emens, L. A. (2022). Current and emerging biologic therapies for triple negative breast cancer. *Expert Opinion on Biological Therapy*, *22*(5), 591–602. doi: 10.1080/14712598.2020.1801627

Sisinni, L., Pietrafesa, M., Lepore, S., Maddalena, F., Condelli, V., Esposito, F., & Landriscina, M. (2019). Endoplasmic Reticulum Stress and Unfolded Protein Response in Breast Cancer: The Balance between Apoptosis and Autophagy and Its Role in Drug Resistance. *International Journal of Molecular Sciences*, *20*(4), 857. doi: 10.3390/ijms20040857

Song, S., Tan, J., Miao, Y., & Zhang, Q. (2018). Crosstalk of ER stress-mediated autophagy and ER-phagy: Involvement of UPR and the core autophagy machinery. In Journal of Cellular Physiology (Vol. 233, Issue 5, pp. 3867–3874). Wiley-Liss Inc. doi: 10.1002/jcp.26137

Sorice, M. (2022). Crosstalk of Autophagy and Apoptosis. *Cells*, *11*(9), 1479. doi: 10.3390/cells11091479

Steigerová, J., Oklešťková, J., Levková, M., Rárová, L., Kolář, Z., & Strnad, M. (2010). Brassinosteroids cause cell cycle arrest and apoptosis of human breast cancer cells. *Chemico-Biological Interactions*, *188*(3), 487–496. doi: 10.1016/j.cbi.2010.09.006

Steigerová, J., Rárová, L., Oklešťková, J., Křížová, K., Levková, M., Šváchová, M., Kolář, Z., & Strnad, M. (2012). Mechanisms of natural brassinosteroid-induced apoptosis of prostate cancer cells. *Food and Chemical Toxicology*, *50*(11), 4068–4076. doi: 10.1016/j.fct.2012.08.031

Sui, X., Chen, R., Wang, Z., Huang, Z., Kong, N., Zhang, M., Han, W., Lou, F., Yang, J., Zhang, Q., Wang, X., He, C., & Pan, H. (2013). Autophagy and chemotherapy resistance: a promising therapeutic target for cancer treatment. *Cell Death & Disease*, *4*(10), e838–e838. doi: 10.1038/cddis.2013.350

Tarantino, P., Morganti, S., & Curigliano, G. (2020). Biologic therapy for advanced breast cancer: recent advances and future directions. *Expert Opinion on Biological Therapy*, *20*(9), 1009–1024. doi: 10.1080/14712598.2020.1752176

Tiwary, R., Yu, W., deGraffenried, L. A., Sanders, B. G., & Kline, K. (2011). Targeting cholesterol-rich microdomains to circumvent tamoxifen-resistant breast cancer. *Breast Cancer Research*, *13*(6), R120. doi: 10.1186/bcr3063

Tran, A. T., Ramalinga, M., Kedir, H., Clarke, R., & Kumar, D. (2015). Autophagy inhibitor 3-methyladenine potentiates apoptosis induced by dietary tocotrienols in breast cancer cells. *European Journal of Nutrition*, *54*(2), 265–272. doi: 10.1007/s00394-014-0707-y

Uttenweiler, A., Schwarz, H., Neumann, H., & Mayer, A. (2007). The Vacuolar Transporter Chaperone (VTC) Complex Is Required for Microautophagy. *Molecular Biology of the Cell*, *18*(1), 166–175. doi: 10.1091/mbc.e06-08-0664

Verwey, M., Nolte, E. M., Joubert, A. M., & Theron, A. E. (2016). Autophagy induced by a sulphamoylated estrone analogue contributes to its cytotoxic effect on breast cancer cells. *Cancer Cell International*, *16*(1), 91. doi: 10.1186/s12935-016-0367-5

Wang, Lijun, Tang, L., Yao, C., Liu, C., & Shu, Y. (2021). The Synergistic Effects of Celastrol in combination with Tamoxifen on Apoptosis and Autophagy in MCF-7 Cells. *Journal of Immunology Research*, *2021*, 1–13. doi: 10.1155/2021/5532269

Wang, Liming, Klionsky, D. J., & Shen, H. M. (2023). The emerging mechanisms and functions of microautophagy. In Nature Reviews Molecular Cell Biology (Vol. 24, Issue 3, pp. 186–203). Nature Research. doi: 10.1038/s41580-022-00529-z

Wang, R., Shang, Y., Chen, B., Xu, F., Zhang, J., Zhang, Z., Zhao, X., Wan, X., Xu, A., Wu, L., & Zhao, G. (2022). Protein disulfide isomerase blocks the interaction of LC3II-PHB2 and promotes mTOR signaling to regulate autophagy and radio/chemo-sensitivity. *Cell Death & Disease*, *13*(10), 851. doi: 10.1038/s41419-022-05302-w

Wehweck, F. S. (2021). Ductal Carcinoma In Situ: Pathology. *Chirurgia (Bucharest, Romania : 1990)*, *116*(5 Suppl), S59–S64. doi: 10.21614/chirurgia.116.5.suppl.S59

Weigelt, B., Geyer, F. C., & Reis-Filho, J. S. (2010). Histological types of breast cancer: how special are they? *Molecular Oncology*, *4*(3), 192–208. doi: 10.1016/j.molonc.2010.04.004

Wen, N., Lv, Q., & Du, Z. (2020). MicroRNAs involved in drug resistance of breast cancer by regulating autophagy. *Journal of Zhejiang University-SCIENCE B*, *21*(9), 690–702. doi: 10.1631/jzus.B2000076

Winters, S., Martin, C., Murphy, D., & Shokar, N. K. (2017). Breast Cancer Epidemiology, Prevention, and Screening. In Progress in Molecular Biology and Translational Science (Vol. 151, pp. 1–32). Elsevier B.V. doi: 10.1016/bs.pmbts.2017.07.002

Wu, Q., & Sharma, D. (2023). Autophagy and Breast Cancer: Connected in Growth, Progression, and Therapy. *Cells*, *12*(8), 1156. doi: 10.3390/cells12081156

Wu, S.-T., Sun, G.-H., Cha, T.-L., Kao, C.-C., Chang, S.-Y., Kuo, S.-C., & Way, T.-D. (2016). CSC-3436 switched tamoxifen-induced autophagy to apoptosis through the inhibition of AMPK/mTOR pathway. *Journal of Biomedical Science*, *23*(1), 60. doi: 10.1186/s12929-016-0275-y

Xu, D., Liu, Z., Liang, M.-X., Fei, Y.-J., Zhang, W., Wu, Y., & Tang, J.-H. (2022). Endoplasmic reticulum stress targeted therapy for breast cancer. *Cell Communication and Signaling*, *20*(1), 174. doi: 10.1186/s12964-022-00964-7

Xu, Z., Huang, B., Liu, J., Wu, X., Luo, N., Wang, X., Zheng, X., & Pan, X. (2018). Combinatorial anti-proliferative effects of tamoxifen and naringenin: The role of four estrogen receptor subtypes. *Toxicology*, *410*, 231–246. doi: 10.1016/j.tox.2018.08.013

Yadav, R. K., Chae, S.-W., Kim, H.-R., & Chae, H. J. (2014). Endoplasmic Reticulum Stress and Cancer. *Journal of Cancer Prevention*, *19*(2), 75–88. doi: 10.15430/JCP.2014.19.2.75

Yao, J., Deng, K., Huang, J., Zeng, R., & Zuo, J. (2020). Progress in the Understanding of the Mechanism of Tamoxifen Resistance in Breast Cancer. *Frontiers in Pharmacology*, *11*. doi: 10.3389/fphar.2020.592912

Yerlikaya, P. O., Mehdizadehtapeh, L., Rencüzoğullari, Ö., Kuryayeva, F., Çevikli, S. S., Özağar, Ş., Odabaş, S. P., Tunçkol, S., Yetim, H., Gürkan, A. Ç., & Arisan, E. D. (2022). Gemcitabine in combination with epibrassinolide enhanced the apoptotic response in an ER stress-dependent manner and reduced the epithelial-mesenchymal transition in pancreatic cancer cells. *Turkish Journal of Biology*, *46*(6), 439–457. doi: 10.55730/1300-0152.2630

Yerlikaya, P. O., & Naxmedova, S. (2022). Epibrassinolide Triggers Apoptotic Cell Death in SK-N-AS Neuroblastoma Cells by Targeting GSK3β in a ROS Generation-Dependent Way. *European Journal of Biology*, *81*(2), 240–250. doi: 10.26650/EurJBiol.2022.1191701

Yun, H. R., Jo, Y. H., Kim, J., Shin, Y., Kim, S. S., & Choi, T. G. (2020). Roles of Autophagy in Oxidative Stress. *International Journal of Molecular Sciences*, *21*(9), 3289. doi: 10.3390/ijms21093289

Zhang, J., Xiang, Q., Wu, M., Lao, Y.-Z., Xian, Y.-F., Xu, H.-X., & Lin, Z.-X. (2023). Autophagy Regulators in Cancer. *International Journal of Molecular Sciences*, *24*(13), 10944. doi: 10.3390/ijms241310944

Zhang, J.-X., Yuan, W.-C., Li, C.-G., Zhang, H.-Y., Han, S.-Y., & Li, X.-H. (2023). A review on the mechanisms underlying the antitumor effects of natural products by targeting the endoplasmic reticulum stress apoptosis pathway. *Frontiers in Pharmacology*, *14*. doi: 10.3389/fphar.2023.1293130

Zhang, N., Chen, Y., Jiang, R., Li, E., Chen, X., Xi, Z., Guo, Y., Liu, X., Zhou, Y., Che, Y., & Jiang, X. (2011). PARP and RIP 1 are required for autophagy induced by 11'-deoxyverticillin A, which precedes caspase-dependent apoptosis. *Autophagy*, *7*(6), 598–612. doi: 10.4161/auto.7.6.15103

Zhao, M., Xu, P., Shi, W., Wang, J., Wang, T., & Li, P. (2024). Icariin exerts anti-tumor activity by inducing autophagy via AMPK/mTOR/ULK1 pathway in triple-negative breast cancer. *Cancer Cell International*, *24*(1), 74. doi: 10.1186/s12935-024-03266-9

Zhou, H., Zhuang, W., Huang, H., Ma, N., Lei, J., Jin, G., Wu, S., Zhou, S., Zhao, X., Lan, L., Xia, H., & Shangguan, F. (2022). Effects of natural 24-epibrassinolide on inducing apoptosis and restricting metabolism in hepatocarcinoma cells. *Phytomedicine : International Journal of Phytotherapy and Phytopharmacology*, *107*, 154428. doi: 10.1016/j.phymed.2022.154428

Zhu, S., Wu, Y., Song, B., Yi, M., Yan, Y., Mei, Q., & Wu, K. (2023). Recent advances in targeted strategies for triple-negative breast cancer. *Journal of Hematology & Oncology*, *16*(1), 100. doi: 10.1186/s13045-023-01497-3

6. SUPPLEMENTARY

Supplementary Table 1. SDS-PAGE gel recipe

	THERMO	
Gel Percentage (%)	**12 (Separating)**	**5 (Stacking)**
H2O	2.3	1.7
30% polyacrylamide (mL)	2.8	0.425
Tris (mL)	1.75 (1.5M pH 8.8)	0.313 (0.5M pH 6.8)
10% SDS (µL)	70	25
10% APS (µL)	47	18.5
TEMED (µL)	14	4.1
Total volume (mL)	7	2.5

Supplementary Table 2. 10X Transfer buffer recipe

10X Transfer Buffer Recipe
30.3 g Tris Base
144 g Glycine
1L ddH_20 pH 8.3

SupplementaryTable 3. ECL solution recipe

ECL			
Solution A		**Solution B**	
dH2O	9 mL	dH2O	9 mL
1M Tris-HCl pH 8.5	1 mL	1M Tris-HCl pH 8.5	1 mL
p-Coumaric acid	45 µL	30% H2O2	6 µL
Luminol	100 µL		
Total volume	10 mL	Total volume	10 mL
Luminol 250 mM		**Coumaric Acid 90 mM**	
0.44 g Luminol		0.148 g p-Coumaric acid	
DMSO to 10 mL		Absolute ethanol to 10 mL	
Store in dark at -20C		Store in dark +4C	

Tris-HCl 1M pH 8.5
8.74 g Tris base
4.42 g Tris HCl
dH2O to 100 mL

Supplementary Table 4. List of chemicals

Chemicals	Brand	Cat No.
(E/Z)-4-hydroxy Tamoxifen	CAYMAN CHEMICAL	17308
0.25% Trypsin-EDTA(1X)	Gibco	25200-056
10X PBS	Serox	SRD-807-500
10X TBS	EcoTech	PBS10x-10
3-Methyladenine (3-MA)	CAYMAN CHEMICAL	13242
4X Laemmli	EcoTech	LSB-4X
Acrylamide/Bis-acrylamide (37.5:1)	EcoTech	AB3751100
Ammonium persulfate (APS)	Sigma-Aldrich	01709-500ML
Asetic asit	Bio-Rad	BL0250001
ATG5 polyclonal antibody	St John's Laboratory	STJ113131-50
Beclin-1 (BECN1) polyclonal antibody	St John's Laboratory	STJ97474
Bradford Assay kit	Thermo Scientific	1856209
Bradford Reagent	Sigma-Aldrich	B6916-500ML
BSA	Sigma-Aldrich	A2153-10GR
Calnexin	CST	#2433
Calreticulin	CST	#12238
Caspase 3	CST	#9662
Caspase 9	CST	#9502
Coomassie Brilliant Blue-G250	MERCK	D273
Crystal Violet	KimyaLAB	V21166.100
DAPI	Thermo	PI62247
DiOC6	Thermo	D273
DMEM	Gibco	11965092
DMSO	Riedel-De-Haën	41640
ECL (Solution A/B)	EcoTech	ECL50
EcoSpin Plasmid Isolation Kit	EcoTech	EcoPI-50x
EGFP-LC3	Addgene	11546

Epibrassinolide	ApolloScientific	BIE0244
Ethanol Pure	ISOlab	920.026.2500
Fetal Bovine Serum (FBS)	Gibco	10270-106
Formaldehyde solution 37%	Sigma	15512-5L-R
GAPDH polyclonal antibody	Boster	A00227-1
GFP-LC3 plasmid	Addgene	11546
Glycine	Bio-Rad	BL-01400202
GRP78 polyclonal antibody	Invitrogen	PA1-014A
Hydrochloric acid %30	KİMYALAB	V00318.905
Hydrogen peroxide	TEKKİM	TK.0880220.01001
Insulin Human Recombinant Zinc Solution	Gibco	12585-014
Infect Transfection reagent	Intron Biotech	15081
IRE1-alpha	ABclonal	A21021
LC3A/LC3B polyclonal antibody	St John's Laboratory	STJ117779-50
Luminol	Sigma-Aldrich	123072
Methanol	Riedel-de-Haën	24229-2.5L
Monodansylcadaverine	CAYMAN CHEMICAL	15571
M-PER	Thermo	78501
MRP1 polyclonal antibody	Invitrogen	PA5-30594
MTT reagent	Bio Basic	NC461720
p62 (SQSTM1) polyclonal antibody	St John's Laboratory	STJ113744-50
PARP1 polyclonal antibody	St John's Laboratory	STJ193190-50
p-Coumaric acid	Sigma-Aldrich	501-984
Penicillin/Streptomycin Solution (100X)	Capricorn Scientific	PS-B
Penicillin/Streptomycin Solution (100X)	SEROX	SLP-508-100
PERK monoclonal antibody	ABclonal	A21255
PDI	CST	#80797
Ponceau S	Sigma-Aldrich	P3504-10G
Propidium iodide	Sigma-Aldrich	P-4170-100MG
Protease inhibitor	Roche	4693116001
Protein Marker (Pre-stained)	EcoTech	PM12
Protein Marker (Pre-stained)	Abbkine	BMM3001

RNAse	EcoTech	EZRA1, EZRA5
SDS	Scharlau	SD0010
Secondary antibody (anti-mouse)	BOSTER	BA1050-0.5
Secondary antibody (anti-rabbit)	CST	#7074
Skim milk powder	Bioshop	SKI400.250
Sodium Chloride (NaCl)	MERCK	1.06404.1000
Sodium Hydroxide (NaOH)	Biosince (SentezLab)	000322
Sodium Hydroxyde Extra Pure	KimyaLab	1310-73-2
TEMED	MERCK	1107320100
Tris base	Sigma-Aldrich	T1503-1KG
Tris HCl	Scharlau	TR0425
Triton X-100	Sigma-Aldrich	T8787-10ML
Trypan Blue (0.4% solution)	EcoTech	TRY-B100
Tunicamycin	Sigma-Aldrich	T7765-1MG
Tunicamycin	CAYMAN CHEMICAL	11445
Tween-20	Sigma-Aldrich	P1379-500ML

Supplementary Table 5. List of devices

Device	**Brand**
Axio Observer 5 Colibri7	Carl Zeiss Microscopy
Azure 300 Chemiluminescent Western Blot Imager	Azure Biosystems
Biometra Fastblot	Analytic Jena
C6 Plus Personal Flow Cytometer	BD Accuri
Centrifuge 5418 R - Microcentrifuge	Eppendorf
Centrifuge 5424 R	Eppendorf
Centrifuge Z 206 A	Hermle
CO_2 incubators (C150) (9040-0078)	BINDER
Digital Orbital Shaker (sk-0180-s)	DLAB
ECLIPSE TS100 (Inverted microscope)	Nikon
FLV1090 Mini Refrigerator	Flavel
Heat blocker	Thermo Scientific
Invitrogen™ Mini Gel Tank	Thermo Scientific
Invitrogen™ Western Blot Wet Transfer Device | Mini Blot Module	Thermo Scientific

Lab Benchtop Mini Centrifuge	ONiLAB's Scientific
Laminar Flow Cabinet /Hood	Labconco
MicroCL 17 Microcentrifuge	Thermo scientific
Milli Q Ultrapure Water Purification System	Merck
Mini Vortex	Isolab
mPAGE® Mini Gel Tank (MGT-4 Millipore)	Merck
Multiskan FC 357 Microplate Photometer	Thermo Scientific
MW151 MAX pH Meter	Milwaukee
Power Supply	VWR
PowerPac™ Basic Power Supply	Bio-Rad
Roller	DLAB
Self-Contained Ice Machine	Scotsman AF 80
Ultra-low Temperature Freezer	Haier
Vertical Laboratory Steam Sterilizers	Nuve
Water Bath VWB 18	VWR